

A STUDY OF FLAME IONIZATION.

A Thesis submitted for the
Degree of Doctor of Philosophy
in the Faculty of Science
at the University of London

by

STANLEY JOHN MELINEK.

Department of Chemical Engineering
and Chemical Technology,
Imperial College of Science & Technology,
London, S.W.7.

July, 1969.

ABSTRACT.

Rates of ion generation in premixed and diffusion flames are investigated by the measurement of saturation currents. The variation of the saturation currents of premixed flames with final flame temperature and stoichiometric ratio is obtained. A porous disc burner is employed to give flat non-adiabatic flames with temperatures between about 1400 and 2100°K.

Flames of four hydrocarbons (methane, ethane, propane, and ethylene) with air and with oxygen are studied. The effects of various additives on premixed and diffusion flames are determined. Additives used include alkali metals, bromine, carbon dioxide, hydrogen, and carbon monoxide. Chemiionization of the alkali metals does not appear to occur except in pure carbon monoxide diffusion flames.

Effective activation energies of the rates of ion generation per unit area of premixed flames are determined. For lean and stoichiometric air flames an average value of 210 kJ mol⁻¹ (50 kcal mol⁻¹) is obtained. It is found that flames with oxygen and rich non-luminous flames with air give higher activation energies and lower saturation current densities.

The rate of ionization above a rich luminous flame

due to thermal ionization of the carbon particles is measured and a value for the work function of 4.6 eV obtained.

The conduction of charge to the electrodes is investigated. It is found that continuing ion generation occurs above the reaction zone of premixed flames and its rate is estimated.

Hydrocarbon diffusion flames are found to give ionization efficiencies (i.e. yields in electrons per carbon atom) of the order of 5×10^{-7} , using several different burners and a range of fuel flow rates. The ionization efficiency is found to be inversely proportional to the pressure.

Results of other workers and those of the present study are compared. Several interesting conclusions concerning the mechanism of chemionization are reached.

ACKNOWLEDGEMENTS.

The author wishes to thank Professor F.J.Weinberg and Dr. J. Lawton for valuable advice and guidance given in the course of this project and during the writing of the thesis. An S.R.C. studentship is acknowledged.

Nomenclature.

a	Distance from flame, electrode separation;
A_f	flame area;
A_p	effective probe area;
e	electron charge;
E	electric field;
E_a	effective activation energy per mole;
f	flow;
h	height above burner surface;
i	current;
i_p	current to probe;
i_t	total flame current;
j	current density;
J	rate of generation of current per unit volume;
J'	value of J at unit distance downstream of flame;
k	charge mobility;
n	density of charged particles of one sign;
n_e/n_c	number of electrons produced per carbon atom input (= ionization efficiency);
p	pressure;
R.	gas constant per mole;
S_u	burning velocity relative to cold reactants;
T	temperature;
T_f	final flame temperature;
T_{CO}	temperature when fuel has been oxidized to H_2O and CO ;

u	gas velocity;
V	voltage;
x	distance;
α	recombination coefficient;
ϵ	permittivity = 8.85×10^{-12} F m ⁻¹ for free space;
ν_a	electron attachment frequency;
ν_d	electron detachment frequency;
ρ	space charge density;
ϕ	stoichiometric ration;

Subscripts.

+	positive ion;
-	negative particle;
i	negative ion ;
e	electron;
s	saturation value.

INDEX.PART I INTRODUCTIONCHAPTER I PHENOMENA

- 1.1. History
- 1.2. Electrical Conduction In Flames
- 1.3. Generation of E.M.F's By Flames
- 1.4. Ionization in Flame Reaction Zones
- 1.5. Effects Of Electric Fields
- 1.6. Rate Of Ionization
- 1.7. Charge Recombination
- 1.8. Mechanism Of Ionization
- 1.9. Utility Of Flame Ionization.

CHAPTER II PRACTICAL ASPECTS OF FLAME IONIZATION

- 2.1. Detection And Measurement
- 2.2. Ionization In Rocket Exhausts
- 2.3. Utilization Of Flame Conductivity
- 2.4. Effect Of Electric Fields On Flames
 - 2.4.1. Chemical Effects
 - 2.4.2. Movement Of Charged Particles
 - 2.4.3. The Wind Effect
 - 2.4.4. Maximum Practical Effects

CHAPTER III SURVEY OF METHODS OF INVESTIGATING
IONIZATION

- 3.1. Experimental Techniques
 - 3.1.1. Probe Methods
 - 3.1.2. Mass Spectrometry
 - 3.1.3. Flame Photometry
 - 3.1.4. Electromagnetic Waves
 - 3.1.5. Conductivity Measurements
 - 3.1.6. Wind Effect
 - 3.1.7. Saturation Current Methods
- 3.2. Derivation Of Rates of Ionization From Ion Concentrations.

CHAPTER IV AIMS AND SCOPE OF PRESENT WORK

- 4.1. Reasons For The Investigation
- 4.2. Aims Of The Present Work
- 4.3. Measurements Made

PART II METHOD

CHAPTER V THE PRINCIPLE OF THE STEADY STATE D.C.
SATURATION CURRENT METHOD

- 5.1. Method
- 5.2. Possible Sources Of Error
 - 5.2.1. Secondary Ionization
 - 5.2.2. Electron Emission From The Electrodes
 - 5.2.3. Influence Of Applied Field
- 5.3. Ion Generation Above The Reaction Zone

CHAPTER VI THE PRINCIPLE OF A.C. AND TRANSIENT
D.C. MEASUREMENT OF SATURATION CURRENT

- 6.1. Alternating Currents
 - 6.1.1. Simplified Theories
 - 6.1.2. Effect Of Space Charge
 - 6.1.3. Discussion
- 6.2. Transient Currents
 - 6.2.1. Experimental Results
 - 6.2.2. Discussion
- 6.3. Summary

CHAPTER VII FLAMES AND BURNERS

- 7.1. Premixed Flames
 - 7.1.1. Flat Premixed Flames.
- 7.2. Diffusion Flames
 - 7.2.1. Types Of Diffusion Flame Used
 - 7.2.2. Determination Of Factors Affecting The Saturation Current
- 7.3. Fuels Studied

CHAPTER VIII CONDUCTION TO THE ELECTRODES

- 8.1. Discussion
 - 8.1.1. Solution For Charges Of Constant Mobility
 - 8.1.2. Divergence Due To Space Charge
- 8.2. Currents To Probes
 - 8.2.1. Effect Of Flame Non-Uniformity

- 8.2.2. Possible Methods Of Making The Current More Parallel
- 8.2.3. Variation Of Probe Current With Height And Potential Of Probe
- 8.3. Negative Conduction
 - 8.3.1. Theory Of Electron Attachment
 - 8.3.2. Experimental Results
 - 8.3.3. Negative Particle Mobility
 - 8.3.4. Ratio Of Electron To Negative Ion Concentration
 - 8.3.5. Evidence Of Ion Generation Above Flames
 - 8.3.6. Effect Of Impurities And Foreign Bodies
 - 8.3.7. Currents To Wires
- 8.4. Positive Conduction
 - 8.4.1. Positive Ion Mobility
 - 8.4.2. Further Evidence Of Ion Generation Above Flames
- 8.5. Ion Generation Above Flames
 - 8.5.1. Current With Low Positive Voltages on Burner
 - 8.5.2. Variation With Height
 - 8.5.3. Comparison Of Different Flames
 - 8.5.4. Variation Of Saturation Current With Electrode Separation
 - 8.5.5. Estimation Of Ionization Zone Thickness
 - 8.5.6. Effect Of Ion Generation Above Flames
 - 8.5.7. Summary

- 8.6. Further Experimental Results
 - 8.6.1. Rectification By Flame
 - 8.6.2. Observation Of Current-Voltage Characteristics
 - 8.6.3. Variation Of Current Due To Flame Movement
- 8.7. Maximum Current Without Breakdown
- 8.8. Summary

CHAPTER IX EXPERIMENTAL DETAILS

- 9.1. Flow System
 - 9.1.1. Use Of Bleed
 - 9.1.2. Seeded Premixed Flames
- 9.2. Burners
 - 9.2.1. Porous Disc Burner
 - 9.2.2. Other Burners Used For Premixed Flames
 - 9.2.3. Burners Used For Diffusion Flames
- 9.3. Electrical Measurements
 - 9.3.1. Electrical Circuit
 - 9.3.2. Safety Measures
 - 9.3.3. Measurements
- 9.4. Measurement Of Final Flame Temperature
 - 9.4.1. Thermocouple Method
 - 9.4.2. Sodium Line Reversal Method
 - 9.4.3. Comparison of Sodium Reversal And Thermocouple Methods
 - 9.4.4. Experimental Procedure

- 9.5. Sources Of Error
 - 9.5.1. Errors In Measuring The Current
 - 9.5.2. Errors In Measuring The Final Flame Temperature
 - 9.5.3. Errors In Measuring Flow And Composition
 - 9.5.4. Discussion

PART III RESULTS

CHAPTER X PREMIXED FLAMES

- 10.1. Air Flames
- 10.2. Oxygen Flames
- 10.3. Hydrogen And Carbon Monoxide Flames
- 10.4. Effect Of Composition On Burning Velocity
- 10.5. Effect Of Additives
 - 10.5.1. Carbon Dioxide
 - 10.5.2. Carbon Monoxide
 - 10.5.3. Hydrogen
 - 10.5.4. Nitrogen
 - 10.5.5. Bromine
 - 10.5.6. Metallic Salts
- 10.6. Luminous Flames
- 10.7. Summary

CHAPTER XI DIFFUSION FLAMES

- 11.1. Results For Methane
- 11.2. Results For Other Hydrocarbons
- 11.3. Counter-Flow Diffusion Flames

- 11.4. Effect Of Experimental Conditions
- 11.5. Effect Of Pressure
- 11.6. Effect Of Additives
 - 11.6.1. Nitrogen
 - 11.6.2. Hydrogen
 - 11.6.3. Carbon Monoxide
 - 11.6.4. Carbon Dioxide
 - 11.6.5. Bromine
 - 11.6.6. Alkali Metals
- 11.7. Ionization Due To Pyrolysis
- 11.8. Reversed Diffusion Flame
- 11.9. Summary

PART IV DISCUSSION

CHAPTER XII PREMIXED FLAMES

- 12.1. Comparison Of Hydrocarbon Flames
- 12.2. Hydrogen And Carbon Monoxide Flames
- 12.3. Effect Of Additives
 - 12.3.1. Addition Of Nitrogen, Carbon Dioxide, Carbon Monoxide
 - 12.3.2. Addition Of Hydrogen
 - 12.3.3. Addition Of Bromine
 - 12.3.4. Addition Of Metallic Salts
- 12.4. Noisy Flames
- 12.5. Effect Of Final Flame Temperature
 - 12.5.1. Effective Activation Energies

- 12.5.2. Alternative Methods Of Calculating The Activation Energy
- 12.6. Maximum Saturation Current Densities And Ionization Efficiencies
- 12.7. Temperature At Which Ionization Occurs
 - 12.7.1. Experimental Evidence
 - 12.7.2. Discussion
- 12.8. Ionization And Flame Propagation
- 12.9. Mechanism Of Ionization
- 12.10. Chemionization
 - 12.10.1. Possible Reaction Schemes
 - 12.10.2. Role Of Excited Species
- 12.11. Sooting Flames
- 12.12. Catalytic Oxidation
- 12.13. Analysis Of Ion Concentration Measurements
- 12.14. Summary

CHAPTER XIII DIFFUSION FLAMES

- 13.1. Variation With Fuel Flow Rate
- 13.2. Counter-Flow Diffusion Flames
- 13.3. Effect Of Additives
 - 13.3.1. Addition Of Nitrogen
 - 13.3.2. Addition Of Hydrogen
 - 13.3.3. Addition Of Carbon Monoxide
 - 13.3.4. Addition Of Carbon Dioxide
 - 13.3.5. Addition Of Bromine

- 13.3.6. Addition Of Metallic Salts
- 13.4. Effect Of Pressure
- 13.5. Effect Of Temperature
- 13.6. Accuracy Of The Results
- 13.7. Discussion
 - 13.7.1. Mechanism Of Ionization
 - 13.7.2. Comparison Of Premixed And Diffusion Flames
 - 13.7.3. Effect Of Premixing And Disequilibrium
 - 13.7.4. Maximum Current Densities Obtainable
- 13.8. Summary

CHAPTER XIV SUMMARY

REFERENCES

APPENDIX

PART I. INTRODUCTION.

CHAPTER ONE.

PHENOMENA.

1.1. History.

It has long been known that flames are capable of conducting electricity. Gißbert (1600) found that electrically charged bodies lose their ability to attract in the vicinity of a flame or on being heated with a flame. Watson (1747) demonstrated the conduction of electricity by flames. More work was done on electricity and flames in the following years. Most of this early work was ingenious but, of necessity, crude and qualitative, and is now mainly of historical interest. However, it is worth recalling in order to provide a background to the present study.

Erman (1802) discovered that a wire in a flame conducts positive electricity more easily than negative. Henley (1774) found that a flame between two electrodes tended to be deflected towards the cathode. Brande (1814) confirmed that flames are deflected by electric fields and that the deflection is usually towards the cathode. It is now known that this phenomenon is due to the ionic wind effect (Calcote, 1949). Brande found also that electrolysis of flame products occurred, acidic gases tending to go to the

anode. Cuthbertson (1802) showed that the heat transfer to electrodes placed near a flame is altered by the application of a field.

1.2. Electrical Conduction in Flames.

A large number of effects regarding flame conduction have been noted. The principal findings will be presented briefly in this section as a series of short statements of fact.

Electrical conduction in flames is non-ohmic (Lawton & Weinberg, 1964). Also there is a maximum current which can be drawn before secondary ionization occurs, and which is termed the saturation current.

Giese (1882) and Schuster (1890) put forward the concept that the conductivity of flames is due to ionization produced in the reaction zone, the current being carried by the movement of charges through the gas, as opposed to being carried by charge transfer between adjacent atoms as in metals. As will be shown, this theory explains the observed characteristics of flames as conductors: their non-ohmic behaviour; the occurrence of electrolysis; the occurrence of a space charge leading to the wind effect; and the existence of a saturation current.

The conductivity of the product gases of a flame can be destroyed by passing them through a strong electric

field (Thomson & Thomson, 1928), the action of which is to remove all the ions.

McClelland (1898) measured the conductivity of the gases above a flame using a quadrant electrometer. He found that the rate of ion recombination is second order.

Since about 1900 many measurements have been made of ion mobilities and the conductivity of flame gases. Not all of the earlier work is reliable. A review is given by Wilson (1931) of work done up to that date, including the measurement of flame conductivities, and ion and electron mobilities. The alteration of flame conductivity due to magnetic fields was measured by him and the deduced electron mobilities from the magnitude of the Hall effect. Flames seeded with easily ionizable metal salts and unseeded flames were studied, and the ionization potential of the metals used was determined.

1.3. Generation of E.M.F's by Flames.

It is often possible to obtain small currents from conductors placed in flames (Hankel, 1851). These currents result primarily from thermal (thermoelectric and caloelectric) effects. The voltages are low, being of the order of one volt or less. The caloelectric effect appears to arise either from the electron temperature in the

reaction zone of flames being anomalously high (Von Engel & Cozens, 1963), or from the high diffusivity of the electrons as compared to positive ions (Lawton, 1965), which causes a net flow of electrons to one electrode. Wilson (1931) showed that there is a potential gradient perpendicular to the flame front due to the tendency of the electrons to diffuse faster than the ions and he calculated and measured its magnitude. The potential difference between two electrodes depends on the temperature difference between them and may arise partly from the quenching caused in their vicinities and the resultant change in the rate of charge generation (Debiesse & Klein, 1964). In addition, the charge density and rate of charge generation vary through the flame. A potential difference can be produced also by differences in the gas composition at two electrodes (Debiesse et al, 1965), which may arise in part from different rates of electron attachment.

If one of the electrodes in a flame is downstream of the other then the voltage obtained can be increased by the charged gas being carried to the downstream electrode. This phenomenon is the electrohydrodynamic effect and appears to have been obtained by Klein (1960).

1.4. Ionization in Flame Reaction Zones.

Much work has been done recently investigating the amount of ionization in flames, its nature, and possible mechanisms. It has been found that ionization greatly in excess of equilibrium values occurs in flames containing hydrocarbons. Moreover, it is found that ionization occurs predominantly in the vicinity of the reaction zone. It reaches its maximum value near the final flame temperature and then decreases towards its equilibrium value (Calcote, 1957). Ionization occurs also in the case of catalytic oxidation of hydrocarbons (Perkins et al, 1963).

All hydrocarbons and most other organic compounds give rise to ionization. Hydrogen, however, and compounds where the carbon is joined to oxygen by a double bond (eg. formaldehyde, carbon monoxide) do not (Sternberg et al, 1962). Hydrogen sulphide and carbon disulphide give negligible ionization with oxygen (Van Tiggelen, 1963) and with air (King, 1962). However, it has been reported that very small concentrations of carbon disulphide in hydrogen do give ionization which appears to be inhibited at higher concentrations (McWilliam, 1961).

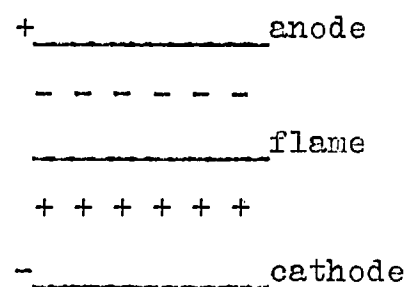
Most of the ionization takes place over a distance of at most 0.5 mm (Calcote, 1957; Wortberg, 1965) for near-limit flames at atmospheric pressure. The distance is

greater at lower pressures (Calcote, 1962). The time taken by the ion generation process is of the order of 1 ms.

The negative charge in flames is carried largely by electrons (Green, 1965). If a negative wire is placed above a flame the current to it is carried by positive ions whereas if the wire is positive most of the current to it is carried by electrons, which have a far greater mobility than ions. For this reason flames conduct more easily to a positive wire, as found by Erman (1802).

1.5. Effects of Electric Fields.

When a flame is placed between two electrodes between which a field is applied, as shown in the diagram, positive ions are drawn towards the cathode and negative charge towards the anode. The electric field acting on the resultant space charge gives an aerodynamic force on the flame, which results in the wind effect. The wind effect has been investigated by Payne and Weinberg (1959). Electric fields can influence also the motion of charged particles in flames. The effects of electric fields on flames are discussed more fully in Ch.II.



1.6. Rate of Ionization.

The ion concentrations and saturation currents of flames vary with the composition of the reactants. Saturation currents increase markedly with the final flame temperature. The ionization process has an apparent activation energy of about 200 kJ mol^{-1} (Lawton & Weinberg, 1964; Van Tiggelen, 1963; Calcote, 1963a). The maximum ion (King, 1958) and electron (Bulewicz & Padley, 1963) concentrations have been found to be proportional to the pressure.

Maximum ion concentrations in hydrocarbon flames at atmospheric pressure are of the order of 10^{16} m^{-3} (Wortberg, 1965) to 10^{19} m^{-3} (Van Tiggelen, 1963), depending on the flame temperature and composition. Saturation currents of adiabatic stoichiometric hydrocarbon/air flames are of the order of 1 A m^{-2} (Lawton & Weinberg, 1964). Lawton & Weinberg also give values for hydrogen/air flames containing hydrocarbons. The ionization efficiency, expressed as the number of electrons produced per carbon atom, is of the order of 10^{-6} for premixed hydrocarbon/air flames (Calcote, 1965). The ionization efficiency increases with temperature (Peeters & Van Tiggelen, 1968).

Since the number of electrons produced is of the order of 10^{-6} per carbon atom, one gram atom of carbon gives

approximately 10^{-6} Faraday or 0.1 coulomb. One gram atom of carbon is equivalent to an energy input of approximately 6×10^5 J, assuming that the fuel has a formula $C_n H_{2n}$. Thus the efficiency of a flame as a source of electrons is approximately 1.6×10^{-7} coulomb per joule, which is equal to 1.6×10^{-7} amp watt $^{-1}$.

1.7. Charge Recombination.

The ion concentration downstream of hydrocarbon flames decays owing to recombination. Near the reaction zone ion-electron recombination appears to predominate (Green & Sugden, 1963). Downstream of the reaction zone recombination may be largely by electron attachment followed by ion-ion recombination (King, 1962). The recombination is second order with a recombination coefficient of the order of $2 \times 10^{-13} \text{ m}^3 \text{ s}^{-1}$ (Calcote et al, 1965), which does not vary greatly with temperature or pressure.

1.8. Mechanism of Ionization.

Ion species found by mass spectrometry in unseeded flames containing hydrocarbons include H_3O^+ , $C_3H_3^+$, CHO^+ , OH^- , and C_2H^- (Green, 1965; Van Tiggelen, 1963). Many other ions, both positive and negative, with molecular weights between 12 (O^+) and about 65, are found, mostly in

small quantities (Van Tiggelen, 1963; Green & Sugden, 1963). Charge exchange occurs, so the ions found are not necessarily those initially produced. The main positive ion downstream of the flame is H_3O^+ (Green & Sugden, 1963). The main negative charges are OH^- and e^- . Ions containing carbon, such as C_2H^- (Green, 1965) and C_3H_3^+ occur downstream of rich flames and tend to predominate.

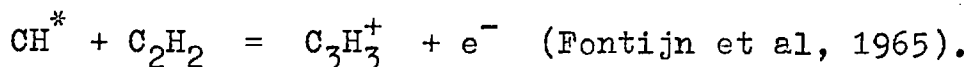
It is thought that the initial ions formed are probably CHO^+ (Bulewicz & Padley, 1963) and possibly C_3H_3^+ (Calcote et al, 1965). The negative charge is probably produced initially as electrons (Mills, 1968), which constitute most of the negative charge in the reaction zone. A proportion of these subsequently attach to give negative ions (Green, 1965). Some negative ions may be formed directly by chemiionization (Calcote, 1965).

Survey papers on this subject have been written by Calcote (1957) and by Sugden (1965). Calcote considers the nature of the charge production and concludes that it occurs by chemiionization.

Calcote (1965) and Green & Sugden (1963) consider possible reaction schemes in detail. The most likely primary ionization reactions appear to be



and possibly



Ionization is not unique to hydrocarbon flames. It also arises when carbon tetrachloride is added to a carbon monoxide/air diffusion flame (Gallaway et al, 1964), or CCl_4 or C_2Cl_4 to premixed carbon monoxide/oxygen flames (Van Tiggelen, 1963). This indicates that ionization can occur in the absence of hydrogen. Ionization occurs also in flames of $\text{C}_2\text{N}_2/\text{O}_2$, NH_3/O_2 , and NO_2/H_2 (Van Tiggelen, 1963). The main positive ion in flames containing nitrogen compounds tends to be NO^+ . This is because NO has a comparatively low ionization potential. Van Tiggelen states that NO^+ is definitely a chemi-ion.

The bulk of evidence suggests that charge production in flames is due to chemi-ionization. However, Perkins et al (1962) give arguments supporting the theory that the ionization is due to the thermal ionization of carbon particles. This seems unlikely (Calcote, 1957), especially in view of the large quantities of ions found in lean premixed flames and the fact that, in diffusion flames, ionization level peaks in the blue premixed region near the burner rim and not in the hotter luminous tip (Kinbara & Nakamura, 1955).

Recently the possibility of ionization by electron collision has been put forward (Von Engel & Cozens, 1965). Clearly the source of ionization in flames has not yet been

finally decided, but much progress has been made.

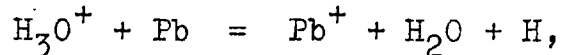
1.9. Utility of Flame Ionization.

For some suggested applications of flame ionization, in particular magnetohydrodynamic generation of electricity (MHD), it would be necessary for the gas to be highly conductive and macroscopically neutral, ie. there would have to be charges of both signs present in equal numbers and high concentrations (ca. 10^{20} ions m^{-3}). However, since ions would be lost by recombination, continuing ionization downstream in the products would probably be required as it is unlikely that the recombination coefficient would be low enough to delay for a sufficient time the loss of most of the ions generated in the reaction zone. Consequently, chemi-ionization in the reaction zone alone might not be suitable in this case (Freck & Wright, 1965).

Sustained charge production can be achieved, for example, by seeding with metallic salts (Arrhenius, 1891). This ionization level can be boosted by chemiionization processes, by addition of low work function materials such as BaO particles, or by the thermal ionization of flame carbon.

Flame ionization can also be increased by the use of augmented flames (flames in which the enthalpy is

increased by the dissipation of electrical energy) at high temperatures (Chen et al, 1965) or by additives which catalyse the ionization or reduce the recombination coefficient. Halogens catalyse the ionization in flames containing alkali metals (Padley et al, 1961). Lead and some other metals increase the electron concentration downstream of hydrocarbon/air flames. This latter effect appears to occur because charge transfer processes, such as



produce positive ions which recombine less rapidly than the ions normally present (Soundy & Williams, 1965). The ion recombination coefficient is also reduced by the addition of small amounts of chlorine (King, 1962) or CH_3Br (Van Tiggelen, 1963). This may be due to the formation of heavy negative ions. Such ions would be likely to recombine less easily than the negative ions otherwise present.

The efficiency of ionization attainable by seeding with metallic salts is much greater than that of chemi-ionization. Ionization of metal atoms can be nearly 100%, depending on the temperature and the metal used, whereas chemiionization gives about one ion pair per 10^6 carbon atoms. Moreover, thermal ionization has the higher activation energy and so is relatively more important at high temperatures.

Seeding with metallic salts tends to be expensive and to cause corrosion. Chemiionization is economical and fast but tends to be short lived. The recombination coefficient for chemi-ions is of the order of 10^2 times that for alkali ions (King, 1963). The rate of ion generation in flames with the same maximum ion concentrations is therefore greater in the case of chemiionization and the time taken to attain the maximum concentration less. Thermal ionization tends to reach its maximum downstream of the reaction zone (Schofield & Sugden, 1965). Chemiionization is most likely to be useful in situations where a high level of continuing ionization is not required, as, for example, in the ionic wind effect and the control of carbon formation.

CHAPTER TWO.

PRACTICAL ASPECTS OF FLAME IONIZATION.

There are many possible applications and practical aspects of ionization in flames, some of which will now be considered.

2.1. Detection and Measurement.

Flame ionization detectors are widely used in gas chromatography. They detect traces of organic compounds in a carrier gas, usually hydrogen, by the ionization produced on combustion. The pure hydrogen flame produces virtually no ionization. The saturation current is proportional to the concentration of the organic compound over a very wide range. The use of these detectors has been extensively investigated by Sternberg et al (1962). They detect hydrocarbons and most other carbon containing compounds. The response for a wide range of organic compounds has been measured. It depends on the composition and structure of the compound, in particular on the number of carbon atoms it contains. The response for very many compounds can be estimated from available data. For hydrocarbons the number of ions produced per molecule is approximately proportional to the carbon number of the molecule (Ackman, 1968). Lovelock (1961) compares the

flame ionization detector with other ionization detectors. Some of these are somewhat more sensitive or in addition detect inorganic compounds. However, the flame ionization detector is the simplest, has the widest range, and is probably the best in most cases where it is desired to detect only organic compounds.

Flame ionization can be used for the detection of flames. The current to an electrode provides a rapid and sensitive means of detecting a flame. The arrival of a flame front at a point can be detected by the use of an ionization gap (Schnauffer, 1934). The response is very rapid. Ionization gaps can be used to follow the progress of a conflagration or to measure flame velocity, and have been used to investigate flame spread in internal combustion engines (Knapp, 1964; Higashino, 1961). Karlovitz (1965) has used a probe to detect the position of the surface of turbulent flames.

2.2. Ionization in Rocket Exhausts.

The ionization in rocket exhausts can cause interference with communications, particularly to and from the rocket (Calcote, 1963a). To minimise this effect it is desirable to reduce the electron concentration. On the other hand highly ionized rocket exhausts could be used to replenish the ionosphere for communication purposes if it

were disrupted by a nuclear explosion. The combustion of one ton a hydrocarbon (propane) produces about 6×10^{22} electrons (Calcote, 1965), which is equal to the number contained in 600km^3 of the ionosphere (Taylor, 1964).

2.3. Utilization of Flame Conductivity.

It is possible to convert the thermal energy of combustion directly into electrical energy by electrohydrodynamic (EHD) and by magnetohydrodynamic generation (Soo, 1968). These methods have the advantage that they require no moving parts. They can operate at high temperatures and are therefore potentially more efficient than conventional methods. It is important however that there be sufficient ionization in the flame products. MHD requires macroscopically neutral gas with high electron concentrations to provide high electrical conductivities. EHD on the other hand requires high concentrations of monopolar ions of low mobility. There are considerable practical difficulties, particularly in the case of MHD. It is not now thought that MHD is economically worthwhile in the United Kingdom (Rotherham, 1967).

Small emf's can arise between electrodes in flames (Von Engel and Cozens, 1963) as a result of thermal or non-equilibrium effects. Such processes are not likely to

provide a practical means of large scale power generation in unseeded flames, however.

A flame can be used as a rectifier or an electronic valve. Heaps (1920) used a flame as an amplifying valve (a triode). He relied on thermal emission from the cathode to provide sufficient current.

Static electricity is a hazard in industry since it can cause explosions. Flame ionization could be used to neutralize static charges. Gilbert (1600) found that charged bodies can be discharged efficiently and rapidly in this way. In this connexion it is interesting to note that combustion products can retain some conductivity for several minutes (Thomson & Thomson, 1928).

The ionization from hydrocarbons can be used to boost the initial ionization in flames seeded with suitable metallic salts to levels above the equilibrium value for the metals (Calcote, 1963a; Knewstubb & Sugden, 1956), or, by charge transfer, to decrease the time in which equilibrium ionization of the metal is attained.

2.4. Effect of Electric Fields on Flames.

Many possible applications of flame ionization depend on the effect of applied electric fields on the flames and flame products. These effects are considered below in greater detail.

2.4.1. Chemical Effects.

There is no conclusive evidence at present that electric fields have any chemical effect on the propagation of non-sooting flames (Guénault & Wheeler, 1932). Many workers have found flames to be affected by electric fields but these effects appear to result from the force exerted by the field on the flame gases. As shown in Ch.XII, there seems to be little direct connection between the flame propagation and ionization processes. One reason for this may be that the number of ions is small compared to the number of molecules present, being not more than about one in 10^5 . Thus, except where the ions are very big, for example charged soot particles, the flame is not likely to be affected appreciably by their removal. However, flame ionization is thought to be important in the inhibition of flames by halogenated hydrocarbons (Mills, 1968).

2.4.2. Movement of Charged Particles.

The application of electric fields to sooting flames has been investigated by Thieme (1912, 1915). Payne & Weinberg (1959), and Place & Weinberg (1966). Soot particles in flames tend to become charged. As a result their motion and residence times can be influenced. It is possible by the use of applied fields to control the site of

deposition and the quantity and nature of the soot produced. The change in the quantity and quality of the soot occur because these depend on the history of the particles and the number of nuclei for soot formation, both of which are influenced by the field. It has also been found that positive ions appear to play an important part in the nucleation and growth of soot particles. Ionization may be important in other flame processes also, in which case it may be possible to control such processes by the application of electric fields or by other wise varying the ion concentration.

The application of electric fields could be used to influence and possibly control flames containing charged macroscopic particles of any type. For example, heat transfer to the reactants might be increased, and with it the burning velocity, by causing the particles to oscillate between the products and the reactants in an alternating field. The residence time of the particles in the flame can be adjusted by suitable combinations of field strengths and frequency. This effect might also be used to control radiation from the flame and the combustion of inflammable particles.

It is possible to electrolyze flame products and to isolate charged species (Thieme, 1915). The maximum rate of separation of a product by electrolysis, per unit area, is normally very low (Lawton & Weinberg, 1964) except perhaps

for very heavy charge carriers such as charged soot particles.

2.4.3. The Wind Effect.

When an electric field is applied to a flame charges are drawn towards the electrodes. The electric field acts on these charges, resulting in forces on the gas, which can lead to a wind (see Ch.I). This effect can be used to alter rates of heat transfer and flame size, shape, and stability (Calcote & Pease, 1951; Payne & Weinberg, 1959; Pejack & Jones, 1968) and to control rates of mixing, entrainment, and flame spread (Mayo et al, 1965). Alternating fields could perhaps be used to increase the turbulence - it is known that flames can be used to convert a.c. electrical signals into sound (Babcock et al, 1967). It is also possible to extinguish flames by the use of applied fields (Calcote, 1957; Nakamura, 1959).

The induction period for flame ignition by a hot wire can be altered by an electric field (Malinowsky & Malyar, 1935). This effect probably results from the influence of the ionic wind on the viability of the flame kernel formed.

The wind effect results from the force exerted by the electric field on the space charge present. For a given current the space charge and therefore the force exerted is greater for charges of low mobility. Since the negative charge is largely carried by electrons it has a higher

mobility than the positive charge and travels to the electrode quicker. There is therefore usually more positive than negative space charge present making the force on the positive space charge greater, giving a net force on the flame towards the cathode. The force obtained and the resultant ionic wind depend on the applied potential, the charge mobilities, and the electrode configuration. The theory is discussed in detail by Lawton et al (1968).

2.5. Maximum Practical Effects.

For a plane flame between two electrodes parallel to it and between which a voltage is applied, it can be shown (Lawton & Weinberg, 1964) that:

i) maximum force due to wind effect = $\frac{1}{2} \epsilon E_b^2 \text{ N m}^{-2}$

where E_b is the breakdown field, which is approximately $3 \times 10^6 \text{ V m}^{-1}$ in air at NTP (Meak & Craggs, 1953);

ii) maximum current density = $\frac{1}{2} \epsilon E_b^2 k/a \text{ A m}^{-2}$

where a is the distance in metres from the flame to the appropriate electrode (that at which breakdown first occurs), and E_b and k are in SI units.

Lawton & Weinberg (1964) also consider cylindrical and spherical configurations.

Many applications of flame ionization, in particular chemical ones, require the drawing of high current densities from the flame. It is therefore necessary to

ensure that the saturation current of the flame is sufficiently large. As shown by the theory, the maximum current obtainable is ultimately limited by the space charge, which causes breakdown at the electrodes. To obtain the maximum current the electrode separation should be a minimum. The minimum electrode separation is ultimately limited by the quenching distance, which is of the order of millimetres or less at atmospheric pressure. The minimum separation for practical purposes would probably be about 5 mm. The breakdown strength of the gas can be increased by certain additives, low temperatures near the electrodes, suitably designed electrodes with no sharp points, and increased pressure. The maximum space charge limited current density is approximately proportional to the pressure for constant electrode separation and constant temperature (see Ch.VIII). Moreover, the quenching distance is roughly inversely proportional to pressure, so it might be possible to have lower electrode separations at higher pressures without affecting the flame. Doing so would further increase the maximum current obtainable.

In order to make use of flame ionization, and to control it, it is desirable to know how much ionization occurs in different flames, its behaviour, and if possible its mechanism. In view of the many potential applications,

there has been a large increase in the amount of research into flame ionization in recent years. Methods of investigating flame ionization are discussed in the next chapter.

CHAPTER THREE.

SURVEY OF METHODS OF INVESTIGATING IONIZATION.

3.1. Experimental Techniques.

A number of methods have been used to measure ion concentrations and rates of ionization in flames. The best method depends on the quantity to be measured and the sensitivity, accuracy, and spatial resolution required. It is desirable where possible to compare results obtained by different methods in order to check their reliability and accuracy.

The principal types of method that have been used are:

- (i) probe methods;
- (ii) mass spectrometry;
- (iii) flame photometric methods;
- (iv) electromagnetic waves and high frequency methods;
- (v) flame conductivity methods;
- (vi) measurement of the wind effect;
- (vii) saturation current methods.

A review of plasma diagnostic techniques is given by Huddleston & Leonard (1965).

3.1.1. Probe Methods.

Probe methods consist of measuring the current versus potential characteristics of a small probe immersed in the flame. Ion and electron concentrations and electron temperatures can be determined in this way (Chen, 1965). The values obtained are those in the vicinity of the probe since the current is drawn primarily from that region. The theory and use of probes in flames is discussed by Calcote (1963b), who used single cylindrical probes, and Travers & Williams (1965), who used spherical double probes.

Probes are capable of giving the ion distribution through a flame (Wortberg, 1965) and probably provide the only method which gives high spatial resolution. It is important to know the variation of ion concentration with distance in order to study the ionization process. The recombination coefficient can be determined from the rate of decay of the ion concentration. The position of the ionization zone shows at what stage in the combustion the ionization occurs. Also, the saturation current density can be estimated from the ion concentration (see below).

The interpretation of data obtained by the use of probes is difficult and not wholly reliable (Salter & Travers, 1965). The theory is complicated and has been subject to modifications (King & Calcote, 1955). However,

ion concentrations obtained by probes for seeded flames have been found to be in quite good agreement with values obtained by resonance light absorption (Carabetta & Porter, 1969).

Probes can disturb the flame by cooling the gases and by obstructing the flow. This may affect the flame physically or chemically, and even change the position of the flame front. Probes can be used only at temperatures low enough to avoid appreciable thermal emission of electrons from the probe, for which reason it is often necessary to provide cooling.

An estimate of the spatial resolution given by a probe can be made by calculating the radius of the region from which the probe collects current, assuming that the probe collects all the ions formed in this region.

For the probe used by Wortberg (1965):

$$j_+ = n_+ e \left(\frac{kT_+}{2\pi m_+} \right)^{\frac{1}{2}} \left(1 + \frac{3}{2^{\frac{1}{2}}} n d r^2 n_0 \ln \frac{2L}{d} \right)^{-1} \quad (1)$$

where n_+ = positive ion density;

j_+ = current density at the probe surface;

m_+ = mass of positive ion

= 3.16×10^{-26} kg assuming a molecular weight of 19
(that of H_3O^+);

T_+ = positive ion temperature;

- d = probe diameter = 0.1 mm;
 n_0 = neutral molecule density;
 L = probe length;
 r = collision radius between ions and neutral molecules;
 k = Boltzmann's constant.

The radius of the region from which the probe current is drawn, x , is given by:

$$\begin{aligned}
 \text{probe current} &= ndj_+L \\
 &= n(x^2 - \frac{1}{4}d^2)L\alpha n_+^2e, \text{ assuming that the} \\
 &\text{rate of generation of positive charge per unit volume is} \\
 &\text{equal to } \alpha n_+^2e, \text{ the rate in equilibrium.}
 \end{aligned}$$

Substituting for j_+ from equation (1) gives

$$\begin{aligned}
 x^2 &= dj_+ (\alpha n_+^2e)^{-1} + \frac{1}{4}d^2 \\
 &= \frac{d}{\alpha n_+^2e} n_+^2e \left(\frac{kT_+}{2nm_+}\right)^{\frac{1}{2}} \left(1 + \frac{3}{2} \frac{1}{2} ndr^2 n_0 \frac{\ln 2L}{d}\right)^{-1} + \frac{d^2}{4} \\
 &= \frac{1}{\alpha n_+} \left(\frac{kT_+}{2nm_+}\right)^{\frac{1}{2}} \left(1 + \frac{3}{2} \frac{1}{2} ndr^2 n_0 \frac{\ln 2L}{d}\right)^{-1} \text{ approximately.}
 \end{aligned}$$

For the specific experiment in question:

$$\begin{aligned}
 T_+ &= 1500^\circ\text{K, assuming } T_+ = T_f x, \\
 r &= 1.8 \times 10^{-10} \text{ m,} \\
 \alpha &= 1.1 \times 10^{-13} \text{ m}^3 \text{s}^{-1}, \\
 L &= 0.05 \text{ m.}
 \end{aligned}$$

$$\begin{aligned}
 \text{Therefore } x^2 &= 400 n_+^{-1}, \\
 x &= 20 n_+^{-\frac{1}{2}}.
 \end{aligned}$$

n_+ in the reaction zone was of the order of 10^{16} m^{-3} . Taking this value gives $x = 0.2 \text{ mm}$. Thus the resolution obtained by Wortberg is of the order of 0.2 mm . It can be seen from his results that this resolution is probably sufficient, the half width of the ion concentration curve being about 1 mm .

Measurements are easier at low pressures because the reaction zone is thicker. The reaction zone thickness is approximately inversely proportional to the pressure (Fristrom & Westenberg, 1955). The ion concentration is approximately proportional to the pressure (King, 1958), in which case the spatial resolution is inversely proportional to the square root of the pressure.

3.1.2. Mass Spectrometry.

Mass spectrometry has been used to investigate flame ionization by several workers (eg. Sugden, 1963; Van Tiggelen, 1963; Calcote et al, 1965; Green, 1965). It is the only method which is capable of identifying the ion species present and giving their relative concentrations. The ions are drawn into the sampling system through a fine hole in a platinum foil by suction. They can be drawn from different parts of the flame and the variation of ion concentration with distance above the burner obtained. Mass spectrometry is capable of high

sensitivity: ion concentrations down to 10^{11} m^{-3} have been measured (Sugden, 1963). However, only relative ion concentrations are given and special calibration is necessary if absolute values are required.

Mass spectrometry has several disadvantages. It is complicated and expensive. Negative ions are difficult to detect (Calcote, 1963a). Charge exchange is liable to occur, particularly in the boundary layer at the entrance hole of the spectrometer, so that the ions detected are not necessarily those extracted from the flame (Green & Sugden, 1963; Bascombe et al, 1963). The size of the entrance hole and other variables have to be selected and varied so as to try to eliminate the effects of charge exchange. Moreover, because it is necessary to place the spectrometer entrance in the flame gases, the flame is likely to be seriously quenched. It is also sometimes difficult to identify ions since mass spectrometry gives only their molecular weight, and there may be several possible ions with the same mass. In this case isotopes can be used to find the molecular formula of the ion.

3.1.3. Flame Photometry.

Flame photometry can be used to obtain the concentration of any species which gives a spectral line.

It has been used to obtain indirectly the rate of ionization of a metal in a flame by measuring the rate of disappearance of neutral molecules (Schofield & Sugden, 1965).

Flame photometry cannot be used to obtain ion concentrations directly because ions give a continuum rather than a line spectrum, except at high energies (Hertzberg, 1944). However, ions and electrons in electric discharges can alter the spectrum as a result of the Stark effect. Their concentration can be deduced from the magnitude of this effect. They can also cause the appearance of lines which are normally forbidden. A review of plasma spectroscopy is given by Cooper (1966). Most of this material is likely to be applicable only at electron temperatures and/or electron concentrations much higher than those usually obtained in unseeded flames.

3.1.4. Electromagnetic Waves and High Frequency Methods.

These involve the use of resonant circuits or microwaves. It is possible to obtain ion and electron concentrations and electron collision frequencies and cross sections by the use of radio frequencies and microwaves. The latter are more suitable for measuring electron concentrations. These methods have the advantage that the flame is not disturbed. Electron concentrations down to

$3 \times 10^{14} \text{ m}^{-3}$ can be detected (Borgers, 1965). In general only poor spatial resolution can be obtained. The best claimed so far is 3 mm (Padley & Sugden, 1962). This resolution is not sufficient to measure the variation of ionization with distance through the reaction zone of flames at atmospheric pressure.

The use of microwave and radio frequency measurements is discussed by Sugden (1963). Microwaves have been used by Padley & Sugden (1962), cyclotron resonance by Bulewicz & Padley (1963) and high frequency resonance methods by Borgers (1965) and Williams (1962). Makios (1965) has used microwave interferometry. With these methods the field strength must be kept sufficiently low to avoid any appreciable increase in the electron temperature.

The use of the Faraday effect was considered. The rotation of the plane of polarization, θ radians, is proportional to $n_e Hl$, where n_e is the electron concentration, H is the magnetic field strength, and l is the path length in the field. The value of l can be maximized by taking a large flame or by the use of multiple reflections (Gaydon, Spokes & Van Suchtelen, 1960). The maximum value of H attainable depends on the volume over which it is required.

It was shown that, if $Hl = 10^7 \text{ A}$, $n_e = 10^{16} \text{ m}^{-3}$,

then $\theta = 3 \times 10^{-8}$ rad for light of wave length 6×10^{-7} m,
 $\theta = 8 \times 10^{-2}$ rad for radiation of wave length 1 mm.

These results show that the use of the Faraday effect to measure electron concentrations would not be practicable using light. It might be feasible using microwaves but any improvement in the resolution attainable would be comparatively small. Thus the use of the Faraday effect does not offer any very great advantages.

3.1.5. Conductivity Measurements.

Conductivity measurements have been used to obtain electron concentrations in the reaction zone of flames by Van Tiggelen (1963). Other workers have measured the conductivity of flame gases above the reaction zone (eg. Wilson, 1931).

Most of the current, particularly in the reaction zone, is carried by electrons since their mobility is much higher than that of ions. For concentration determinations it is necessary to know the electron mobility, which has a value of about $0.25 \text{ m}^2 \text{ V}^{-1} \text{ s}^{-1}$ at atmospheric pressure (see Ch. VIII).

The conductivity method has to be applied with care, for two reasons. Firstly, a voltage drop occurs in the vicinity of the electrodes. This drop can be allowed for

by varying the electrode separation. Secondly, for measurements of the electron concentration in the reaction zone the thickness of the ionization zone must be estimated. The value obtained for the electron concentration then represents an average over this distance.

The reaction zone thickness is difficult to measure because of its small value at atmospheric pressure and of optical distortion (Weinberg, 1963). Van Tiggelen (1963) used a formula, based upon his theory of flame propagation, to obtain the reaction zone thickness. He assumed that the ion concentration was constant over the distance. It appears that the flame thickness which he calculated represents that of the preheat zone rather than that of the reaction zone (Van Wouterghem & Van Tiggelen, 1954). Bradley & Matthews (1967) found that in a CO flame with methane added, the zone of maximum rate of ion generation was not coextensive with the zone of maximum heat release rate. Thus the thickness of the ion generation zone is not necessarily equal to the reaction zone thickness. The ion concentration, n , downstream of the ion generation zone is given by $dn/dt = -\alpha n^2$. Thus the ion concentration remains high for a distance of the order of $u\alpha^{-1} n_{\max}^{-1}$ where u is the flow velocity and α the recombination coefficient, which is about $2 \times 10^{-13} \text{ m}^3 \text{ s}^{-1}$ (Calcote et al, 1965).

3.1.6. Wind Effect.

The wind effect results from the action of the applied field on charge carriers within all the gas between the electrodes, as has been discussed in Ch. II, and not primarily from the action of the field on those of the reaction zone, which is a very thin region of relatively low field. The magnitude of the wind effect therefore cannot be used to estimate the number of ions in the reaction zone, as has been assumed in the past (Calcote, 1949, 1963a).

3.1.7. Saturation Current Methods.

The distribution of the saturation current density of a flame can be recorded by ion photography (Weinberg, 1966a). The charge striking an electrode is passed through a photographic plate, giving an image of the flame, which image is liable to be distorted. The current from the flame to the electrode tends to diverge due to the space charge. This distortion could be reduced by using a collimator consisting of a cylindrical insulating surface round the path of the current. This would become charged and in equilibrium no current could go to the insulator. The current at the surface of the insulator would therefore become parallel to this surface. This effect could also be used to concentrate the current into a smaller area. A magnified

image of the flame could be obtained by allowing the current to diverge.

Ion photography is primarily a qualitative method. It gives a detailed image of the flame from point to point. Its use to obtain actual values of the current would be approximate and cumbersome. The method has the disadvantage that it takes up to 15 minutes to obtain a photograph.

A more convenient and accurate method of obtaining saturation current densities is by the direct measurement of saturation currents. The use of saturation current measurements is described by Lawton & Weinberg (1964). The method has been used also by Arrington et al (1965), Peeters & Van Tiggelen (1968), and, in connection with gas chromatography, by Sternberg et al (1962) and others.

The principle of saturation current measurements is that when a field is applied to a flame ions are extracted. The current obtained increases as the voltage is increased. Usually it reaches a steady value and then does not change appreciably with further increases in voltage until very high fields are attained, when secondary ionization and breakdown occur, giving a sudden increase in current. The current reaches the steady value when all the ions produced in the flame are being withdrawn and collected before they can recombine. This current is the saturation current. Under

conditions of high saturation currents and large electrode separations breakdown can occur before the saturation current is attained.

The measurement of saturation current gives the total rate of ionization in the flame and is the only direct method of obtaining this quantity. The method is simple, unambiguous, exact, and rapid. Most of the methods of investigating ionization discussed above measure the ion concentration, which results from a balance between ion generation and ion recombination. Saturation current measurements give the rate of ion generation directly and ion recombination is not involved. Moreover, the saturation current is more fundamental than the ion concentration in the flame and it is of more importance for applications involving the use of applied electric fields.

A disadvantage of the saturation current technique for some purposes is that it does not give any spatial resolution through the reaction zone. However, in many cases it is necessary to know only the total rate of ionization and its variation with temperature. The problem of resolution is not a serious one in connection with investigation of the kinetics and mechanism of the ionization process because it is found that the ionization occurs over a narrow region near the final flame temperature (Bradley &

Matthews, 1967), so that the temperature is approximately constant. Most of the spread of the ionization detected by probes is due to convection and diffusion and not to an extended source.

3.2. Derivation of Rates of Ionization from Ion Concentrations.

All the quantitative methods of investigating ionization discussed above, except saturation current measurements, give ion or electron concentrations or relative concentrations. Rates of ion generation can be obtained from these concentrations, although the accuracy is limited by the spatial resolution attainable, and by uncertainty of the values of the rate of diffusion and the recombination coefficient, α . α is not necessarily constant (Gaydon & Wolfhard, 1960).

The saturation current density is given by the formula

$$j_s = \int_{-\infty}^{\infty} \alpha n^2 dx,$$

where n is the positive ion concentration.

If the rate of ion generation is constant, then, ignoring diffusion,

$$dn/dt = J/e - \alpha n^2,$$

where J is the rate of generation of current per unit volume,

so that J/e is the number of ion pairs generated per unit volume per unit time.

If the ionization commences at $t = 0$ then

$$n = 0 \text{ at } t = 0$$

$$t = \frac{1}{2(J\alpha/e)^{\frac{1}{2}}} \ln \frac{1 + (e\alpha/J)^{\frac{1}{2}} n}{1 - (e\alpha/J)^{\frac{1}{2}} n}.$$

For large values of t : $n = (J/e\alpha)^{\frac{1}{2}}$

$$J = n^2 \alpha e$$

$$\alpha \propto n^2 \quad (2)$$

For small values of t : $n = Jt/e$

$$J = ne t$$

$$\alpha \propto n \quad (3)$$

The time taken to reach equilibrium is of the order of $ne/J = (\alpha n)^{-1}$, putting $J = n^2 e \alpha$. For longer times equation (2) can be used, and for shorter times equation (3). Thus for high ion concentrations or comparatively slow changes $J \propto n^2$. For low ion concentrations and fast changes $J \propto n$. In most cases the maximum rate of ion generation can be taken to be proportional to the square of the maximum ion concentration.

CHAPTER FOUR.

AIMS AND SCOPE OF PRESENT WORK.

4.1. Reasons for the Investigation.

As shown in Ch. II it is often desirable to know the amount of ionization in flames. Some actual and potential applications, eg. flame ionization detectors used for analysis, require a precise knowledge of the value of the saturation current, and others, eg. M.H.D., a knowledge of the electron or ion concentrations. The prevailing ion concentration results from a balance between ion generation and ion recombination. Thus the more fundamental quantity is the saturation current, which is the maximum available current and represents the rate at which ions are produced by the flame.

Most potential application of flame ionization require high ion concentration or high available currents for maximum efficiency. For applications requiring the maximum current density which can be drawn without breakdown, the saturation current density should not be less than the breakdown value, $\frac{1}{2} \epsilon k E_p^2 / a$. For these reasons it is important to obtain information on ionization in flames, in particular to know whether the saturation current is sufficient to give the maximum practical effect.

It is desirable to know the saturation currents for a large range of flames, in order to select the most suitable flame for any application, eg. to select the flame with the lowest fuel throughput or lowest final flame temperature which will give sufficient current. Moreover, investigation of flame ionization and its mechanism by means of saturation current measurements may throw light on fundamental ionization processes and may lead to the discovery of more efficient ways of producing and controlling ionization, and to a better understanding of processes affected by the ionization, such as the nucleation and growth of soot particles in flames. In addition, flames are a convenient medium for measuring the reaction rates of ion reactions in general (Calcote, 1965).

4.2. Aims of Present Work.

The aim of the present work is to obtain information on available currents for a large variety of flames, to find how this varies with the factors concerned, and where possible to draw conclusions about the mechanism and kinetics of the ionization process.

The method of measuring saturation currents was chosen because as mentioned above they provide a fundamental measurement of the rate of reaction that, unlike ion

concentrations, is independent of both charge exchange and the recombination process. In addition this quantity is that required for many practical purposes. Another advantage of the technique is that because current measurements can be taken quickly, a wide coverage is possible. This is especially valuable when dealing with many additives.

The use of alternating and transient fields was considered because it was thought that it might be possible to draw larger ion fluxes from the flame by this means. The maximum current that can be drawn in a steady state d.c. system is limited by the space charge, which ultimately causes breakdown at the electrodes. With an alternating field there would be ions of each sign present on each side of the flame. This would tend to reduce the net space charge and might permit larger ion fluxes to be drawn from the flame without breakdown at the electrodes. Transient d.c. fields also have apparent advantages. Thus, before any field is applied there is no net space charge outside the flame, so that when a voltage is suddenly applied it is possible to draw a large current from the flame initially. It was thought that it might be possible by means of these methods to measure saturation currents in excess of the maximum space charge limited current in the steady state d.c. case and the investigation of this possibility was one of

the aims of this project.

4.3. Measurements Made.

The conduction of charge in the flame products and the possibility of continuing ion generation above the flame were investigated. This is necessary to establish the validity and feasibility of the proposed method of measuring the total rate of ion generation in the flame and to assess the feasibility of possible applications and the probable behaviour of flame gases subjected to applied fields. Measurements were made of the variation of current with applied voltage and electrode separation and estimates made of ion mobilities.

Flames containing hydrocarbons were investigated and saturation currents measured over a wide range of reactant composition and of final flame temperature. Measurements were mostly at atmospheric pressure, but some were at lower pressures. Lean, rich, and sooting premixed hydrocarbon/air flames were investigated. Rates of generation of charge in the luminous gases above sooting flames were measured. Several hydrocarbons were used. Work was also done on premixed flames with oxygen and on diffusion flames. Measurements were made on pure carbon monoxide and hydrogen flames and on flames of these gases with small amounts of hydrocarbon added.

Hydrocarbon flames with hydrogen, carbon monoxide, or nitrogen added were studied. The effects of some other additives of interest were also investigated, principally carbon dioxide, bromine, and some metallic salts. The hydrocarbon fuels used were methane, ethane, propane, and ethylene. The final flame temperatures of the premixed hydrocarbon flames ranged from about 1450°K to about 2100°K .

Carbon monoxide and hydrogen were added in small quantities to some premixed hydrocarbon flames to see how these gases affect the saturation current. It was hoped to deduce from their effect whether the ionization occurred before or after the oxidation of carbon monoxide in the flame (see Ch. VII).

Many premixed flames were burnt with oxygen instead of air, to find the effect of dilution with nitrogen. Also it was thought that the results for flames with oxygen might be easier to interpret theoretically since the oxygen concentration is more nearly constant through the flame. By the use of oxygen flames a wider range of fuel concentrations can be investigated.

Carbon dioxide is produced in large concentrations by all hydrocarbon flames. This gas was therefore added to some flames to study its effect.

Metallic salts were added to some flames to test

the theory that the boost in metal ion concentration given by hydrocarbon addition to seeded flames is due to charge transfer (see Ch. I), in which case the total saturation current should be equal to the sum of that due to thermal ionization alone and that due to chemi-ionization without seeding.

Bromine and methyl bromide were added to some flames. Halogen containing compounds are commonly used as flame inhibitors. Since they have high electron affinities (Creitz, 1961), these substances were added to see if they also affect the flame ionization. If flame ionization is catalyzed by free electrons as suggested by Von Engel & Cozens (1965) the addition of electronegative substances, which reduce the concentration of free electrons (King, 1962), should cause a reduction of the saturation current.

The reactant compositions and final temperatures of the premixed flames were measured and the variation of saturation current with temperature and composition obtained. Effective activation energies for the ionization process were calculated from the results. The variation of the saturation currents of diffusion flames with the variables involved, in particular the fuel flow rate, was also investigated. The mechanism and kinetics of the ionization process was also considered.

PART II. METHOD.

CHAPTER FIVE.

THE PRINCIPLE OF THE STEADY STATE D.C. SATURATION
CURRENT METHOD.

5.1. Method.

In the present work rates of ion generation were studied using the steady state d.c. saturation current method employed by Lawton & Weinberg (1964). In this technique the flame is situated between two electrodes between which a d.c. field is applied and the maximum current obtainable from the flame without secondary ionization is measured.

5.2. Possible Sources of Error.

For the saturation current method to give accurate unambiguous results it is necessary that:

- 1) no breakdown or secondary ionization occurs above the flame;
- ii) no electron emission from the electrodes occurs;
- iii) the total rate of ion generation in the flame and the saturation current are not altered by the field.

5.2.1. Secondary Ionization.

Secondary ionization and breakdown occur when the

field at any point reaches the breakdown strength of the gas. The field increases with distance from the flame. The electrode separation should therefore be kept as small as practicable. When secondary ionization occurs the current increases rapidly for any further increase in potential. All current measurements must therefore be taken at a potential where the current has reached its maximum value but does not increase appreciably for a small increase in applied potential.

5.2.2. Electron Emission from the Electrode.

Thermionic emission of electrons could occur from the electrodes if they were sufficiently hot. It has been suggested that electrons can be emitted also from cold electrodes in seeded flame products (Turcotte & Friedman, 1965). It is unlikely that this cold cathode emission occurs in unseeded flames. Moreover most saturation current measurements on premixed flames were taken with the burner negative, for the reasons given in Ch. VIII, in which case, because the electrode immersed in the flame products is the anode, the current cannot be affected by electron emission from it. If there were any appreciable amount of electron emission from either electrode this would be shown by the saturation currents depending on the polarity of the burner, which was not found to be the case.

5.2.3. Influence of Applied Field.

The total rate of ion generation in non-sooting flames should not be appreciably altered by an applied field unless the flame as a whole is, which is unlikely. The rate of ion generation in the reaction zone itself is not likely to be altered greatly since its thickness is insufficient for the ions and electrons within it to acquire very much energy from the field. If there is any effect due to the field on the rate of ionization in the flame then the saturation current should vary with the field and polarity. Lawton & Weinberg (1964), using non-sooting premixed flames, found no such effect. The current reached a constant value beyond a certain potential. There is no conclusive evidence that electric fields have any chemical effect on flames, even after many experimental studies. The wind effect can be made negligible.

Diffusion flames which are not fully stabilized (ie. flames the position of which is not fixed by a surface on which they burn, or aerodynamically) are more likely to be affected physically by a field induced wind (Payne & Weinberg, 1959; Nakamura, 1959), in which case the current is likely to be dependent to some extent on the strength and polarity of the field. Whether this is so should be investigated.

In the case of sooting flames the field alters the carbon particle concentration (Place & Weinberg, 1966). However, the saturation current is not greatly affected by the field polarity.

If the current does not reach a completely flat plateau as the voltage is increased but continues to increase slowly until the onset of secondary ionization, then the current can be measured at fixed voltage intervals and the rate of ionization taken at the point where the current increases least for a given voltage increase.

5.3. Ion Generation Above the Reaction Zone.

If there is an appreciable rate of ion generation above the reaction zone then the saturation current will be a function of the electrode separation. This gives a means of studying rates of ion generation above the reaction zone. Ionization is likely to occur above the reaction zone of sooting flames. Appreciable ionization is less likely to occur above non-sooting flames. It was considered necessary nevertheless to check whether the saturation current varied with the electrode separation for the flames investigated.

CHAPTER SIX.THE PRINCIPLE OF A.C. AND TRANSIENT D.C. MEASUREMENT
OF SATURATION CURRENT.

The use of alternating and transient fields is a possible alternative to the constant field method of measuring rates of ion generation which was used by Lawton & Weinberg (1964) as discussed in the preceding chapter. Alternating fields would extract ions of each sign from the reaction zone into the gas on either side. The net space charge density would be low, so that it might be possible to draw any ion flux density at lower applied voltages. The current that can be drawn in the d.c. case is limited by the space charge built up on either side of the reaction zone. If a transient voltage is applied it will be possible to draw a large current initially before any space charge has built up. Thus by the use of alternating or transient fields it may be possible to obtain larger ion flux densities from flames and to measure higher rates of ion generation than is possible by applying a constant d.c. field. It is also of interest to know what change if any is produced in the mean ion flux and ion distribution when an a.c. field is applied. For these reasons the theory of a.c. and transient fields was developed.

6.1. Alternating Currents.

When considering alternating currents it is necessary to distinguish between ion flux and current. The current observed is that in the external circuit to the electrodes. The current between the electrodes can result from the capacitance and from ions moving backwards and forwards, as well as from the net movement of ions to the electrodes.

6.1.1. Simplified Theories.

i). Thomson and Thomson(1928) give a simplified theory for an a.c. field applied to a flame. They assumed that the electrons oscillate as a cloud of constant thickness about the reaction zone while the positive ions remain stationary.

ii). The charges in a flame subject to an a.c. field can be considered to consist of two blocks of uniform ion density, n , and opposite charge oscillating in opposite directions about the reaction zone. Let the blocks extend distance l from the reaction zone at the maximum of each oscillation. Then $l = 2 \times 2^{\frac{1}{2}} E_{\text{rms}} k/w$ where k is the ion mobility, and w the angular frequency of the field. On average the ions are in the presence of charge carriers of the opposite sign for 0.363 of the time. Recombination occurs during this time. The total rate of ion recombination

per unit area is therefore $0.363 \propto n^2 l = 1.03 \propto n^2 E_{\text{rms}} k/w$. This is equal to the total rate of ion generation.

6.1.2. Effect of Space Charge.

The above simplified theories do not take into account the space charge field due to the ions. This is often of the same order as the applied field. It tends to cause the ion cloud to spread out and it should be taken into account.

If all the ions have the same mobility, k , then the net ion flux at any point x , is equal to $kE(n_+ - n_-)$.

$$\epsilon dE/dx = (n_+ - n_-)e.$$

$$\begin{aligned} \text{Therefore} \quad f &= \frac{\epsilon k E}{e} \frac{dE}{dx} \\ &= \frac{1}{2} \frac{\epsilon k}{e} \frac{d^2 E^2}{dx^2}. \end{aligned}$$

The ion concentration decreases with distance from the flame due to recombination. Also, while the ion concentration at the flame is high, that at the electrodes is low since the average ion concentration near the electrodes for a given field and ion flux must be of the same order as in the d.c. case as at no point in the cycle are ions of each sign present simultaneously there. As a result of the decrease in ion concentration the gas conductivity decreases and E_{rms} therefore increases with increasing distance from

the flame. The mean net ion flux is equal to $\epsilon k (2e)^{-1} (dE_{\text{rms}}^2/dx)$. Thus an a.c. field causes an ion flux away from the flame.

If there is no recombination then the ion flux must be constant outside the flame (assuming ion generation occurs only in the flame). dE_{rms}^2/dx is then constant and E_{rms}^2 increases linearly with distance from the reaction zone, as in the d.c. case.

The case where the mobilities of the positive and negative charges, k_+ and k_- respectively, are constant but not necessarily equal to each other will now be considered:

$$\text{positive ion current, } j_+ = n_+ k_+ E e, \quad (1),$$

$$\text{negative particle current, } j_- = n_- k_- E e. \quad (2),$$

where n_+ , n_- are the respective particle densities.

$$\text{Ion flux density, } f = (j_+ - j_-)/e \quad (3),$$

$$\text{current density, } j = j_+ + j_- \quad (4).$$

$$\text{Therefore, } j_+ = \frac{1}{2}(ef + j) \quad (5),$$

$$j_- = \frac{1}{2}(ef - j) \quad (6).$$

From Gauss' Law:

$$\epsilon dE/dx = (n_+ - n_-)e.$$

Substituting for n_+ , n_- from (1) and (2):

$$\frac{dE}{dx} = \frac{1}{\epsilon E} \left(\frac{j_+}{k_+} - \frac{j_-}{k_-} \right).$$

$$\text{Therefore } \frac{dE^2}{dx} = \frac{2}{\epsilon} (j_+/k_+ - j_-/k_-) \quad (7)$$

$$\frac{dj_+}{dx} = -\frac{dj_-}{dx} \quad (8), \text{ from (4),}$$

$$= -\propto n_+ n_- e \quad (9).$$

Therefore
$$\frac{d^2 E_{\text{rms}}^2}{dx^2} = \frac{2}{\epsilon} \left(\frac{1}{k_+} + \frac{1}{k_-} \right) \frac{dj_+}{dx}, \text{ from (7) \& (8),}$$

$$= -2(k_+^{-1} + k_-^{-1}) n_+ n_- e / \epsilon, \text{ from (9).}$$

A more general form of this equation was derived by Thomson & Thomson (1928) for the d.c. case.

Substituting for j_+ , j_- in (7) from (5) and (6):

$$dE^2/dx = (k_+^{-1} + k_-^{-1})ef/\epsilon + (k_+^{-1} - k_-^{-1})j/\epsilon \quad (10).$$

At higher frequencies and/or low ion densities, it is necessary to take into account the displacement current, giving

$$dE^2/dx = (k_+^{-1} + k_-^{-1})ef/\epsilon + (k_+^{-1} - k_-^{-1})(j/\epsilon - dE/dt).$$

$\bar{j} = 0$, assuming that the field and current are the same on both sides of the flame.

Therefore
$$dE_{\text{rms}}^2/dx = (k_+^{-1} + k_-^{-1})e\bar{f}/\epsilon \quad (11)$$

It has been assumed that k_+ , k_- are constant. In most cases a large part of the negative charge is carried by electrons. k_- is then the resultant effective negative particle mobility, which is much greater than k_+ , and varies with distance because of electron attachment.

It is assumed above that the frequency of the a.c. field is much less than the collision frequency of the charges. Otherwise they will not have time to attain their terminal velocities. The collision frequency of electrons in flames is about $8 \times 10^{10} \text{ s}^{-1}$; that of ions is believed to be of the order of 10^8 s^{-1} (Borgers, 1965). It is also assumed that the charges do not move far during each cycle and that n_+ , n_- do not depart greatly from their mean value.

Because the ion concentrations are higher with a.c. than with d.c. fields the results could be substantially affected by the flow velocity. This effect has been ignored.

6.1.3. Discussion.

Alternating fields can be used to spread the charge produced in a flame over a large volume. This process could be used to increase the number of ions present by reducing the rate of recombination. Since ion generation occurs mainly or only in the reaction zone, the use of alternating fields to draw ions out of flames could be used to investigate rates of recombination.

The ion flux density at any point is given by:

$$\begin{aligned} \bar{I} &= \frac{\epsilon}{e} \left(\frac{1}{k_+} + \frac{1}{k_-} \right)^{-1} \frac{dE^2}{dx} \text{rms} && \text{from (11)} \\ &= \frac{k \epsilon}{2e} \frac{dE^2}{dx} \text{rms} && \text{when } k_+ = k_- = k. \end{aligned}$$

In the d.c. case, $f = \epsilon k_{\pm} / (2e) (dE^2/dx)$.

The maximum ion flux that can be drawn is limited by the maximum field attainable without breakdown. Thus it can be seen that a.c. fields do not in general permit the extraction of greater ion fluxes than d.c. fields. The average magnitude of the field is less than the maximum value. Moreover, the breakdown strengths of gases in a.c. fields tend to be lower than in d.c. fields (Meek & Craggs, 1953).

6.2. Transient Currents.

6.2.1. Experimental Results.

The transient current on suddenly applying or removing an external field across a flame was observed on a cathode ray oscilloscope. The flame was burnt on a Botha-Spalding burner similar to that used by Lawton & Weinberg (1964). The field was removed by shorting out the voltage source (a 9-volt battery in series with a 10^6 ohm resistance). The current was observed by feeding the voltage drop across a 10^7 ohm resistance into the CRO. A detailed trace was obtained. The trace when the field was removed was a series of decreasing peaks in alternate directions. The trace when the field was applied was less regular, consisting of a series of maxima rapidly decaying to the steady state value.

6.2.2. Discussion.

The purpose of studying transient conditions was partly an attempt to circumvent the space-charge limitation on steady-state saturation current measurements. It was thought originally that the initial current, until the space charge built up, would be the saturation current, even for a low applied voltage, giving a convenient method of measuring the saturation current, which would not be subject to the breakdown limitation. An estimate of the quantities involved shows that the initial current is primarily due to the charge initially present in the flame (the equilibrium charge).

The ion concentration downstream of the reaction zone is given by $dn/dt = \alpha n^2$, where n is the concentration of ions of each sign. Integrating this gives the number of ion pairs per unit area in the distance in which the ion concentration halves to be $\alpha^{-1} u \ln 2$. The minimum number of ion pairs per unit area is thus of the order of $\alpha^{-1} u \ln 2$, which, taking $u = 1 \text{ m s}^{-1}$, $\alpha = 10^{-13} \text{ m}^3 \text{ s}^{-1}$, is approximately 10^{13} m^{-2} . Wortberg (1965) found there to be approximately 3×10^{13} ion pairs per m^2 . The field necessary to extract these ions is equal to $3 \times 10^{13} \text{ e}/\epsilon$, which is 0.6 MV m^{-1} . Thus the field necessary to remove the equilibrium charge is approaching the same order as the

maximum field (3 MV m^{-1}) which can be applied in the steady state case. The use of transient currents therefore does not appear to offer any very great advantage in overcoming the breakdown limitation. The method is more complicated than the steady state method. It would be further complicated by the short time periods involved and the capacitance between the electrodes. For these reasons the steady state current was used for all subsequent measurements.

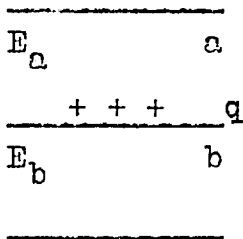
The transient current could be used to investigate the equilibrium charge or the mobilities of the charged species, but the method would be much more complicated than steady state measurements.

It is interesting to consider what current flows when the applied field is removed and the electrodes are both earthed. The average field between the electrodes is zero. Thus there is an external field due to image charges which has a value equal and opposite to the average space charge field. For example, if all the charge is close to one electrode it can be shown that the external field will be such as to drive the charge into that electrode.

The flame can be considered as a source of electrons of effectively infinite mobility. In this case the field at the flame must be zero. Consider the case where there is initially a region of positive space charge

outside the flame. Some electrons will be drawn out of the flame leaving a positive space charge at the flame. The original positive space charge and that induced at the flame start to move in opposite directions. As the original charge travels to the electrode more space charge is induced at the flame and the process is repeated. A series of current peaks in opposite directions results. This was observed on the cathode ray oscilloscope.

Consider a layer of space charge, with charge q per unit area, between two electrodes, as shown in the diagram. The fields, E_a , E_b , are given by:



E_a a

+ + + q

E_b b

—————

$$E_a = E_b + q/\epsilon, \text{ from Gauss' Law,}$$

where a , b are the distances to the electrodes.

Potential difference between the electrodes = $aE_a + bE_b$
 = 0 for no applied potential.

$$\text{Therefore } E_a = qb(a+b)^{-1}/\epsilon \quad (12),$$

$$E_b = qa(a+b)^{-1}/\epsilon.$$

The current density observed is $\epsilon(dE/dt)$ where E is the field at one electrode, given by equation (12). The observed current density is therefore equal to qv divided by the electrode separation, where v is the velocity of the charge. Thus the current recorded in transient measurements is not the rate at which charge arrives at the electrodes,

which can make interpretation of the results more difficult.

6.3. Summary.

It has been shown that alternating current measurements and transient direct current measurements give little if any advantage over the steady state d.c. method for measuring saturation current densities. For this reason all saturation current measurements were taken using the steady state d.c. method.

CHAPTER SEVEN.FLAMES AND BURNERS.

Flames are fast exothermic reactions, which usually occur at high temperatures, although "cool flames" can occur with final temperatures between 200 and 400°C (Gaydon & Wolfhard, 1960). Flames can exist over a wide range of pressures (Fristrom & Westenberg, 1965) and compositions.

The reaction zone of flames is a region of very high gradients of temperature and composition and very rapid and intense chemical reaction, sometimes accompanied by marked disequilibrium (Weinberg, 1966b). This makes the detailed study of flame kinetics very difficult. For this reason and because for most practical purposes it is not necessary to understand flame mechanisms in detail, it is only recently that the structure of flames has been extensively studied, and the processes involved are still only incompletely understood.

Flames can be propagating or stationary, depending on whether the reactants are initially stationary or whether they flow from a burner at an appropriate velocity.

This work is concerned with stationary flames of common gaseous fuels, with air or oxygen, mostly at atmospheric pressure. These flames are the easiest to

obtain and take measurements on and they include those types which are of most practical importance.

Flames can be divided into two main classes, premixed flames and diffusion flames, depending on the initial state of mixing of the reactants. In premixed flames the reactants are initially perfectly mixed. In diffusion flames the reactants are initially separate and mix in the reaction zone. Flames intermediate between premixed flames and diffusion flames can be obtained (Fristrom & Westenberg, 1965). Flames can be usefully subdivided according to whether the gas flow is laminar or turbulent.

7.1. Premixed Flames.

In premixed flames the reactants are mixed on a molecular scale before entering the front and the flame moves relative to the reactants. It consists of a preheat zone, a reaction zone, and products. The flame speed is limited by the reaction rate and the transport processes and depends on the initial composition of the reactants and the final flame temperature.

Most commonly used types of premixed flames are basically free burning and very nearly adiabatic. They have low heat loss and over most of their area are not close to any surface.

7.1.1. Flat Non-Adiabatic Premixed Flames.

For the present work, flat non-adiabatic flames, stabilized by heat loss to the burner, were used. This type of premixed flame has often been used for experimental purposes (eg. Kaskan, 1957). The flame is stabilized, by heat loss to the burner surface, a short distance downstream of a flat porous plug through which the reactants pass (see Fig. VII (1)). The flame burns at that distance from the burner at which the burning velocity is equal to the flow velocity of the reactants. If the flame moves closer, the increase in the heat loss decreases the burning velocity so that the flame moves back to the equilibrium position. The principle of this type of flame is discussed by Botha & Spalding (1954). The burners used are described in Ch.IX.

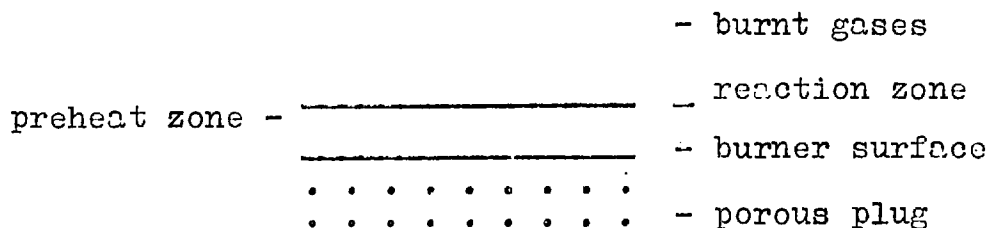


Fig.VII(1).

Flat non-adiabatic premixed flames stabilized downstream of a cooled plug were used for the present work for the reasons discussed below:

- i) the variation of the saturation current density, j_s , with the final flame temperature, T_f , is needed to

obtain the effective activation energy of the ionization reaction. By the use of this type of flame, T_f can be altered independently of the reactant composition by varying the flow velocity. This method clearly is preferably to varying T_f by dilution, since this alters the composition as well as T_f ;

- ii) the saturation current density of adiabatic flames, if too high to measure directly by the saturation current method because of the breakdown limitation, can be obtained by extrapolating values for non-adiabatic flames;
- iii) the flame burns very close to the surface of the burner so that high current densities can be obtained before breakdown by utilising electron conduction in the hot products and ion conduction in the cold reactants;
- iv) the flames obtained by use of a suitable burner are flat and of reasonable size and uniform;
- v) the area of the flame is constant and easily determined;
- vi) the flame is easily stabilized a short distance from the burner. Its position is then fixed and known within narrow limits. The shape and position of the flame are not appreciably altered by the wind effect;
- vii) the reactants of these flat flames being premixed gases effectively avoids the presence of easily

ionizable impurities such as metallic salts. All common substances which give appreciable ionization at the flame temperatures used (up to about 2100°K) are solids with negligible vapour pressures at room temperature. Since all the reactants pass through the flow system and the disc, solid particles would tend to be filtered out;

- viii) the gaps between the particles of which the discs used were composed were very small, which prevents the flame flashing back and causing an explosion;
- ix) any premixed flame is completely defined by the initial composition and the final flame temperature, because the final flame temperature is a function of the burning velocity and the reactant composition only (Botha & Spalding, 1954), and does not depend appreciably on the surface temperature of the disc (Yumlu, 1959). A flame of fixed composition can therefore be defined by one variable only. This makes presentation and analysis of the results much easier.

To measure j_s versus T_f at constant composition it is necessary to quench the flame. In order to obtain information about ordinary flames it is desirable that the processes occurring in quenched flames are similar to those in unquenched flames and that the variation of j_s with

temperature is due to the change in temperature and not the change in the amount of quenching or loss of radicals to the disc. Although quenching and pre-cooling are different processes, the loss of heat to the burner surface appears to be equivalent to pre-cooling the reactants. Slight quenching should have the same effect as pre-cooling. This assumption was made by Kaskan (1957) and by Botha & Spalding (1954).

7.2. Diffusion Flames.

In diffusion flames the reactants are initially separate and have to mix in order to burn. The reactants diffuse into the reaction zone from opposite sides. The rate of reaction is primarily diffusion limited. Diffusion flames are discussed by Gaydon & Wolfhard (1960, Ch.VI) and by Sternberg et al (1962), amongst others.

The reaction occurs close to the stoichiometric surface between the reactants. This is the surface at which in the absence of combustion the reactants would be in stoichiometric proportions. The reactant concentrations at the reaction zone are low and almost no reactant passes through the reaction zone without being consumed. Before reaching the reaction zone, the fuel is preheated in the absence of oxidant. This preheating can last for a

comparatively long period since the fuel has to reach the reaction zone by diffusion. In the case of hydrocarbon fuels, pyrolysis usually occurs on the fuel side of the flame, resulting in soot formation and yellow luminosity.

Diffusion flames are more convenient for most practical purposes than premixed flames and are safer in view of their immunity from a flash back. Moreover, diffusion flames can be used for reactants which are too reactive to be premixed.

Diffusion flames have no burning velocity and the history of the reactants does not depend only on their initial composition but also on the aerodynamics, geometry, and size of the system.

Most diffusion flames used in practice are partially premixed or have a small region which is premixed. This assists in the stabilization of the flame.

The most common type of diffusion flame is that on cylindrical burner ports. These are often partially premixed, as in the bunsen flame. Partially premixed turbulent diffusion flames stabilized in combustion chambers have many important applications, including jet engines and gas turbines. It is possible to obtain flat diffusion flames, such as those given by the Parker & Wolfhard burner (Wolfhard & Parker, 1949), and flat counter-flow diffusion

flames (Pandya & Weinberg, 1963). Flat flames have been used for research purposes. A diffusion flame usually forms where the products of a reaction containing excess fuel comes into contact with the surrounding air.

Diffusion flames are used industrially more than premixed flames but they have been studied less in fundamental research because they are less amenable to theoretical analysis. In particular their structure is more complicated. As shown above, diffusion flames differ from premixed flames in a number of respects. Although some measurements have been taken on ionization in diffusion flames (Kinbara & Nakamura, 1955; Place & Weinberg, 1966; Pejack & Jones, 1968) most saturation current measurements on flames have been on premixed flames (Lawton & Weinberg, 1964). For this reason and because of their importance practically it was felt that measurements should be taken of the saturation currents of some diffusion flames.

Although free burning diffusion flames are liable to be affected by applied fields (Payne & Weinberg, 1959) measurements were made on these flames since it is precisely the saturation currents of flames disturbed by fields which are most likely to be of interest for practical purposes.

7.2.1. Types of Diffusion Flame Used.

Measurements were made on "batswing" flames and on circular flames produced by directing a jet of fuel vertically upwards against a horizontal plate. The latter were reasonably flat and consisted of a single layer; a field could be applied between an electrode beneath the flame and the plate above it, when the flame was disturbed comparatively little. The "batswing" burner gives a thin flame with a large area, and electrodes can be placed close together on either side of the flame, although the flame is liable to be affected by the field. Because of their large areas and the small electrode separations which can be used, the circular flame described and the "batswing" burner are likely to permit the measurement of high saturation currents before breakdown. Measurements were also taken with flames on nozzles (cylindrical burner ports) because these are most representative of practical diffusion flames. The saturation current and rate of fuel consumption were also measured for a candle flame.

Measurements were taken with the flat counter-flow diffusion type of flame used by Pandya & Weinberg (1963). Flames of this type seem ideally suited to investigating the saturation currents of diffusion flames. They have the following advantages:

- i) the flame is likely to be less affected by the applied field since its position is closely determined by the aerodynamics of the opposed jets;
- ii) because the flame is flat the electrode separation can be made small, permitting high currents to be drawn;
- iii) the flame being a single layer reduces the likelihood of breakdown and secondary ionization;
- iv) the area of the flame is easy to measure;
- v) the incident fuel and oxidant fluxes are known;
- vi) since the flame does not usually touch the electrodes the effect of quenching is small and the risk of shorting or of emission from the electrode is minimized;
- vii) by the use of the counter-flow diffusion burner it is easier to burn diffusion flames with oxidants other than air;
- viii) if required, the variation of the saturation current density over the flame could be measured by the use of an insulated probe in one of the electrodes.

7.2.2. Determination of Factors Affecting the Saturation Current.

In order to elucidate the effect of all possible factors it is important to measure the variation of the saturation current with all the variables, in particular

electrode separation and configuration, burner size, flow velocities, and gas composition. It is also necessary to measure the current at several voltages and to check the effect of reversed polarity.

It was attempted to determine the effect of flame size and shape on the saturation current. The variation of saturation current with fuel flow was measured. Flame areas at zero applied voltage were also measured.

The saturation currents of diffusion flames are for the whole flame rather than for a unit area, since the saturation current per unit area is likely to vary with position in the flame. A calculated saturation current density would therefore be an average over the whole flame.

7.3. Fuels Studied.

The fuels used were certain representative hydrocarbons, carbon monoxide, and hydrogen. The oxidant was air or oxygen. The first three members of the paraffin series and an olefin (ethylene) were investigated to obtain the effect of the carbon number and structure of the fuel molecule. The gases taken are easily obtainable and commonly used.

Acetylene was not fully investigated because this gas forms an explosive compound (cuprous acetylide) with copper. Copper and brass were used in the flow system and

burners. The formation of cuprous acetylide might have led to ignition of the premixed gases in the flow system. However, a few measurements were taken with an acetylene diffusion flame on a quartz nozzle using a flow system containing no copper.

Hydrocarbon combustion appears to occur in two stages (Burgoyne & Hirsch, 1954; Friedman and Nugen, 1959; Scheller & McKnight, 1959), reaction to H_2O and CO , and then the oxidation of the CO to CO_2 . The temperature at which the first stage is substantially complete will be designated T_{CO} and the final flame temperature T_f . Carbon monoxide and hydrogen were added in small quantities to some premixed hydrocarbon flames in order to alter T_{CO} and T_f independently. The addition of CO might be expected to increase T_f without affecting T_{CO} appreciably, while by the substitution of hydrogen for carbon monoxide it is in principle possible to alter T_{CO} without altering T_f . It is stated by Chase & Weinberg (1963) that the kinetics of a reaction occurring during the oxidation of the hydrocarbon to CO and H_2O should depend on T_{CO} and not T_f . Varying T_{CO} and T_f independently ought to show whether the ionization occurs at T_f or T_{CO} .

Small quantities of other additives were added to some flames, as discussed in Ch.IV.

CHAPTER EIGHT.CONDUCTION TO THE ELECTRODES.

8.1. Discussion.

The total rate of charge generation in flames was measured by determining the saturation current from each flame to electrodes placed on either side. Although convection and diffusion occur to some extent, the charge is carried to the electrodes primarily by the field. It is thus necessary to investigate conduction to the electrodes in order to design a suitable system.

Most potential applications of flame ionization depend on the behaviour of the charge in an electric field, i.e. on the mobility. Where high currents are required it is necessary to have a high mobility in order to limit the voltage and power requirements and to avoid breakdown. Applications depending on the force exerted by the field on the gas give the maximum effect for a given current if the mobility is low. It is of interest therefore to know the behaviour of charges in the flame gases.

It may be desired to measure the saturation current of part of a flame so as to investigate the variation with position in the flame of the saturation current per unit area, in order, for example, to avoid edge effects or to

increase the accuracy of the flame saturation current measurements by confining them to the most uniform part of the flame only. This can be done by having a separate electrode or probe which collects the current from just part of the flame. It is necessary to know the area of the flame from which the current flows to such a probe or the proportion of the total current collected. The lines of current flux will not generally be parallel, because space charge tends to make tubes of current diverge. Cooling of the flame gases near the periphery may decrease the charge mobility and thereby cause the current to converge into the region of high temperature, where the mobility is highest. Another factor to be considered is variation of the gas composition, in particular the presence of any impurities.

Magnetic fields can be ignored since the currents are low compared with the net charge present.

8.1.1. Solution for Charge of Constant Mobility.

In the presence of a flow velocity u and with ions of one sign only present

$$j = ne(kE + u)$$

From Gauss' law, $ne = \int \rho dx$ in the one-dimensional case.

Therefore $j = \epsilon kE' dE'/dx,$

$$\text{where } E' = E + u/k$$

$$= 0 \text{ at } x = 0 \text{ for subsaturation,}$$

$$\begin{aligned} \text{whence } E' &= (2j/\epsilon k)^{\frac{1}{2}} x^{\frac{1}{2}} \\ E &= (2j/\epsilon k)^{\frac{1}{2}} x^{\frac{1}{2}} - u/k \\ V &= (2/3) (2j/\epsilon k)^{\frac{1}{2}} x^{3/2} - ua/k. \end{aligned}$$

The last equation shows that a current can be obtained even at negative applied voltages. This is the principle of the electrohydrodynamic generator.

Ion mobilities in flames are of the order of $0.0017 \text{ m}^2 \text{V}^{-1} \text{ s}^{-1}$ (see below). The flow velocity is usually of the order of 1 ms^{-1} or less and can therefore be ignored for fields greater than 10 kV m^{-1} . The general equations giving the field in the steady state are then:

$$\begin{aligned} \underline{j} &= k n e \underline{E} \\ \text{div } \underline{E} &= n e / \epsilon \\ \text{div } \underline{j} &= 0 \\ \underline{E} &= \text{grad } \phi \end{aligned}$$

In principle these equations can be solved for any electrode configuration. In practice it is normally necessary to make simplifying assumptions.

8.1.2. Divergence due to Space Charge.

It is usual to assume a one-dimensional field in calculating currents between two electrodes. This assumption can lead to errors. These errors are, however, not very serious if the electrode separation is less than half the flame width (Davies & Evans, 1967).

Consider an initially uniform narrow tube of charge of area A and radius r , subject to a field E and carrying a current i . Since the tube is narrow E_z , j , and n would not vary appreciably across it (E_z is the axial field).

$$\text{From Gauss' law, } \epsilon d(\Delta E_z)/dz = neA \quad (1)$$

where z = distance along axis.

$$i = kE_z neA \quad (2).$$

Substituting for neA from (1):

$$\epsilon d(\Delta E_z)/dz = i/(kE_z) \quad (3).$$

$$A = \pi r^2$$

$$\begin{aligned} \text{therefore } dA/dz &= 2\pi r dr/dz \\ &= 2\pi r E_r/E_z \end{aligned}$$

where E_r is the radial field.

From Gauss' law, $E_r = neA/(2\pi r \epsilon)$ approximately.

$$\text{Therefore } E_z dA/dz = neA/\epsilon$$

Substituting for neA from (2)

$$E_z dA/dz = i/(\epsilon kE_z) \quad (4)$$

$$= AdE_z/dz + E_z dA/dz, \quad \text{from (3).}$$

$$\text{Therefore } A dE_z/dz = 0.$$

$$\text{Therefore } E_z = \text{constant}$$

$$\text{and } A = A_0 + iz/(\epsilon kE_z^2) \quad \text{from (4).}$$

Thus for a narrow beam the field is constant and the area increases linearly with distance.

8.2. Currents to Probes.

In the cases envisaged in the present work it was thought that divergence might play a significant role. Because of the difficulty of obtaining mathematical solutions valid over the wide range of operations it was considered necessary to carry out an experimental investigation. The burner was one electrode. Another electrode was placed above the flame and parallel to the burner. Both electrodes were larger than the flame in order to give an approximately parallel field. The centre of the upper electrode consisted of an insulated probe. Details of the apparatus are given in Ch. IX. Measurements were taken of the total current to the upper electrode, i_t , and that to the probe, i_p . It was found that the ratio i_p/i_t tends to vary and is not always equal to the ratio of the probe area to the flame area. The value varies with applied voltage, and electrode separation.

Values of i_p/i_t were obtained for various electrode separations and with the burner positive and negative. The ratio of the probe area to the total area was 0.32 in one case. The mean value of i_p/i_t was approximately equal to this, although it tended to be higher with the burner negative, particularly at electrode separations above 30 mm. The value of i_p/i_t ranged from about 0.26 to 0.40.

Some measurements were made with the burner negative since this is the easiest way to measure saturation currents. It was found that the probe current tended to go through a maximum when the voltage was near the minimum required to draw the saturation current. As the voltage was increased the probe current reached a maximum and then decreased to a steady value of up to about 30% lower than the maximum. When the electrode separation was increased with a constant applied voltage the probe current reached a maximum of up to twice its value for low separations before decreasing. The total current decreased continuously. The region of hot gas above the flame became narrower with height, as could be seen by placing a wire across the gas stream and observing the shortening of the length which glowed as it was raised. The particle mobility would therefore be lower above the edge of the flame, which would tend to cause the current to converge towards the probe at larger electrode separations.

8.2.1. Effect of Flame Non-Uniformity.

Moving the upper electrode across the matrix burner used and measuring the probe current showed that the saturation current density was about 30% lower at the centre of the flame than near the edge. At higher applied voltages the field near the centre of the burner would

therefore have been higher, making the equipotentials convex with respect to the burner, which would tend to make the current converge downstream. The lower saturation current density near the centre of the matrix was probably due to the flame temperature being lower there. Because the matrix was hotter at the centre, the viscosity of the gas would have been higher there and the flow lower. It will be apparent from the results that a temperature difference of only 25 K would account for a 30% change in saturation current. In fact, the flame on the hot matrix could be seen to burn closer to the surface at the centre. The higher current at the edge of the matrix did not appear to be due to electron emission since the edge was not observed to be overheated and no current was obtained after the flame was extinguished. These results emphasise the importance of using a burner giving uniform flow and good heat conduction. The ratio i_p/i_t tended to a constant value at high applied voltages but was up to 50% lower at low voltages.

The variation of i_p/i_t with the stoichiometric ratio, ϕ , was measured for ethylene/air. The value was approximately constant up to $\phi = 1.1$ and then fell. This fall was due to ionization occurring in the secondary flame formed by the excess fuel burning in the surrounding air. This adds to i_t but not to i_p .

For ethylene/oxygen flames on a porous disc burner it was found that i_p/i_t was approximately equal to the ratio of the probe area to the flame area for very lean flames but that the value was up to about 50% lower for somewhat richer flames. The temperature and probe saturation current were measured across one flame ($\phi = 0.68$, $T_f = 1500^\circ\text{K}$). The temperature at the edge was found to be about 20 K higher than at the centre, and the current about four times as great. The low value of i_p/i_t for less lean oxygen flames thus appears to be due to the saturation current density being much greater near the edge, which might result from dilution with the surrounding air and from a resultant increase in the final flame temperature. Dilution of a non-adiabatic oxygen flame with air is likely to raise the temperature, since the burning velocity would otherwise be reduced, giving blow off.

8.2.2. Possible Methods of Making the Current more Parallel.

At higher voltages, the external field can largely overcome the space charge field and force the tubes of current to become more parallel. Measurements of the saturation current to the probe should be taken where possible at voltages at which the probe current has reached a constant value as the voltage is increased.

The use of an insulating chimney as a collimator

to make the current more parallel was considered. In equilibrium the current must travel parallel to its surface. This has been discussed more fully in Ch III in connection with ion photography.

The divergence of the current from the flame could also be reduced by making the upper electrode the same size and shape as the flame and/or having a series of insulating apertures which would restrict the divergence of the current.

Some measurements were made using an asbestos chimney around the flame gases between the electrodes. This arrangement gave a steadier probe current which was more uniform over a larger region. However, the use of a chimney was cumbersome. It was liable to conduct additional current between the electrodes. The improvement obtained was probably mainly due to reduced disturbance by draughts and reduced cooling of the gas above the flame, which could give a more uniform temperature distribution.

The flow and temperature distribution can be made more uniform by the use of an upper electrode consisting of a matrix which allows gas to pass through it, instead of a water cooled copper electrode as used initially. A matrix electrode can be run hot to reduce cooling of the gases. Such an electrode was constructed and was used for most of the subsequent measurements. It was confirmed that electron

emission did not take place from the matrix electrode when hot, by blowing out the flame and observing that no further current flowed.

The use of a pilot flame round the flame investigated, to render the current more parallel, was considered. Such a flame would increase the effective area of the burner and reduce edge effects. It is necessary to have a flame of sufficient size if measurements of the current from part of it are to be taken. The use of a pilot flame, however, would require the building of a special burner and careful matching of the main flame and the pilot flame. It did not appear that the advantages to be gained made the use of a pilot flame worthwhile.

It should be possible to make the current from the flame to the upper electrode more parallel by placing insulated wires or grids parallel to the electrodes. The equipotentials would have to be parallel to these wires and the field would therefore be perpendicular to them. An insulated wire was placed half way between the burner and the upper electrode. A slight reduction of the maximum in the current to the probe was obtained. The burner was negative and the inter-electrode separation 40 mm. Copper and platinum wires had similar effects. Several copper wires gave a greater effect. The excess of the maximum probe

current over that at higher voltages was reduced by about 40%. To make the current parallel might require several coarse gauzes, which would impede the passage of the current. It was found that the presence of wires in flames, particularly if contaminated, could greatly affect the current and its distribution. This effect is discussed below.

8.2.3. Variation of Probe Current with Height and Potential of Probe.

The probe in the centre of the water cooled copper upper electrode used for most of the earlier measurements could be raised or lowered relative to the rest of the upper electrode. The variation of the probe current with the probe height relative to the electrode was measured. It was found that each 0.1 mm vertical displacement of the probe altered the current by 4%. Thus it is necessary that the probe be positioned accurately. The measurements were taken with an applied voltage of 330 V and an electrode separation of 37 mm.

The variation of the probe current with the probe voltage relative to the rest of the upper electrode was investigated by placing resistances in series with the probe, measuring the current and calculating the probe voltage. Measurements were taken with the burner negative and an electrode separation of 37 mm. It was found that i_p was

reduced by about 0.06 μA for each volt on the probe. This result was obtained at three different voltages on the burner (90, 330, 440 V). A resistance of R ohms in series with the probe, which changes the probe voltage by $10^{-6} i_p R$ volts (where i_p is in microamps) therefore reduces the probe current by the fraction $6 \times 10^{-8} R$. Thus the reduction of the probe current due to the resistance of the microammeter (maximum resistance 2×10^4 ohms) was negligible.

8.3. Negative Conduction.

A considerable amount of work, both experimental and theoretical, has been done on the conduction of negative charge in gases (Loeb, 1955). Much of the experimental work, particularly that on electron attachment, has been performed at low temperatures and/or at low pressures and/or with additives, in particular alkali salts, to increase the ion concentration. Most of the work has been confined to pure gases. Since the quantities involved vary in a complex manner with particle energies and densities, these results cannot easily be applied to combustion products consisting of complex mixtures of gases at high temperatures and atmospheric pressure. Also, the gases downstream of a flame are not always in equilibrium, in particular radical concentrations and, in some flames, the electron temperature (Bradley & Matthews, 1967) tend to be too high.

Negative charge is carried in gases by electrons and negative ions. Since the mobilities of these differ by a factor of about 10^3 it is important for practical purposes to know what proportion of the charge is carried by each. The fraction of electrons in equilibrium increases with temperature. Investigating the conduction of negative charge gives a means of estimating the proportion of the charge carried by free electrons and how this varies with distance from the flame. It can also indicate whether the negative charge is produced at the flame as negative ions or as electrons. This is of interest in investigating the mechanism of the ionization.

Near the reaction zone there are more electrons than negative ions (Green, 1965). Further downstream some electrons attach to give negative ions. The ion-ion recombination coefficient is probably several times the ion-electron recombination coefficient (Gaydon & Wolfhard, 1960). Thus it is likely that an important process of electron loss in the flame products is electron attachment followed by ion-ion recombination (King, 1962). Ion-electron recombination also occurs (Green & Sugden, 1963). This may be the main recombination process in the region of high ion concentration near the reaction zone.

Electron decay downstream of flames has been

investigated by Williams (1962) and King (1962). Both found the decay to be first order. Positive ion recombination is second order (King, 1962).

When the burner is made the cathode the current above the flame is mainly by negative conduction with the current from the flame to the burner being due to positive ions. For sub-saturation currents the surplus positive ions are held back by the field and mainly recombine within a short distance downstream of the flame. The absence of positive ions farther above the flame is desirable to eliminate recombination and enable the electron/negative ion behaviour to be elucidated more easily, as proposed by King (1962). In particular the electron attachment frequency and the equilibrium electron concentration can then be estimated. In addition, potentially greater spatial resolution can be obtained by the measurement of the variation of field strength than by microwave or resonance methods.

8.3.1. Theory of Electron Attachment.

Assuming a one-dimensional system, the absence of positive ions, negligible flow velocity and diffusion, first order kinetics for the electron attachment and detachment, and given that the electron attachment frequency, ν_a , and the frequency of electron detachment, ν_d , do not vary with

position or field, it can be shown (see the Appendix) that

$$E \frac{d^2}{dx^2} (E^2) = \frac{2j}{\epsilon k_i k_e} (\nu_a + \nu_d) - \left(\frac{\nu_a}{k_e} + \frac{\nu_d}{k_i} \right) \frac{d(E^2)}{dx} \quad (5)$$

where x = distance from burner, E = field, j = current density.

From (5), $\frac{d(E^2)}{dx} = \frac{2j}{\epsilon} \frac{\nu_a + \nu_d}{\nu_a k_i + \nu_d k_e}$ at large x .

$$\begin{aligned} \text{Therefore } \frac{2j}{\epsilon} \frac{d(E^2)}{dx}^{-1} &= \frac{\nu_a k_i + \nu_d k_e}{\nu_a + \nu_d} \\ &= \text{constant} \\ &= k_- \end{aligned} \quad (6)$$

k_- is called the negative particle mobility by comparison with the case where there are particles of only one mobility, k , present, when

$$\begin{aligned} k &= j/(neE) \\ &= j (\epsilon EdE/dx)^{-1} \quad \text{since } dE/dx = 4\pi ne \\ &= 2j (\epsilon d(E^2)/dx)^{-1} \end{aligned} \quad (7)$$

From (6),

$$(\nu_a k_i + \nu_d k_e) = (\nu_a + \nu_d) k_-.$$

$$\begin{aligned} \text{Therefore } \frac{\nu_a}{\nu_d} &= \frac{k_- - k_i}{k_e - k_i} \\ &= n_e/n_i \end{aligned} \quad (8).$$

The results can be analysed approximately by assuming that all the space charge is due to negative ions (because $k_e/k_i = 10^2$ to 10^3 , so that comparatively small quantities of electrons can give rise to dominant currents),

when:

$$en_i = \epsilon \frac{dE}{dx} \quad \text{from Gauss' law,}$$

where n_i is the negative ion concentration.

$$j_i = en_i k_i E \quad (9),$$

where j_i is the negative ion current density.

$$\begin{aligned} \text{Therefore } j_i &= \epsilon k_i E \frac{dE}{dx} \\ &= \frac{1}{2} \epsilon k_i \frac{d(E^2)}{dx} \end{aligned} \quad (10).$$

$$j_e = j - j_i,$$

where j_e is the electron current density.

$$n_e = \frac{j_e}{Ek_e} \quad (11)$$

giving n_e , the electron concentration.

$$\begin{aligned} \frac{dj_e}{dx} &= - \frac{dj_i}{dx} \\ &= \text{net rate of electron loss} \\ &= - \nu_a n_e + \nu_d n_i \end{aligned} \quad (12),$$

from which ν_a , ν_d can be estimated.

Solutions for $\nu_d = 0$ have been worked out by Lawton (1963).

8.3.2. Experimental Results.

In order to investigate negative conduction, a potential difference, V , was applied across a lean premixed ethylene/air flame at atmospheric pressure stabilized above

the surface of a rectangular matrix burner of area 20 cm^2 , as described in Ch IX. The burner was made the cathode. The distance, a , between the burner and the upper electrode was varied by one centimetre intervals and the current, i_t , measured as a function of voltage at each position. From this data the field E and the charge density ρ can be obtained. Graphs of i_t versus voltage were plotted for each value of a (Fig. VIII(1)), from which were obtained graphs of V versus a by cross plotting.

8.3.3. Negative Particle Mobility.

The gradient, at any point, of the graphs of V versus a is equal to the field, E . Graphs of E^2 versus distance from the burner, x , are given in Fig.VIII(2) for various values of i_t .

The graphs of E^2 versus x at constant i_t give:

$$dE^2/dx = 1.16 \times 10^{10} \text{ V}^2 \text{ m}^{-3} \text{ at } i_t = 4 \text{ } \mu\text{A},$$

$$dE^2/dx = 2.8 \times 10^{10} \text{ V}^2 \text{ m}^{-3} \text{ at } i_t = 10 \text{ } \mu\text{A}.$$

Substituting these results into equation (7) gave $k_- = 0.039$ and $0.0405 \text{ m}^2 \text{ V}^{-1} \text{ s}^{-1}$ respectively. These values are in close agreement, which indicates that the results are reliable. Thus k_- is about $0.040 \text{ m}^2 \text{ V}^{-1} \text{ s}^{-1}$. King (1962) obtained an order of magnitude value of $0.1 \text{ m}^2 \text{ V}^{-1} \text{ s}^{-1}$. This higher value of k_- may have been due to his flame being hotter.

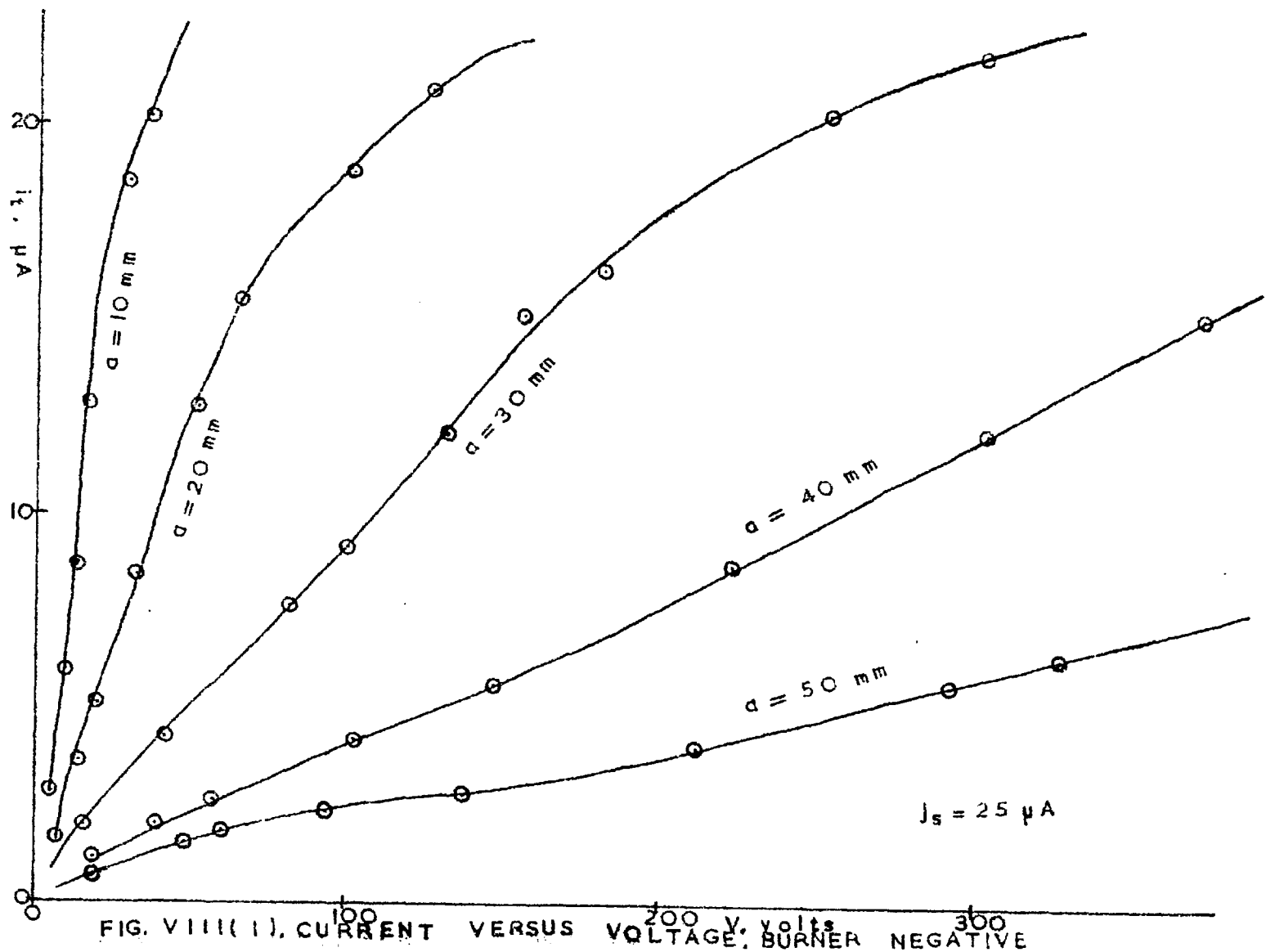


FIG. VIII (1), CURRENT VERSUS VOLTAGE, BURNER NEGATIVE

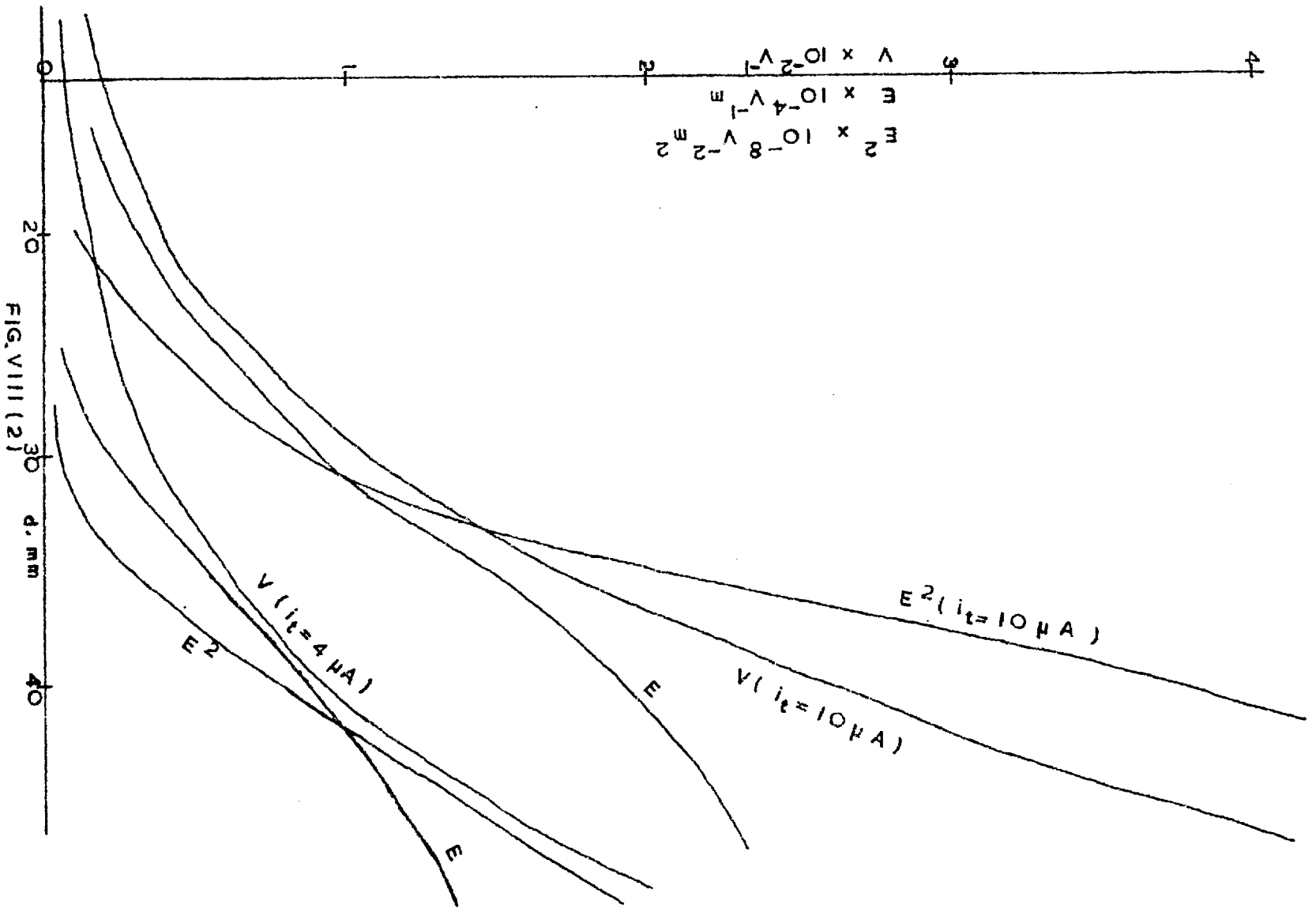


FIG. VIII (2)

The graphs obtained show that the fields near the flame were low, which confirms that all or most of the negative charge from the flame is formed initially as electrons. $d(E^2)/dx$ was much lower near the flame than farther downstream, even for near saturation currents.

8.3.4. Ratio of Electron to Negative ion Concentration.

The ratio of the electron to negative ion concentration can be obtained from the effective negative particle mobility and the electron and negative ion mobilities.

A wide range of values for the electron mobility has been given in the past. It is now accepted that its value is of the order of $0.2 \text{ m}^2 \text{ V}^{-1} \text{ s}^{-1}$ in flames at one atmosphere (Wilson, 1931; King, 1962). Van Tiggelen (1963) takes a value of $0.25 \text{ m}^2 \text{ V}^{-1} \text{ s}^{-1}$. It should be remembered, however, that the electron mobility depends on the magnitude of the applied field (Meek & Craggs, 1963) and on the temperature.

The negative ion mobility should have about the same value as the positive ion mobility, for which a value of $0.00175 \text{ m}^2 \text{ V}^{-1} \text{ s}^{-1}$ was obtained (see below). Evaluating equation (8) taking $k_e = 2500$, $k_i = 0.00175$, $k_- = 0.040 \text{ m}^2 \text{ V}^{-1} \text{ s}^{-1}$ gives the ratio of the electron to negative ion concentration, n_e/n_i , to be 0.18.

8.3.5. Evidence of Ion Generation Above Flames.

As x increases j_i increases and, from equation (10), $d(E^2)/dx$ must increase. Therefore, when x is less than an arbitrary value, h ,

$$\frac{d(E^2)}{dx} > \frac{x}{h} \left(\frac{d(E^2)}{dx} \right)_{x=h}$$

giving

$$E^2 > \frac{1}{2} \frac{x^2}{h} \left(\frac{d(E^2)}{dx} \right)_{x=h}$$

$$E > \frac{x^2}{h} \left(\frac{dE}{dx} \right)_{x=h} \quad (13)$$

Putting $x = h$ in equation (13) gives

$$E > h \, dE/dx \text{ at any point.} \quad (14)$$

The intercept, E_0 , on the E axis of the tangent to the graph of E versus x is given by

$$E_0 = E - x \, dE/dx.$$

Therefore, from equation (14),

$$E_0 > 0 \quad (15)$$

It can be seen that the graphs of E versus x (Fig.VIII(2)) are not in accordance with equation (15). Tangents give negative intercepts on the E axis. It thus appears that the field does not start to increase appreciably for some distance from the flame. This effect may be due to the presence of some positive ions which neutralize the negative space charge. Whether any positive ions are present could be checked using a Langmuir probe.

It is unlikely that many positive ions are carried downstream of the flame by the flow velocity. The field near the flame was about 3 kV m^{-1} . The positive ion mobility in flames is normally about $0.0017 \text{ m}^2 \text{ V}^{-1} \text{ s}^{-1}$ (see below) in which case a flow velocity of 5 m s^{-1} would be required. The actual flow velocity was not more than about 1 m s^{-1} . However, ions or charged particles of exceptionally low mobility might perhaps be carried downstream. The average mobility downstream would tend to decrease because of the small ions, which have the highest mobility, recombining more quickly in accordance with Langevin's theory (Langevin, 1905).

The most probable reason for the delay in the rise in E^2 is ionization occurring downstream of the flame because of excited species or of disequilibrium. Because the negative particle mobility is much higher than the positive ion mobility, the positive ions would be removed more slowly and could neutralize the negative space charge. Ionization downstream of the reaction zone of about 1% of the saturation current should be sufficient to provide a large enough positive ion concentration. Whether the amount of ionization occurring above the flame is appreciable compared with the saturation current can be checked by varying the electrode separation.

It is shown below that ionization does occur downstream of some flames investigated. Estimates are made of the rate of ion generation for different flames and its variation with height above the flame. Whether the effect is large enough to affect appreciably the validity of the assumption that all charge originates in the reaction zone will be considered.

8.3.6. Effect of Impurities and Foreign Bodies.

The effect of impurities and foreign bodies on negative charge conduction in the flame products was investigated. It was found that an insulated wire placed between the flame and a probe in the centre of the upper electrode could greatly reduce the current to the probe when the burner was negative. The total saturation current to the whole upper electrode was not appreciably reduced, which shows that the current not going to the probe was diverted to the rest of the upper electrode. The probe current was not greatly affected by the wire when the burner was positive.

The reduction of the probe current due to a thin wire tended to be greater when the wire was nearer the burner and when the wire was hot. Thinner wires were more effective than thick ones. Typical current reductions were 50% for a wire still cool and 95% for a hot wire. Various wires were tried, including copper (various diameters),

nichrome (5 thou), platinum rhodium (2 thou), platinum, and also a glass filament. The average reduction of the probe current was of the order of 60%. A clean 2 thou. diameter platinum wire gave the smallest current reduction, which was of the order of 30%.

The effect of various substances on a platinum wire were tried. Large reductions in the probe current were given by starch (75%), a handled wire, ammonium nitrate (90%, but short lived), Fe_3O_4 (80%), sodium chloride (80% short lived), POCl_3 , and methyl red (short lived). PbO_2 , MgO , Zn , Br_2 , sulphur, carbon, and ammonia solution did not appear to affect the probe current appreciably. In some cases this may have been due to their being driven off or destroyed before the wire could be positioned and the effect observed.

A nichrome wire on the burner reduced the probe current by about two-thirds. An attempt was made to see if this resulted from any substance released by the wire. The rate of loss of mass of the wire, which weighed 66 mg, was found to be under about 0.1 mg/hr. It is possible, of course, that any loss of metal from the wire was counteracted by an increase in mass due to oxidation.

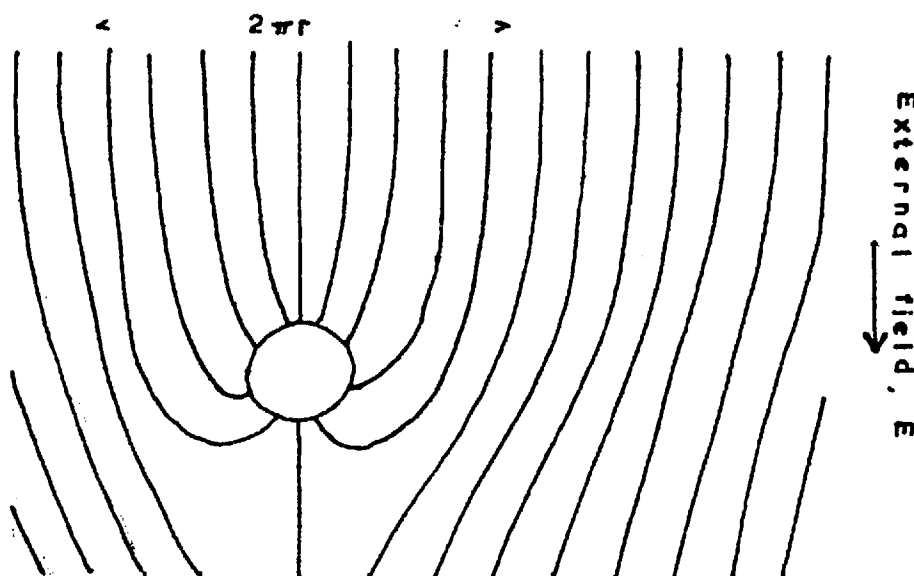
Measurements were made to investigate from how wide a region current is diverted by a wire. A gauze with

a small hole in it was placed in front of the probe in the upper electrode to obtain higher spatial resolution of the current density distribution. A nicraloy wire of about 0.2 mm diameter was placed on the burner and the current distribution scanned by moving the upper electrode horizontally. It was found that the current density above the wire was reduced by over 90% over a distance of more than 20 mm.

The electrode separations used in these experiments were about 50 mm. The negative voltage applied to the burner was about 400 V. The upper electrode and probe were at earth potential. A lean premixed ethylene/air flame was used.

It does not appear that appreciable electron emission occurred from the wires. All wires were insulated when held above the flame. The probe and upper electrode were earthed. Any emission would have tended to increase the current.

When a wire of radius r in a field E is fully charged it creates at its surface a field E in the opposite direction so that no more charge can reach the wire. $2\pi rE$ lines of force therefore leave the wire, as shown in the diagram overleaf. These form a shadow, initially about $2\pi r$ wide, above the wire, which no ions travelling along



SHADOW DUE TO WIRE

the external field lines can enter. A 2 thou. nichrome wire gave a 96% reduction of current over 20 mm, a 20 thou. nicraloy wire a 90% reduction over 20 mm. Thus the shadows cast by these wires is far greater than can be explained electrostatically.

It appears that the wire or something emanating from it causes the transformation of electrons to ions of low mobility which create a negative space charge in the wake of the wire and divert most of the current away. Electron attachment may occur at or near the surface of the wire. The effect does not appear to be due to the cooling effect of the wire since thin wires and hot wires were more effective. It might be due to catalysis, leading to the

formation of stable negative ions.

If the charges in the gas have a range of mobilities with fraction f_i of the current density being carried by charges of mobility k_i where $i = 1, 2, \dots, n$ then the effective mobility, k , is given by:

$$\begin{aligned} \text{space charge} &= \sum \frac{jf_i}{Ek_i} \\ &= j/(kE), \end{aligned}$$

$$\text{giving} \quad \frac{1}{k} = \sum \frac{f_i}{k_i} \quad (16)$$

For example, if 99% of the ions have mobility 10^{-3} and 1% have mobility 10^{-6} then $k = 0.091 \times 10^{-3}$. Thus the effective mobility can be greatly reduced by small proportions of ions of very low mobility.

The root mean square distance any substance travels by diffusion in time t is equal to $(2Dt)^{\frac{1}{2}}$, where D is the coefficient of diffusion. The time taken for the products to go from the wire to the upper electrode was of the order of 0.05 s and D is about $2 \times 10^{-4} \text{ m}^2 \text{ s}^{-1}$. Thus anything emanating from a wire could spread over a distance of about 10 mm by the time it reached the upper electrode. This effect is sufficient to explain the width of the region over which the current can be affected by a wire.

Experiments were carried out to see if current

could be diverted to the probe by a wire not directly beneath it. It was found that a small increase in the probe current could be produced in this way. The effect of a gauze with a 20 mm square hole was tried. It was found that with the hole under the probe the probe current could be increased threefold. The effect was greatest when the gauze was near the burner. This effect is due to the current being deflected away from the edge of the hole towards the probe.

These results shew that care must be taken to avoid impurities or any foreign bodies or hot surfaces in the flame, particularly in a flux of electrons, i.e. when determining saturation current densities by measuring probe currents with the burner negative.

8.3.7. Currents To Wires.

Some effects described by Waroux (1964) were investigated. The current from an unoxidised positive copper wire in a flame was found to increase rapidly after about five seconds and then to decrease slowly over a similar period. The initial increase appeared to be connected with the heating up of the wire and the subsequent decrease with its oxidation. Experiments were carried out using 26 gauge copper wire. The current increase of up to about 400% obtained at a low voltage (100 V) was much greater

than the increase (about 25%) obtained at a near saturation voltage. The current to a hot oxidized wire was up to double that to a cold oxidized wire. When the applied field was removed by shorting it out a large momentary back current was observed on a cathode ray oscilloscope, which suggests that the decrease in current was due to a back e.m.f. For example, electrons emitted thermionically from the wire may form a sheath.

The currents, measured using a microammeter, to initially unoxidized 26 gauge copper wires about 13 mm long in series with a megohm resistance are given below:

Applied voltage, V	33	98	212
Initial current, μA .	0.9	2.4	4.5
Maximum current, μA .	1.2	3.8	7.4
Subsequent current, μA .	1.0	2.6	5.1

The current maxima were less marked than they would otherwise have been, because of the megohm resistance, which was placed in series with the wire to protect the microammeter in the event of the wire sagging and touching the burner. These results indicate that there is a back e.m.f. produced, the magnitude of which depends on the history of the wire.

8.4. Positive Conduction.

8.4.1. Positive Ion Mobility.

Current voltage characteristics were obtained with the burner positive for several values of the electrode separation, a , to obtain the positive ion mobility, k_+ .

For subsaturation (j less than j_s)

$$E^2 = 2jx/\epsilon k_+$$

$$\begin{aligned} \text{giving } k_+ &= (8/9)ja^3 V^{-2} \epsilon^{-1} \\ &= (8/9) \epsilon^{-1} a^3 dj/dV^2 \end{aligned} \quad (17).$$

Measurements of current versus voltage were made for several different flames on the porous disc burner. The burner was positive. The electrode separation was 10 mm and the flame area 19.8 cm^2 . The following results were obtained:

$V^2, \text{ volt}^2 \times 10^4$	0.04	1.0	6.0	11.0	16.0
$i_t, \mu\text{A}$	0.13 to 0.45	0.7 ± 0.03	2.6 ± 0.05	4.3	5.8
$di_t/dV^2, \mu\text{A V}^{-2}$		ca.0.40	0.38	0.34	0.30

These results confirm that the current at low voltages is much greater than if i_t were proportional to V^2 . Substituting into equation (17) the value of $dj/dV^2 = 10^4$ to $16 \times 10^4 \text{ volt}^2$ gives the positive ion mobility to be $0.00175 \text{ m}^2 \text{ V}^{-1} \text{ s}^{-1}$.

King (1962) and Wilson (1931) give the positive ion mobility to be about 1 to $2 \times 10^{-4} \text{ m}^2 \text{ V}^{-1} \text{ s}^{-1}$. However, this does not appear to be correct for ions in flame products. The predominant positive flame ion is H_3O^+ (Green & Sugden, 1963). The mobility of this ion at N.T.P. is about $3 \times 10^{-4} \text{ m}^2 \text{ V}^{-1} \text{ s}^{-1}$ (see Mitchell & Ridler, 1934). Simple kinetic theory, assuming the molecules and ions to act as solid spheres, gives the mobility to be proportional to $T^{\frac{1}{2}}$. The temperature of the flames used was about 1600°K , giving a mobility of about $7 \times 10^{-4} \text{ m}^2 \text{ V}^{-1} \text{ s}^{-1}$. More precise kinetic theory, taking into account dipole interactions, gives $k\varrho = \text{constant}$ (Langevin, 1905), where ϱ is the density of the gas. $k\varrho$ tends to vary comparatively little with temperature (Massey & Burhop, 1952). The assumption that $k\varrho$ is constant gives $k \propto T$ giving $k = 0.00164 \text{ m}^2 \text{ V}^{-1} \text{ s}^{-1}$ at the flame temperatures. This value is in good agreement with the value of 0.00175 obtained above.

It does not appear that electron emission occurred from the upper electrode when the burner was positive (although it has been suggested that electrons can be produced in the vicinity of cool electrodes in seeded flames (Turcotte & Friedman, 1965), since the current ceased immediately the flame was extinguished. Moreover, similar currents were obtained using either the hot matrix upper electrode, which

was not cooled, or the water cooled upper electrode.

8.4.2. Further Evidence of Ion Generation Above Flames.

The above results show that the current with the burner at a positive voltage of 20 V and an electrode separation of 10 mm was about 0.3 μA or 0.15 mA m^{-2} . Taking the maximum field to be 4 kV m^{-1} and assuming only positive charge was present, Gauss' law gives the total charge present to have been 3×10^{-8} coulomb m^{-2} . To give the observed current this charge would have required a velocity of 50 m s^{-1} , which is much greater than the flow velocity and the probable drift velocity due to the field. Thus it does not appear that the current at low positive voltages is carried solely by positive ions travelling from the reaction zone. It has been shown that it is unlikely that electron emission occurs from the upper electrode. The most likely explanation for the current at low positive voltages being higher than expected is that ion generation continues above the flame, since positive ions formed near the upper electrode would have less distance to travel.

8.5. Ion Generation Above Flames.

It has been suggested that some ion generation occurs above hydrocarbon flames. This was investigated by two methods as discussed below: by measurement of the current

to an electrode with low positive voltages on the burner; and by observing the variation of the saturation currents of flames with electrode separation.

8.5.1. Current with Low Positive Voltage on Burner.

If positive ions are formed in the vicinity of the upper electrode, at the rate of J/e per unit volume, a sheath of thickness z would be formed in which all the positive ions generated go to the upper electrode. Assume that the negative charge formed has infinite mobility and ignore diffusion, since the sheath would be thick.

At distance $(z-x)$ from the upper electrode the current density $j(x)$ is given by $j(x) = Jx$.

$$\begin{aligned} \epsilon dE/dx &= \text{space charge density} \\ &= j(x)/(k_+E) \\ &= Jx/(k_+E). \end{aligned}$$

Therefore, integrating and taking $E = 0$ at $x = 0$ since the current below the sheath is carried by negative charge of infinite mobility,

$$E^2 = (J/\epsilon k_+)x^2.$$

Therefore, integrating,

$$V = \frac{1}{2} (J/\epsilon k_+)^{1/2} z^2.$$

Therefore
$$z = \frac{1}{2} k_+^{1/4} \epsilon^{1/4} V^{1/2} J^{-1/4}$$

Hence the total current density, $j = Jz$

$$= (\epsilon k_+)^{1/4} \epsilon^{-1/4} (2V)^{1/2} J^{3/4}$$

$$\text{Thus } J = (4/k_+ \epsilon)^{-1/3} (j/V^{1/2})^{4/3} \quad (18).$$

Graphs of j versus $V^{1/2}$ for low positive voltages on the burner for three flames are shown in Fig.VIII(3). These give, at low voltages, approximately straight lines passing near the origin, indicating that the current was primarily due to ionization above the flame. Measurement of the current at low voltages with the burner positive thus provides a means of determining the rate of ionization above the flames.

The flame represented by the middle curve in Fig. VIII(3) was an ethylene/air flame. At 14 V the total current was 0.2 μA . The current to a probe of area 5.8 cm^2 was 0.18 of the total. Thus the current density produced near the upper electrode was about 0.062 mA m^{-2} . The positive ion mobility has been shown to be about 0.00175 $\text{m}^2 \text{V}^{-1} \text{s}^{-1}$. This value will be assumed in all the following calculations. The rate of current generation, J , which occurred near the upper electrode is thus given by

$$\begin{aligned} J &= (4 \times 0.00175)^{-1/3} (6.2 \times 10^{-5} \times 14)^{4/3} \text{ from (17)} \\ &= 10 \text{ mA m}^{-3}. \end{aligned}$$

For another flame the current to the upper electrode at an electrode separation of 10 mm and at 21.8 V was about 0.307 μA , which gives the rate of ionization, J , 10 mm above the flame to have been 14 mA m^{-3} .

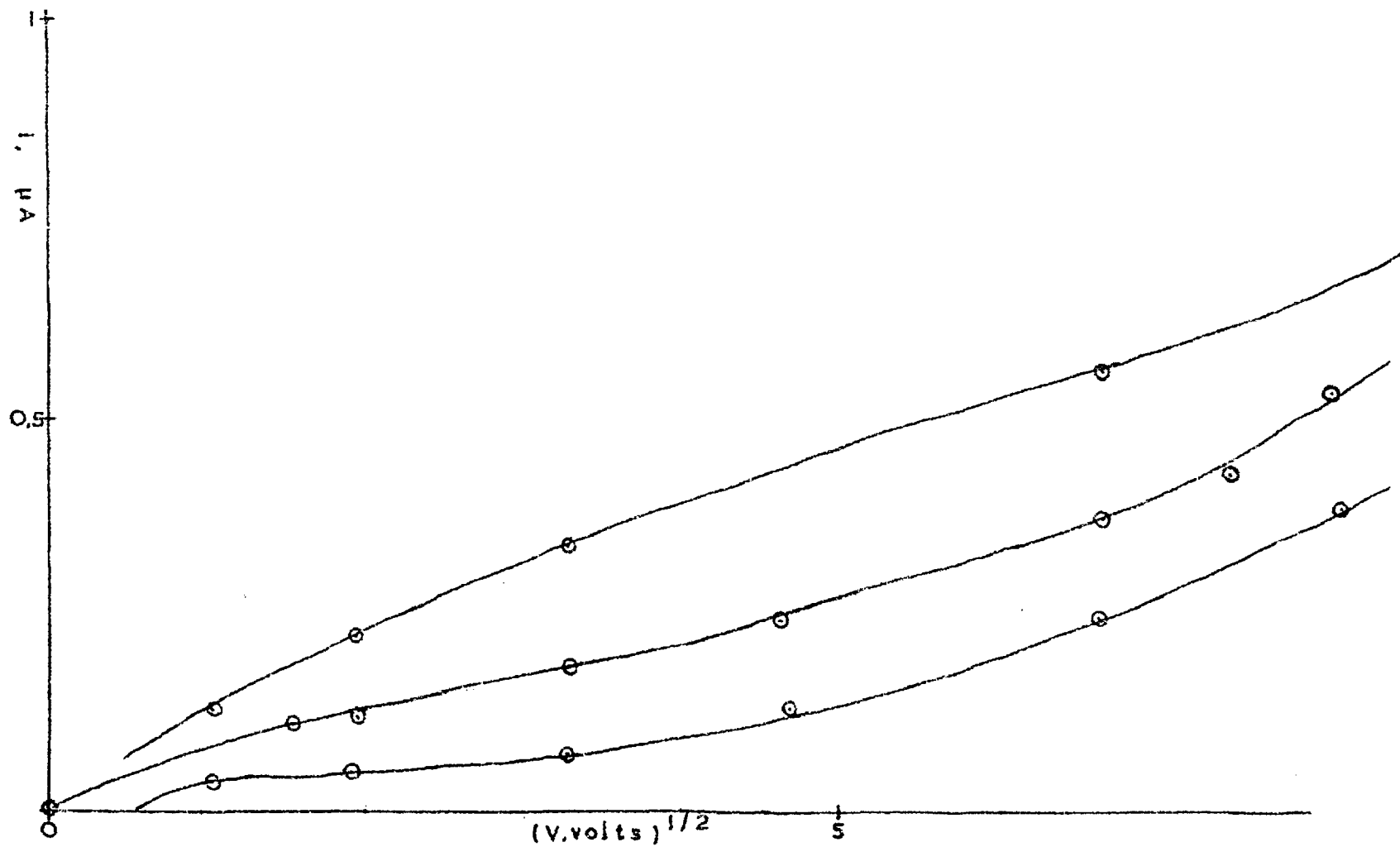


FIG.VIII(3), CURRENT VERSUS VOLTAGE, BURNER POSITIVE

The current measured must come from a zone of thickness j/J , which was about 5 mm. The spatial resolution obtained was therefore of this order.

The rate of ion generation found per unit volume is less than the saturation current density of most hydrocarbon/air flames, which explains why this ionization above flames has not been detected before.

8.5.2. Variation with Height.

It was decided to investigate the variation of the rate of ionization with height above the flame. The results shown in Fig.VIII(4) were obtained for the variation with electrode separation, a , of the current to an upper electrode. The burner was at a positive voltage of 21.8 V. These results give

$$i \propto a^{-1.48}$$

From (18) $J \propto i^{4/3}$.

Therefore $J \propto a^{-1.97}$, which shows the rate of ionization above the flame is approximately inversely proportional to the square of the height above the flame. This fact rules out the likelihood of this ionization being due to the thermal ionization of impurities.

8.5.3. Comparison of Different Flames.

Measurements were made to find rates of ionization above different flames and the variation with the flame

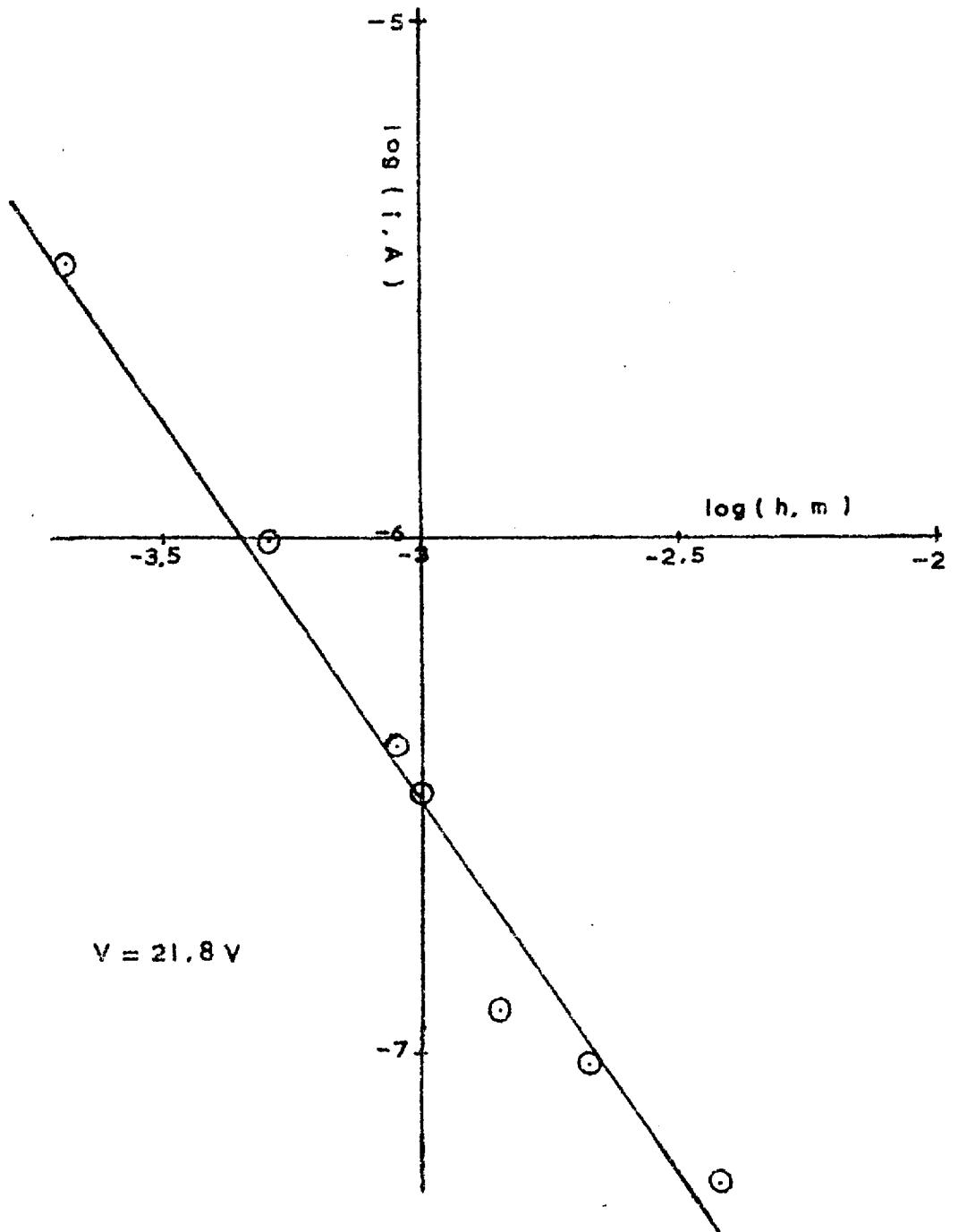


FIG. VIII (4). CURRENT VERSUS ELECTRODE SEPARATION

saturation current density. Results are given below:

Probe area = 5.8 cm^2 , electrode separation = 10 mm.

Lean $\text{C}_2\text{H}_4/\text{O}_2$

Saturation current to probe, $(i_p)_s$, μA	0.313
Current to probe with burner at +10V, $(i_p)_+$, μA	0.017

Lean $\text{C}_2\text{H}_4/\text{air}$

$(i_p)_s$, μA	0.24	0.55	2.7	7.0	14.0	16.0
$(i_p)_+$, μA	0.014	0.019	0.037	0.05	0.07	0.085

Rich $\text{C}_2\text{H}_4/\text{air}$

$(i_p)_s$, μA	0.15	0.15	6.5	10.0	14.5	20.5
$(i_p)_+$, μA	0.010	0.013	0.06	0.05	0.065	0.09

Lean $\text{C}_2\text{H}_4/\text{CO}/\text{air}$

$(i_p)_s$, μA	2.0	2.2	2.5	4.3	7.5	17.5
$(i_p)_+$, μA	0.033	0.034	0.039	0.037	0.065	0.08

These results show that flames with different compositions but the same saturation current density give similar values of J . $(i_p)_+$ tends to increase as $(i_p)_s$ increases. $(i_p)_+$ varied over a much smaller range (0.01 to 0.09 μA) than $(i_p)_s$ (from 0.15 to 20 μA). It is not to be expected that there would be an exact relationship between

$(i_p)_+$ and $(i_p)_s$ since flames with the same saturation currents but different compositions have different burning velocities so that the time which elapses before the gas reaches the upper electrode varies.

The fact that $(i_p)_+$ varied over a factor of about ten is further evidence that it is due to ionization occurring above the flame. If ionization occurred only in the reaction zone, the current at subsaturation voltages should be independent of the saturation current.

Results are given below for some oxygen flames:

Flame area = 18 cm²

electrode separation = 10 mm.

CH₄/O₂

Total saturation current, i_s , μA	0.08	0.18
Total current with burner at 10 V, i_+ , μA	0.039	0.043

C₂H₄/O₂

i_s , μA	0.20	0.31	0.50	1.2	1.6	3.9	9.0
i_+ , μA	0.031	0.029	0.031	0.055	0.048	0.060	0.064

CO/C₂H₄/O₂

i_s , μA	0.70
i_+ , μA	0.070

The values of i_+ all lie within a range of 0.029 to 0.070 μA . There is a tendency for i_+ to increase with i_s .

If 0.18 of the current at low voltages goes to a probe of area 5.8 cm^2 , as found for air flames, then the effective area of the column of flame gases is $5.8/0.18 = 32 \text{ cm}^2$. Assuming this area and taking $i_+ = 0.029 \mu\text{A}$, which corresponds to $i_s = 0.31 \mu\text{A}$ for ethylene/oxygen, gives, by substitution in (18), volume rate of ionisation above flame, $J = 1.2 \text{ mA m}^{-3}$. The rate of ionization per unit distance interval above the flame is then $0.0032 \text{ m}^2 \times 1.2 \text{ mA m}^{-3} = 3.8 \mu\text{A m}^{-1}$, which should be observable.

8.5.4. Variation of Saturation Current with Electrode Separation.

Measurements taken of the saturation currents of a methane/oxygen and two ethylene/oxygen flames showed clearly that the saturation current varies somewhat with electrode separation, confirming that ionization occurs above these flames. Increases in saturation current of 10 to 50% were obtained.

For a lean ethylene/oxygen flame the saturation current was 0.24 μA for an electrode separation of 6 mm and 0.314 μA at 25 mm. Assuming the rate of ionization to be proportional to h^{-2} and integrating gives the rate of ionization 10 mm above the flame to be (from equation (20)) $5 \mu\text{A m}^{-1}$, which is in good agreement with the value

of $3.8 \mu\text{A m}^{-1}$ calculated from the current with the burner at a low positive voltage for a flame giving a similar rate of ionization.

It was confirmed for another ethylene/oxygen flame that the saturation current was the same ($0.5 \mu\text{A}$) within the experimental error both with the burner positive and negative, which shows that it is unlikely that cold cathode emission occurred.

8.5.5. Estimation of Ionization Zone Thickness.

The current density to a probe in a plane electrode for ethylene/air flames with the burner at +10 V was about 0.04 and 0.1 mA m⁻² when the saturation current density was 1 and 10 mA m⁻² respectively. These values correspond to $J = 6$ and 15 mA m^{-3} respectively (from substitution in equation (18)). The electrode separation was 10 mm.

Assuming that the ionization occurs from $h = h_1$ at a rate proportional to h^{-2} ,

$$J = J' h^{-2}$$

where J' is the value of J at unit height.

$$\begin{aligned} j_s &= \int_{h_1}^{\infty} J' h^{-2} dh \\ &= J' h_1^{-1}. \end{aligned} \tag{19}$$

Contribution to j_s between $h = h_1$ and $h = h_2$

$$= J' (h_1^{-1} - h_2^{-1}). \quad (20)$$

Thus if $j_s = 1 \text{ mA m}^{-2}$, $J' = 0.6 \text{ } \mu\text{A m}^{-3}$ at $h = 1 \text{ m}$, then $h_1 = 0.6 \text{ mm}$ and 50% of the ionization occurs over 0.6 mm. If $j_s = 10 \text{ mA m}^{-2}$, $J' = 1.5 \text{ } \mu\text{A m}^{-3}$ then $h_1 = 0.15 \text{ mm}$ and 50% of the ionization occurs over 0.15 mm.

The results show that the current with low positive voltages on the burner, and therefore J' , vary much less than j_s . Thus the proportion f of the ionization occurring beyond an arbitrary given height above the flame is greatest for flames with low saturation current densities.

The distance over which 50% of the ionization occurs gives a measure of the ionization zone thickness. Equations (19) and (20) show that this distance is of the order of J'/j_s . The above figures, which are based on average experimental values, show that the ionization thickness is typically of the order of 0.3 mm. It tends to be greater for flames with low saturation current densities.

8.5.6. Effect of Ion Generation Above Flames.

If 50% of the ionization occurs in 0.3 mm then $h_1 = 0.3 \text{ mm}$. The saturation current density at $h_2 = 10 \text{ mm}$ is then 97% of that at $h_2 = \infty$, which confirms that for a typical flame with a typical electrode separation the saturation current density measured is near the maximum potential saturation current density. Thus the ionization

downstream of the flame is unlikely to affect appreciably the accuracy of the saturation current method for most flames.

$$\begin{aligned} dn/dt &= -\alpha n^2 + J/e \\ &= -\alpha n^2 + (J'/e) h^{-2} \\ &= -\alpha' n^2 \end{aligned} \quad (21)$$

where α, α' are the real and apparent recombination coefficients respectively, and e is the electronic charge.

$$n = u(\alpha' h)^{-1} \text{ approximately,}$$

where u is the flow velocity.

$$\text{Therefore } h = u\alpha'^{-1} n^{-1}.$$

Thus, substituting for h in equation (21),

$$\begin{aligned} dn/dt &= -(\alpha - \alpha'^2 J' e^{-1} u^{-2}) n^2 \\ &= -\alpha' n^2. \end{aligned}$$

Thus continuing ionization above the flame at a rate proportional to h^{-2} would not be detected by ion concentration measurements since the ion concentration still decays in accordance with a second order law. The apparent recombination coefficient is however reduced.

8.5.7. Summary.

It has been shown that ionization occurs above hydrocarbon flames. This has been measured by two different methods: measurement of the current to an upper electrode with low positive voltages on the burner, and measurements of the saturation currents of flames at different electrode

separations. These methods give values in approximate agreement. The distance over which most of the flame ionization occurs was estimated. It was shown that the rate of ionization above flames is insufficient to appreciably affect the accuracy of saturation current measurements in most cases. It would be of interest to measure the variation of the rate of ionization above flames with flame composition and temperature and its decay with time, and to investigate other hydrocarbons as well as ethylene. However, this topic was not pursued further since the principal aim of the project is to measure saturation currents of flames.

8.6. Further Experimental Results.

8.6.1. Rectification by Flames.

A variable alternating potential (from a Variac) was applied across a flame and the current observed on a cathode ray oscilloscope. Partial rectification was obtained. This effect results from electrons, which carry most of the current when the burner is negative, having a higher mobility than positive ions (see Section 1.4). The amount of rectification varied with the flow rates of the fuel and air. The maximum rectification corresponded, at least approximately, to a stoichiometric mixture, for which the flame would be closest to the burner. The current was the greater the smaller the cold gap between the flame and the burner, this

gap having a high resistance. The current often increased as the flame dropped just before going out.

8.6.2. Observation of Current-Voltage Characteristics.

A circuit was set up so that the current-voltage characteristics of a flame could be displayed on a cathode ray oscilloscope. The X deflection was proportional to the applied voltage and the Y deflection to the current obtained. It was hoped that this arrangement would provide a rapid means of obtaining the required relationship. A 50 Hz a.c. field of variable voltage was applied. The trace obtained was approximately of the shape expected but it was not a single well defined line. Because of the build up of charge and capacitance effects the curve was distorted and hysteresis occurred. The position of the trace could not be measured accurately. It was concluded that the characteristics could be obtained more accurately by measuring the steady state d.c. currents and voltages with a galvanometer.

8.6.3. Variation of Current Due to Flame Movement.

The current in a bunsen flame due to an electric field obtained by connecting a high tension battery between the burner and a gauze above the flame was observed by the use of a cathode ray oscilloscope. The trace obtained moved

up and down because of the movement of the flame. There was a definite maximum current corresponding to the flame touching the gauze. This gives a convenient method of demonstrating the movement of the flame.

If a voltage less than that required to extract the saturation current is applied to a flame then the current depends on the flame position and the charge mobility. The charge mobility depends on the gas temperature and composition. Thus the current at sub-saturation voltages could provide a means of monitoring variations in the flame position, temperature and composition. In particular it might provide a convenient way of detecting substances with high electron affinities. Such substances can reduce the electron concentration (King, 1962), giving a lower negative ion mobility and thereby reducing the current.

8.7. Maximum Current Without Breakdown.

The work on conduction in flame gases in the present study has shown that the negative particle mobility is much greater than the positive ion mobility. The former was found to be about $0.040 \text{ m}^2 \text{ V}^{-1} \text{ s}^{-1}$ in the hot gas; the latter about $0.00175 \text{ m}^2 \text{ V}^{-1} \text{ s}^{-1}$. The charge mobility in the cold space between the flame and the burner would be about $3 \times 10^{-4} \text{ m}^2 \text{ V}^{-1} \text{ s}^{-1}$ for positive ions and somewhat greater than this for negative charge, depending on the proportion of electrons which attach in the cold gas.

The maximum current density that can be drawn without secondary ionization, j_b , is equal to $\frac{1}{2} \epsilon E_b^2 k / a \text{ A m}^{-2}$ (Lawton & Weinberg, 1964) where E_b is the breakdown field in V m^{-1} , a is the distance from the flame to the electrode in metres, and k is the charge mobility in $\text{m}^2 \text{V}^{-1} \text{s}^{-1}$. Breakdown occurs when aj/k exceeds a critical value on either side of the flame. The largest current without breakdown can be drawn when the higher k is utilized on the side of the flame on which a is larger. Thus higher saturation current densities can be measured without secondary ionization when the burner is negative and the current in the space above the flame is carried by negative charge. For this reason most of the saturation current measurements were made with the burner negative.

The breakdown strength of air is about 3 MV m^{-1} at N.T.P., being less at higher temperatures and more at small electrode separations (Meek & Craggs, 1953). For $E_b = 3 \text{ MV m}^{-1}$, $k = 2.5 \times 10^{-4} \text{ m}^2 \text{V}^{-1} \text{s}^{-1}$, $a = 1 \text{ mm}$ the maximum current which can be drawn without breakdown in the cold space between the flame and the burner is 10 A m^{-2} . Taking E_b above the flame to be 0.6 MV m^{-1} , with $k = 0.03 \text{ m}^2 \text{V}^{-1} \text{s}^{-1}$, $a = 10 \text{ mm}$ gives the maximum current which can be drawn without breakdown above the flame with negative conduction to be 5 A m^{-2} . In practice secondary ionization tends to

occur at lower current densities than this because of deviations from the ideal of plane, smooth electrodes. The saturation currents of most of the premixed hydrocarbon/air flames to be measured are under 1 A m^{-2} (Lawton & Weinberg, 1964). These magnitudes confirm that the saturation current method is capable of measuring the required saturation current densities without secondary ionization.

$k \propto p^{-1}$ and $E_b \propto p$ approximately (Meek & Craggs, 1953), giving $j_b \propto E_b^2 k/a$

$$\propto p/a$$

$$\propto \frac{\text{pressure}}{\text{electrode separation} \times \text{temperature}}$$

Lawton & Weinberg (1964) have calculated maximum practical effects obtainable by applied fields without breakdown. They assumed a minimum electrode separation of 5 mm. Although this value is probably the minimum for practical purposes, flames can be burnt at smaller separations - it was found that counter-flow diffusion flames could be obtained at electrode separations of 1 to 2 mm. To minimize the likelihood of breakdown plane parallel electrodes should be used.

The voltage drop, V , between the flame and each electrode is given by

$$V = (2/3) (2j/\epsilon k)^{1/2} a^{3/2} \text{ volt,}$$

where a and k are the appropriate distance in metres and

mobility in $\text{m}^2 \text{V}^{-1} \text{s}^{-1}$ respectively, and convection and diffusion are ignored. Thus the voltage is proportional to $(a^3 k^{-1})^{\frac{1}{2}}$. The distance from the flame to the upper electrode is about 10 mm and that from the flame to the burner of the order of one tenth of this. The voltage drop between the flame and the upper electrode is therefore of the order of 3 to 150 times that between the burner and the flame, depending on the polarity. Hence the total voltage required to draw a given current is much less when the conduction above the flame is by negative conduction. ie. when the burner is negative. The results obtained confirm that for a given arbitrary current and electrode separation the voltage required is less when the burner is negative.

8.8. Summary.

In this chapter factors affecting the current to probes, the behaviour of negative and positive charge in flame gases, and ionization above flames have been investigated. Charge mobilities have been obtained. It was found that negative conduction is extremely sensitive to the presence of many impurities. Their introduction beneath a probe diverted the current away from a large area and greatly reduced the current to the probe. This effect could be used as a means of detecting impurities. It might also be useful in gas chromatography.

It was shown that ion generation continues above

non-luminous premixed hydrocarbon flames. The rate of this ion generation was measured by two methods, which gave results in reasonable agreement.

It was shown that the saturation current method is accurate and capable of measuring the saturation current densities required. In particular it was shown that sufficiently large current densities can be drawn before breakdown and that the applicability of the method is not appreciably affected in most cases by ion generation above the flame. Indeed, measurement of saturation current as a function of electrode separation provides a method for studying ion generation in the product gases. Precautions which should be taken and limitations of the saturation current method have been discussed.

CHAPTER NINE.EXPERIMENTAL DETAILS.

9.1. Flow System.

A suitable flow system was designed to control and measure the flow of reactants to the flame. Needle valves were used to control the flows and pressures.

A typical simple flow system, which was used for earlier measurements, is shown in Fig.IX(1). Air was obtained from the laboratory air supply, or from a pump, A. The latter gave a steadier flow. The air was passed through a cotton wool filter, C, to remove any oil and then through drying towers, D, filled with silica gel. Other gases were obtained from cylinders. Two-stage regulators were used to reduce the pressure to about one atmosphere. The gases from the cylinders did not need to be dried since the gas in the cylinders is at high pressure so that even if it is saturated with water the percentage of water is negligible. Calming volumes, B, F, were used to reduce fluctuations in the gas flow. The gas flows were measured by means of capillary meters, E, G, of the type used by Pandya & Weinberg (1963). These were calibrated for each gas used by means of a bubble meter. The gas flow at N.T.P. is a function of hp , where h is the pressure drop across the capillary and p is the pressure just downstream.

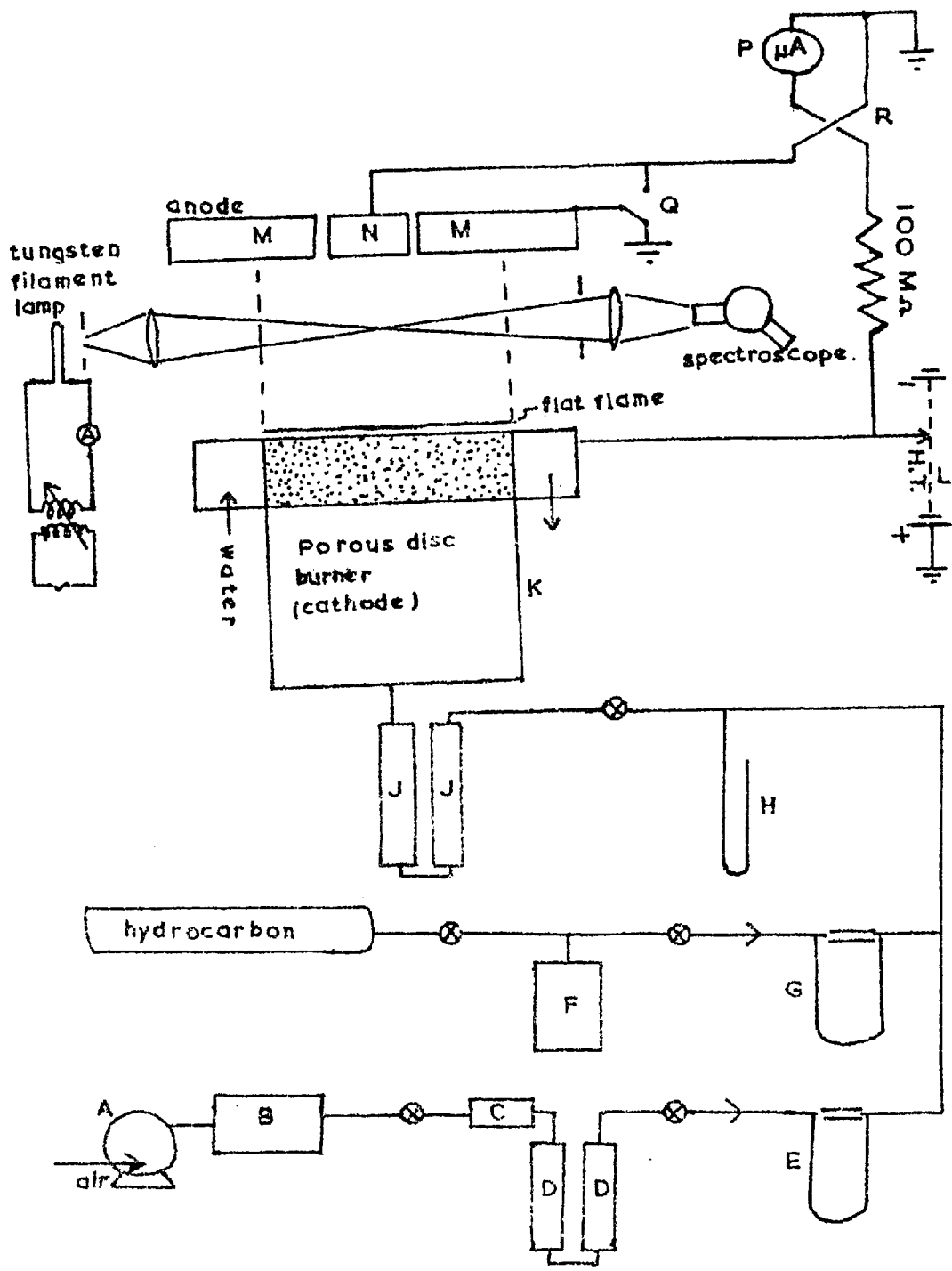


FIG. IX (1), FLOW SYSTEM AND ELECTRICAL CIRCUIT

The gases were mixed in mixing towers, J, filled with glass beads and pieces of tubing. The mixing towers were bound with adhesive tape to prevent the scattering of broken glass in the event of an explosion. They were also surrounded by a zinc screen and placed behind a board. Flame traps consisting of metal matrices were placed in the flow lines to arrest flash back. After use the system was often purged with air or nitrogen to avoid leaving an explosive mixture in it.

The final flow system built is shown in Fig.IX(2). It permitted four gases to be metered separately and each to be fed to either (or both) of two burners. This arrangement allowed measurements to be taken on flames with more than two constituents and allowed the flow and composition of the gas to two burners to be adjusted and metered independently for measurements on counter-flow diffusion flames.

An extraction system was set up to remove harmful or obnoxious products which might be produced by rich flames or flames containing sodium chloride or other halogen compounds.

9.1.1. Use of Bleed.

The flow to a premixed flame could be varied

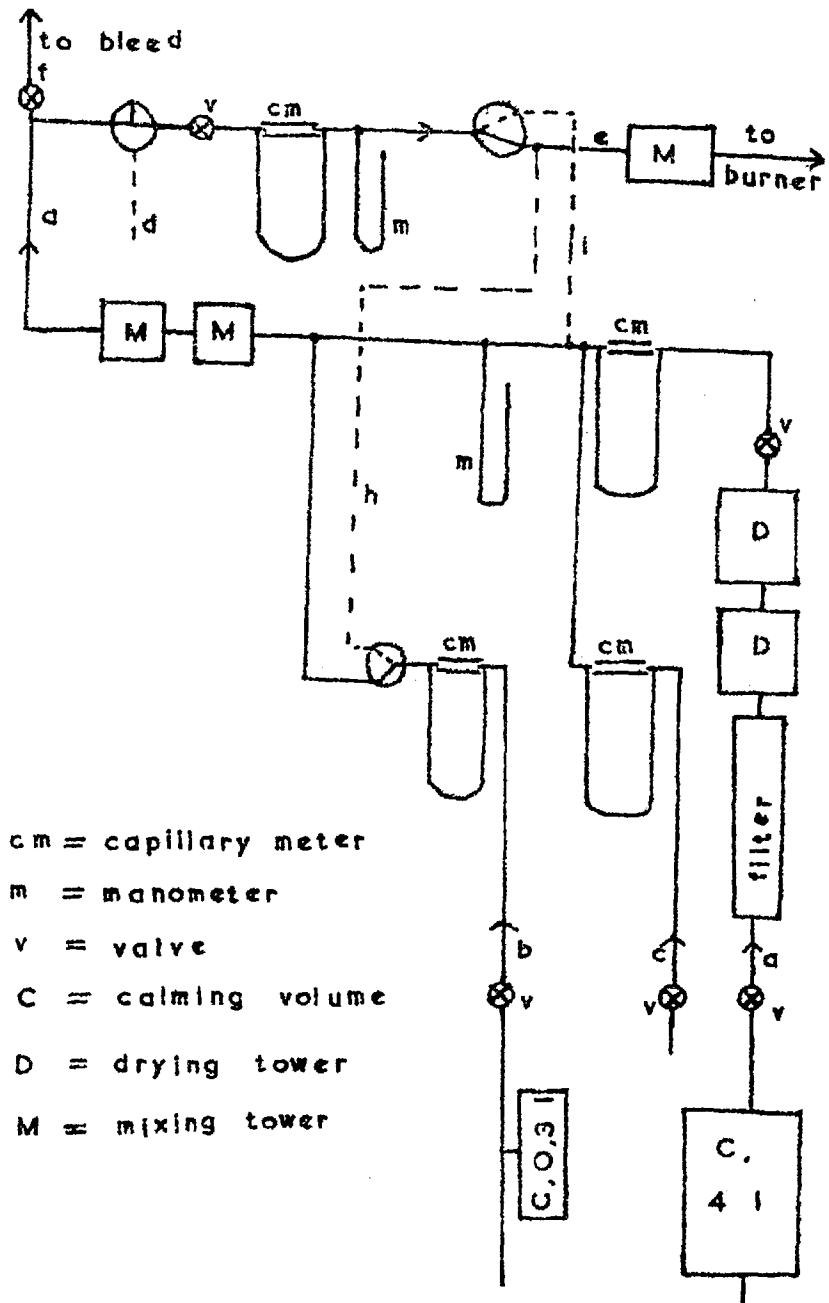


FIG. IX (2), FLOW SYSTEM

without changing the reactant composition by using one burner as a bleed. By suitable adjustment of the valves, a proportion of the premixed gas could be bled off through the bleed while the total flow, and the pressure of the meters measuring the flow of the gas constituents, were kept constant. The gas going to the burner could be passed through one of the flow meters. A meter upstream of the burner can be useful for correlating flames of different flows but : of the same composition. Fig.IX(2) shows the flow system as set up for use with a bleed. The dotted lines (d,h,i) are not used with this arrangement. There are three inlets (a,b,c). The metered gases are divided between the line to the burner, e, and that to the bleed, f.

9.1.2. Seeded Premixed Flames.

The mixture burnt was slightly lean (5.5 l. min^{-1} of air, 2.0 l. min^{-1} of CO). A Meker burner was used, which gave an approximately flat flame of 4 cm^2 area. The salts were introduced in the form of a spray of the aqueous solution given by an atomiser. For the flame with sodium, a solution of sodium carbonate was used. For those with lead, a solution containing 10.4 g lead nitrate and 0.25 g sodium acetate in 98 cm^3 of water was employed. A field was applied between the burner and an electrode above it.

The burner was made the anode. It was found that the use of a shield of nitrogen to prevent secondary air reaching the flame did not alter the current.

9.2. Burners.

For premixed flames it is necessary that the burner gives uniform flow and good heat extraction to keep the burner surface cool and at a constant temperature and to give a uniform flame.

It was decided to employ a flat flame for the reasons given in Ch.VII. Several types of burner were tried, including a fine gauze in a frame, resting on a bed of bronze powder, and a burner consisting of a rectangular matrix flame trap, supplied by Amal Ltd., water-cooled round the edge. The former gave insufficient cooling of the burner surface, which tended to become red hot. The matrix burner, also, did not give sufficient heat extraction to give a uniform flame for all the throughputs and compositions used.

9.2.1. Porous Disc Burner.

The type of directly cooled porous disc burner used by Yumlu (1959) appeared to be the best way to obtain the maximum rate of heat extraction. A burner designed to hold cylindrical discs one inch thick and of two inches diameter was developed and built (Fig.IX(3)). Later, a second

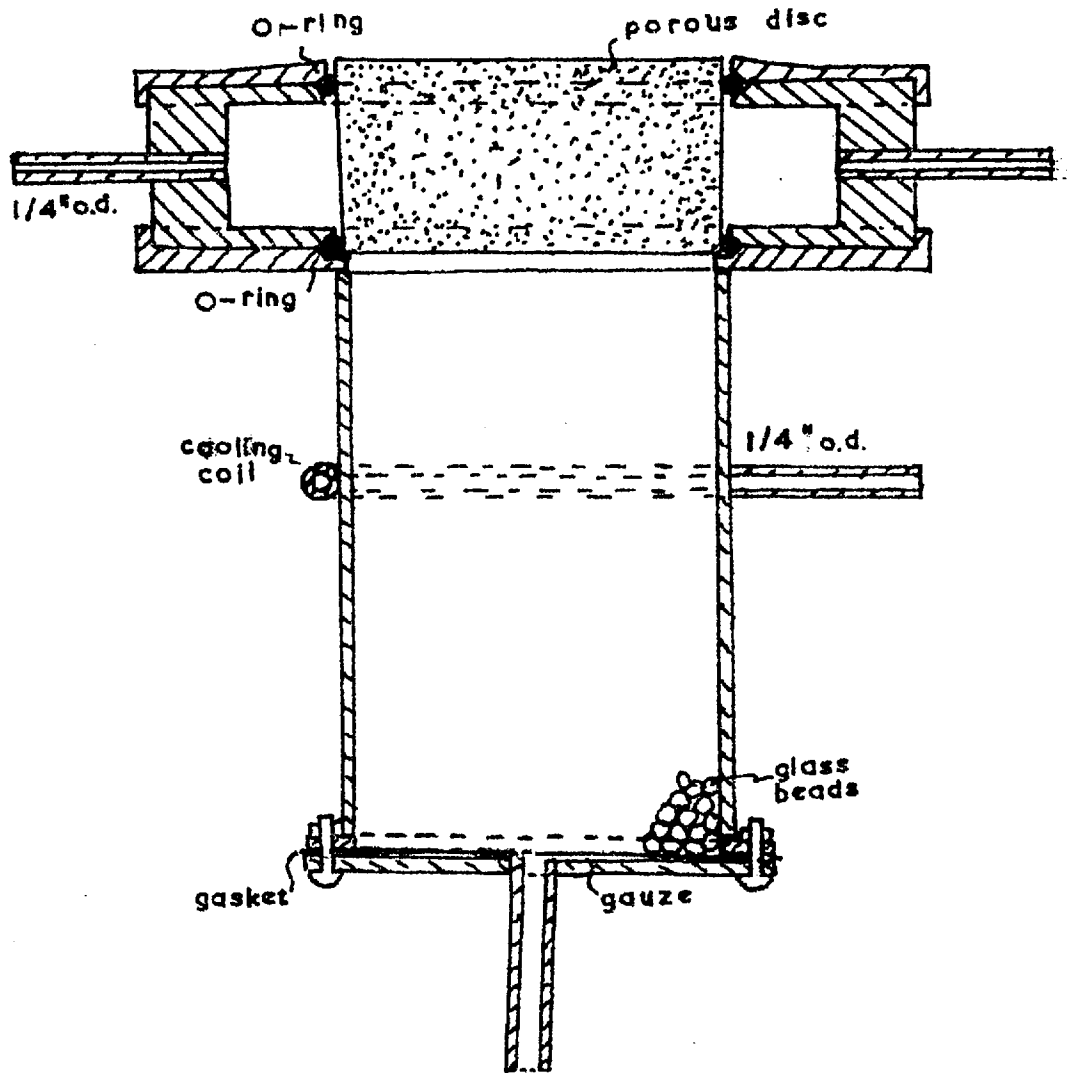


FIG. IX (3), POROUS DISC BURNER

burner was made. Water circulated round the disc and solder-sealed directly cooled discs could be used, or smaller discs shrink-fitted or push-fitted into sleeves of the right size. Two compressed O-rings prevented the water escaping and secured the disc in place. Discs could be easily interchanged, which was necessary since several discs had to be tried to find the one which gave the most uniform flame. The disc surfaces deteriorated as a result of impacts, prolonged overheating, corrosive chemicals, or the deposition of soot, so that the disc needed to be changed often (or the other side used). The discs could be cleaned by washing with dilute ammonia solution.

It was found that direct-cooled porous discs were capable of giving extremely high rates of heat extraction (up to 800 W, equal to 400 kW m^{-2}) without the surface becoming hot. The main disadvantage of this porous disc burner is the large pressure drop across the disc (up to half an atmosphere). For this reason $\frac{1}{2}$ " thick discs were sometimes used instead of 1" thick ones.

Several 2" diameter 1" thick porous sintered bronze discs made by Sintered Products Ltd were obtained. Some were sealed with solder round the circumference. This operation was difficult because it is necessary to avoid damaging the disc surface, to prevent solder from penetrating

into the interior of the porous disc, and not to damage the disc by overheating. The circumference of the disc must be completely sealed to prevent water penetrating the disc or gas escaping from it.

Because it was difficult to tin the discs effectively without damaging them, some discs were fitted with brass sleeves instead, which prevented water entering the discs or gas escaping from the circumference. The heat transfer through the sleeve was not as good as with direct cooling, but was still adequate. The disc in use acquired a temperature of the order of 100°C , which would not affect the flame appreciably (Yumlu, 1959). Reduced heat transfer at the circumference of the disc should not significantly affect the uniformity of the flow across the disc. The flow distribution may be marginally altered since the higher disc temperature will mean that a given difference in temperature would alter the gas viscosity and flow by a smaller ratio.

The disc temperature could be estimated by the increase in the pressure drop as the disc heated up. The pressure drop is proportional to the volumetric flow rate multiplied by the gas viscosity. Thus it is proportional to the average disc temperature to the power of $3/2$. In one case the pressure drop increased from 43 to 58

millimetres of mercury, indicating a disc temperature of 85°C.

The increase in the disc temperature due to the lesser conduction across the sleeve is a disadvantage since it causes the flow to alter slowly until the disc reaches its equilibrium temperature, increasing the time taken for the flow and flame composition to reach a steady state after any alteration, and causing an initial drift in the quantities being measured. This effect occurs also without the sleeve but its magnitude is smaller since the disc remains cooler. Measurements were not taken until the quantities being measured reached steady values.

When a disc is surrounded by a brass sleeve the disc can become hot while the sleeve remains relatively cool. Because the disc cannot expand freely, as it can without the sleeve, stretching of the sleeve or compression of the disc can occur. The result was that after repeated use the disc tended to become loose or to rise in the sleeve, particularly after stabilizing flames with high rates of heat loss to the disc. The disc was liable to emerge suddenly from the burner because of the pressure drop across it. This was potentially dangerous since it could allow the flame to burn past the disc and ignite gas in the burner and flow system. To prevent discs being pushed up out of the sleeves some discs and sleeves were made tapered so that the discs were

slightly wider at the bottom. The discs were push-fitted into these sleeves.

9.2.2. Other Burners Used for Premixed Flames.

All the results for premixed flames given in Ch.X, except those for flames containing bromine or metallic salts, were obtained using the porous disc burner. The results for premixed ethylene/air flames given in Ch.VIII were obtained using a rectangular matrix burner water-cooled round the edge.

The measurements to determine the effect of bromine (in premixed and diffusion flames) were taken using an Egerton-Powling matrix burner (Egerton and Thabet, 1952). The measurements on the effect of seeding premixed flames with metallic salts were made using a Meker burner.

9.2.3. Burners Used for Diffusion Flames.

The types of diffusion flame on which measurements were made are discussed in Ch.VII. Measurements on counter-flow diffusion flames were obtained using the burner of Pandya & Weinberg (1963) or using the two porous disc burners facing each other. The burners used for measurements on free burning diffusion flames consisted of various nozzles. The electrodes were simply metal plates or gauzes. The results obtained and further details of the experimental arrangements are given in Ch.XI.

9.3. Electrical Measurements.

9.3.1. Electrical Circuit.

The circuit used is shown in Fig.IX(1). The burner, K, was maintained at a high potential by several HT batteries, L, or by a Brandenburg 20 kV unit. The upper electrode, M, and probe, N, were at near earth potential. The current to the upper electrode and probe were measured by a microammeter, P. A two-way switch, Q, either earthed the rest of the upper electrode or connected it to the probe, enabling either the probe current or the total current to be measured. The burner potential was obtained by measuring the current to earth through a high resistance of known value. The same microammeter was used to measure the current to the probe and upper electrode and the voltage, by means of a reversing switch, R. This arrangement saved the expense of having two meters and saved bench space. The microammeter had five scales with full scale deflections from one microamp. A second reversing switch was installed, before the microammeter, to avoid having to reverse the leads every time the polarity was changed.

9.3.2. Safety Measures.

To make the system safer during connecting up and use, the current from the high voltage source was limited by

high resistances. Because of the desirability of limiting the current to the burner, it was necessary that the resistance from the burner to earth should be very high. The burner supports were therefore insulated and the cooling water to and from the burner was passed through several yards of narrow-bore tubing. The water was expelled into a sink through an earthed metal tube in order to prevent fluctuations in the resistance to earth, which would otherwise cause fluctuations in the potential of the burner. The maximum resistance of the microammeter was 20,000 ohms. The leakage resistance from the upper electrode had to be much higher than this value for accurate current measurements to be obtained.

de Gruchy (1953) has considered ways of protecting galvanometers against high fault currents and discussed possible effects of overloading. Since it was not intended to operate at near breakdown voltages it was decided to limit the maximum current by resistances in series with the voltage source and to use the microammeter without any further protection in most cases.

A Pt/Pt-Rh thermocouple was used to measure the flame temperature. The potential difference was measured using the microammeter. A reversing switch enabled the same meter to be used to measure the voltage and flame

current. The voltage source was turned off while temperature measurements were made, to avoid errors due to any effect of the field and to avoid possible damage to the microammeter if the thermocouple broke. It was found that the thermocouple reading was altered by the equivalent of a few degrees when the field was on.

The thermocouple was left in position during current measurements for convenience and to eliminate any random error due to its being replaced in slightly different positions. To avoid error due to current flowing to the thermocouple, the current to the thermocouple was included in the current measured. For this purpose the thermocouple was connected to the microammeter through a high resistance. The thermocouple was also connected to earth through a neon bulb, which did not conduct at low voltages, in order to protect the microammeter in the event of the thermocouple breaking and touching the burner.

9.3.3. Measurements.

The circuit used included facilities for measuring either the total flame current or the current to a probe. The measurement of probe current avoids edge effects and permits measurements to be taken on a selected part of the flame, which may be more uniform than the rest. The variation of probe current across the flame can be used to

check the uniformity of the flame. As mentioned previously, it is often necessary to measure probe current in the case of rich flames since secondary combustion of the excess fuel occurs in the surrounding air and this adds to the total current.

As shown in Ch.VIII, the proportion of the total saturation current going to the probe, i_p/i_t , is not constant. It would therefore appear to be more reliable to measure the total current in most cases. The total current is larger and easier to measure. It gives the current density directly where the flame is uniform and i_p/i_t is constant. For runs giving constant i_p/i_t the total current was measured. For rich or non-uniform flames the probe current was recorded. The average value of i_p/i_t for the system was obtained on each occasion by making measurements on several lean hydrocarbon/air flames. The area of flame from which current went to the probe was estimated from this value of i_p/i_t .

The disturbance of free burning diffusion flames by longitudinal fields obtained by placing an electrode above the flame can be comparatively small (Nakamura, 1959). The large electrode separation necessary would be likely to limit greatly the current which could be drawn without breakdown. Placing an electrode along the axis of the flame,

with a cylindrical electrode round the flame, was found to be impracticable, as the flame was not sufficiently steady. Measurements on diffusion flames on nozzles and with the batswing burner were therefore carried out with electrodes on either side of the flame to obtain the minimum electrode separation in order to maximise the saturation current which could be drawn, although this arrangement distorted the flames.

9.4. Measurement of Final Flame Temperature.

The final flame temperature of premixed flames was measured because it is of the most important variables affecting the rate of ionization in flames (see Ch.I). Its value is needed to calculate the effective activation energy of the ionization process, and to find the saturation current density for adiabatic flames, if required, by extrapolation.

The temperature was measured by two methods: by thermocouple and by sodium line reversal.

9.4.1. Thermocouple Method.

The thermocouples used were 0.001" diameter Pt/13%Rh-Pt, which were joined by touching the wires together at high temperature. The resistance of the thermocouple was of the order of 10 ohms. The thermal

e.m.f. was measured by a microammeter of resistance 20,000 ohms, which was calibrated against a potentiometer. Fig. IX(4) shows the variation with height above the burner of the temperature measured by an uncoated thermocouple for two ethylene/air flames. It can be seen that the apparent temperature gradient is greater near the flame, which suggests that catalytic heating or recombination may have occurred at the thermocouple surface. The temperature gradients exceeded those due to radiation from the hot gases, calculated from data given by Perry (1963) and shown in Fig. IX(4) by solid straight lines. Thus the higher temperature gradients appear to have been partly due to conduction. It was difficult to estimate the precise flame temperature or where the temperature given by the thermocouple was equal to the flame temperature. Coating the thermocouple made little difference, so uncoated thermocouples were used. The flame temperature was taken to be equal to that given by a thermocouple 6 mm above the burner. It can be seen from Fig IX(4) that this is approximately correct, assuming that the dotted lines, representing the straight part of the graphs extrapolated back to the flame, give the actual flame temperatures. A radiation correction was made to the thermocouple using the equation employed by Kaskan (1957).

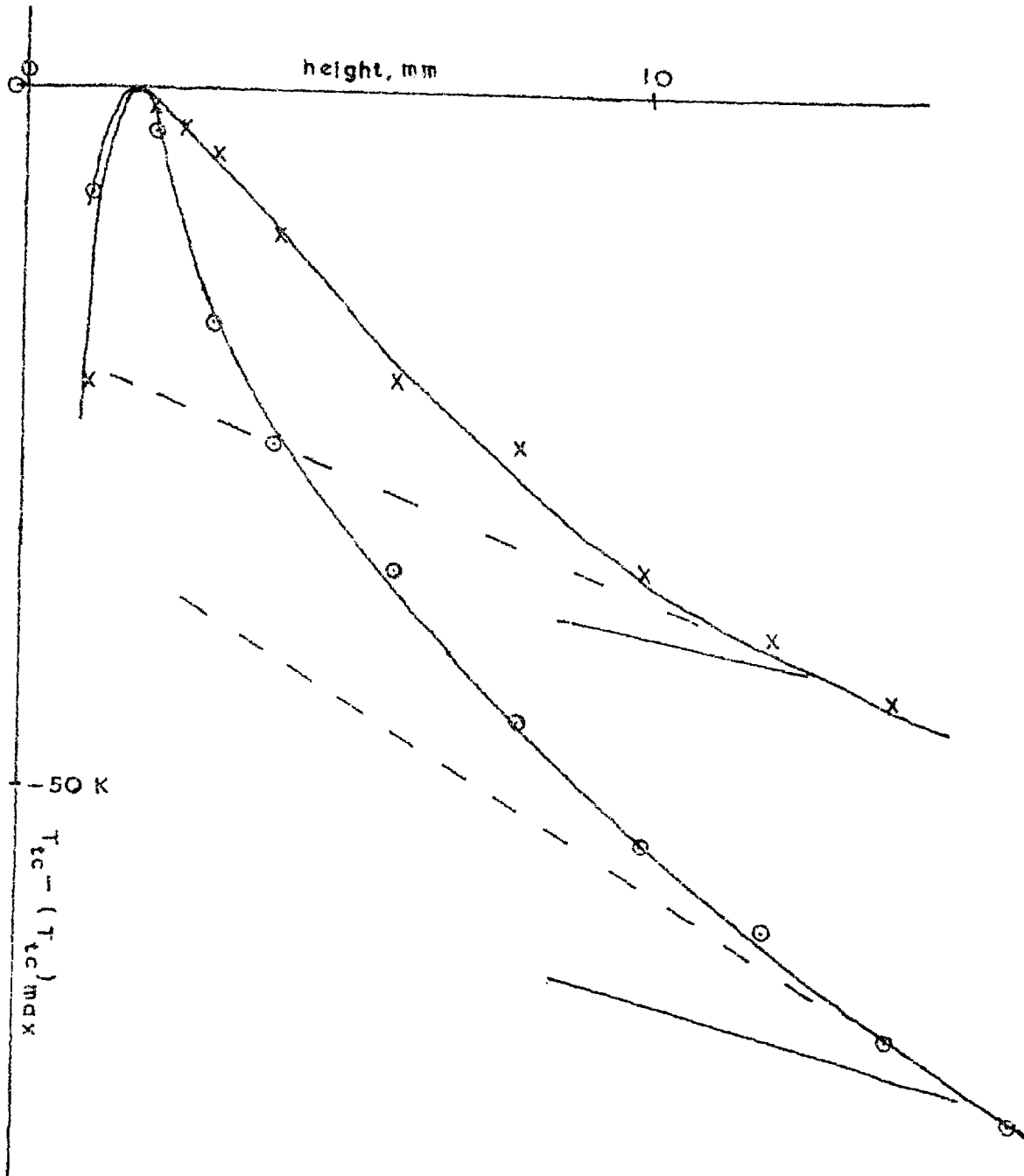


FIG. IX (4). THERMOCOUPLE READING
VERSUS HEIGHT ABOVE FLAME

9.4.2. Sodium Line Reversal Method.

The sodium line reversal method of temperature measurement is described e.g. by Gaydon & Wolfhard (1960). The sodium was introduced in the form of borax on a platinum wire or (for very hot flames) placed on the disc. It was found that borax lasted longer than sodium chloride and was easier to collect on a wire. Sodium chloride can lead to the formation of harmful oxides of chlorine. The sodium line reversal temperature was measured 5 to 10 mm above the flame and no corrections were necessary. The experimental system is shown in Fig IX(1).

Measurements of the sodium reversal temperature, T_{Na} , were made on methane/air flames of the same stoichiometric ratio (1.25) on two different occasions, the apparatus being set up before each run. The following results were obtained:

Run 1.	S_u , m/s	0.103	0.118	0.141	0.165	0.190	0.224	0.232
	T_{Na} , °K	1785	1826	1871	1904	1929	1943	1988
Run 2.	S_u , m/s	0.145	0.162	0.198	0.210	0.230		
	T_{Na} , °K	1885	1919	1948	1976	2003		
	T'_{Na} , °K	1879	1903	1943	1958	1978		

T'_{Na} is the temperature estimated from the results of Run 1 by plotting a graph of T_{Na} versus S_u . These measurements show that Run 2 gave results 14 K higher on

average than Run 1, which indicates that the systematic error is of the order of ± 10 K. The random error appears to be of the order of 8 K. The error due to inaccuracy in the measurement of S_u , assuming the latter to be of the order of 2%, is about 4 K.

9.4.3. Comparison of Sodium Reversal and Thermocouple Methods.

The sodium line reversal method is less reliable at lower temperatures because of the lower intensity and the difficulty of accurately calibrating the source at lower temperatures. Measurements at lower temperatures (up to about 1820°K) were therefore made by the thermocouple method. At higher temperatures the thermocouple method is less reliable owing to the high radiation correction. At very high temperatures the thermocouple melts and the sodium line method must be used.

Measurements taken to compare temperatures given by the thermocouple method, T_{tc} , and by the sodium reversal method, T_{Na} , for air flames gave the following results:

Fuel	CH_4	C_2H_6	C_3H_8
ϕ	1.04	0.91	1.02
$T_{Na}, ^\circ\text{K}$	1826	1820	1825
$T_{tc}, ^\circ\text{K}$	1810	1817	1810

These results show that for lean and stoichiometric flames the temperatures given by the two methods are in very good agreement.

The following results for rich flames are given in the order in which they were obtained:

Run 1, CH_4/air , $\phi = 1.3$.

T_{Na} , °K	1687	1727	1801
T_{tc} , °K	1692	1679	1744

Run 2, CH_4/air , $\phi = 1.64$.

T_{Na} , °K	1754	1794
T_{tc} , °K	1762	1717

These results for rich flames show that the first temperature measurement in each run obtained by the thermocouple agrees with the sodium line reversal method but that subsequent measurements are lower. Thus it seems likely that the temperatures given by the thermocouple for rich hydrocarbon flames is low as a result of carbon being deposited on the thermocouple, which would increase the heat loss by radiation. Carbon deposited on the thermocouple as a result of fluctuations in the composition of the gas would not be burnt off in rich flames. These results show that the thermocouple method is not suitable for rich flames.

9.4.4. Experimental Procedure.

For most of the results the temperature was measured for each flame. For others the temperature was measured for several flames at a fixed composition but different burning velocities and a graph plotted of temperature versus burning velocity. Current measurements were also taken for several flames at this composition and different burning velocities and their temperatures read off the graph. This was done partly for convenience and, for very hot flames, because the borax had to be placed on the disc, so that the temperature and current could not be measured for each flame without washing the disc to remove the borax after each temperature measurement. Plotting the flame temperature versus the burning velocity also helped to reduce the random errors in the former, the latter being measurable more accurately.

9.5. Sources of Error.

9.5.1. Errors in Measuring the Current.

Any error in the microammeter reading would be small. The microammeter was accurate to 2%. Measurements taken with an applied voltage but no flame showed that stray currents were negligible. Measurements taken with a flame but no applied voltage showed that the current at zero

voltage was also negligible and could be ignored. The resistance of the microammeter was different for each range. Readings were taken on different scales to verify that the current was not reduced by the meter resistance. The resistance from the upper electrode to earth and that from the probe to the rest of the upper electrode were also re-measured periodically.

The flame area was taken to be equal to the area of the disc. The possible error due to this assumption is estimated at 2%. The proportion of the total current which goes to the probe is not constant (see Ch.VII) and was measured, using lean air flames, for each set of results. The error in the saturation current densities derived from probe current measurements due to inaccuracy of the estimated probe areas was estimated at less than 5%.

If the current potential curve does not have a flat plateau there is, to that extent, no precise saturation current. Premixed flames were found to give flat plateaux, as did most diffusion flames within about 10%. These results indicate that the rate of ion generation is not directly affected by the field.

Whether ionization of impurities contributes appreciably was checked by taking measurements on H_2 and CO flames. Such ionization was found to be negligible for premixed flames.

9.5.2. Errors in Measuring the Final Flame Temperature.

Errors in the temperature measurement for premixed flames are the most serious inaccuracy since the current varies steeply with the flame temperature (see Ch.I).

The flame temperature varied across the discs. An attempt was made to measure the temperature at a point near the average value. The average error due to the variation across the discs was estimated at about 10 K.

The error in the thermocouple temperature due to uncertainty in the radiation correction is thought to be of the order of 10 K. That due to catalytic heating and uncertainty of the height at which the thermocouple gives the correct flame temperature is probably of the same order. The error due to inaccuracy of the assumed thermocouple resistance and the voltage drop across the microammeter is estimated to be under 5 K.

The sodium line reversal method is thought to be valid outside the reaction zone (Greig, 1965). Systematic errors in the method are discussed by Gaydon & Wolfhard (1960) and by Snellerman (1967) and may be up to 20 K.

The above estimates show that the total systematic error in the temperature measurements is not greater than 25 K. Comparison of the results given above for measurements taken on different occasions or by the two methods indicate that it is less.

9.5.3. Errors in Measuring Flow and Composition.

The purity of the hydrocarbon gases used was approximately 95% or more in most cases, most of the impurity being other hydrocarbons. The gases were assumed to be pure except in the case of methane used for some of the measurements, which contained 14% of air.

The errors in the measured flows and stoichiometric ratios are probably of the order of 2% and can be ignored since the saturation current varies comparatively little with composition.

9.5.4. Discussion.

Systematic errors matter less when obtaining the variation of current with temperature and calculating the effective activation energy, since if all the saturation currents are wrong by a constant factor the value obtained for the activation energy is unaltered. Random errors can be reduced by taking large numbers of measurements.

It has been estimated that the accuracy of the current density measurements is of the order of 5% and that of the temperature of the order of 25 K or less. This shows that the proposed method is suitable for investigating the variation of saturation current and that it is capable of giving reasonably accurate results.

The random errors are difficult to predict and their importance can best be estimated from the scatter of the results.

PART III RESULTS.CHAPTER TEN.PREMIXED FLAMES.

All the results in this chapter are for flames at atmospheric pressure and were obtained with electrode separations of about 15 mm.

Mixture strengths are given in terms of the stoichiometric ratio, ϕ , which is defined by

$$\phi = \frac{c_f/c_o}{(c_f/c_o) \text{ for stoichiometric mixture}}$$

where c_f , c_o are the initial concentrations of fuel and oxygen respectively.

Thus ϕ is unity for stoichiometric mixtures, greater than one for mixtures containing excess fuel, and less than one for mixtures containing excess oxygen

10.1. Air Flames.

For lean air flames it was found that the ratio of the probe saturation current, i_p , to the total saturation current, i_s , was approximately equal to the ratio of the probe area to the flame area. The saturation current density was therefore taken to be equal to i_t divided by the flame area, A_f . For rich flames, because of the surrounding diffusion flame, the saturation current density was taken to

be equal to i_p divided by the effective probe area, A_p , where $A_p = A_f \times (i_p/i_t$ for lean air flames). The results for non-luminous flames are given in Table X(1).

Graphs of $\log j_s$ versus $10^4/T_f$ °K (Figs. X(1- 11)) were plotted for all the flames. These graphs were straight lines over the greater part of their length. The gradients are given below:

Flame	ϕ	$\frac{d(\log j_s)}{d(10^4 / T_f \text{ } ^\circ\text{K})}$	Flame	ϕ	$\frac{d(\log j_s)}{d(10^4 / T_f \text{ } ^\circ\text{K})}$
CH ₄ / air	0.6	-1.28	C ₂ H ₆ / air	0.70	-1.14
	0.87	-0.96		0.91	-1.06
	1.04	-1.27	C ₂ H ₄ / air	0.52	-1.44
	1.25	-1.72		0.69	-1.52
	1.30	-1.82		0.85	-0.94
	1.39	-1.99		1.05	-0.89
	1.64	-5.6		1.17	-1.00
C ₃ H ₈ / air	0.69	-0.82	1.61	-1.59	
	1.02	-0.32	1.83	-2.50	
	1.27	-1.6	2.0	-3.62	
			2.4	-4.28	

10.2. Oxygen Flames.

The ratio of the probe current to the total current was not generally equal to A_p/A_f for oxygen flames. For richer flames ($\phi = 0.25$ to 1.0) it was less. However,

i_p/i_t was found to be constant within the experimental error for each composition over the range of burning velocities studied. i_t was measured because it was larger and therefore subject to smaller errors. Where i_p/i_t differed from A_p/A_f by more than 10%, the average value, $(i_p/i_t)_{av}$, is given and the saturation current density taken to be equal to $(i_p/i_t)_{av} i_t / A_p$.

Some hydrocarbon/oxygen flames were noisy. When the upper electrode was lowered the noise became louder and the saturation current increased. Observation of the saturation current on a cathode ray oscilloscope showed that the current from noisy flames varied periodically. The amplitude of this oscillation was of the order of $\frac{1}{2}\%$ of the mean current for quiet flames, 3% for nearly quiet flames, and up to 50% for the most noisy flames. Hydrogen added to noisy flames made them quiet and reduced the saturation current. Results for flames with hydrogen added lay on straight lines whereas those for noisy flames gave higher saturation currents. About 5% of hydrogen was therefore added to some flames to make them quiet. The final flame temperatures were found to be unaffected by the addition of this amount of hydrogen to noisy or quiet flames. Results with hydrogen are shown on the graphs (Figs. X(8- 10)) by x, those without by +. The results are given in Table X(2).

Graphs of $\log j_s$ versus $10^4/T_f$ °K for hydrocarbon (/hydrogen)/oxygen flames are given in Figs.X(8 - 11). All the graphs were approximately straight lines over most of their length except that for propane/oxygen at $\phi = 0.275$. The gradients are given below:

Flame	ϕ	% H ₂	$d(\log j_s)/d(10^4/T_f \text{ °K})$
CH ₄ /H ₂ /O ₂	0.187	0	-1.52
	0.187	3.4	-1.69
	0.30	0	-1.43
	0.30	4.9	-1.37
	1.00	0	-1.62
	1.51	0	-2.41
C ₂ H ₆ /H ₂ /O ₂	0.152	0	-1.69
	0.262	0	-1.89
	0.272	4.8	-1.31
C ₃ H ₈ /H ₂ /O ₂	0.150	0/2.9	-1.45
	0.275	5.1	-1.35
C ₂ H ₄ /H ₂ /O ₂	0.155	0/2.9	-1.55
	0.254	0/4.6	-1.43

10.3. Hydrogen and Carbon Monoxide Flames.

The saturation currents of some flames of hydrogen, carbon monoxide, and both these gases together, in which chemi-ionization is thought to be absent, were measured to

see if any ionization was obtained. The results are given in Table X(3).

10.4. Effect of Composition on Burning Velocity.

The burning velocities of some methane flames were measured to establish the dependence on composition. The results are given in Table X(4).

10.5. Effect of Additives.

10.5.1. Carbon Dioxide.

Carbon dioxide was added to a number of premixed hydrocarbon/air flames. In every case the final flame temperature was increased and the saturation current was decreased. Up to 15% of CO_2 was added. The saturation current was reduced by up to 40% compared with flames with the same final temperature but without CO_2 added.

The effect of adding carbon dioxide to a premixed ethylene/oxygen flame (see section 10.5.2) is illustrated in Fig.X(14), which shows that for this flame the saturation current was increased.

About 12% of carbon dioxide added to premixed hydrogen/air flames containing a little methane reduced the temperature by 44 K in one case but reduced the current by only 8%. In the other case the temperature was also considerably reduced but i_s was increased.

15% of carbon dioxide was added to a premixed CO/air flame containing a small amount of methane. The temperature decreased by 15 K, which corresponds to a reduction of the saturation current of about 14%, assuming an activation energy of 210 kJ mole^{-1} . The current was reduced, however, by 38% from 0.37 to 0.23 μA .

The above results indicate that carbon dioxide reduces the saturation currents of premixed hydrocarbon/air flames and CO/air flames containing a small amount of hydrocarbon, but tends to increase it in the cases of flames with oxygen and hydrogen/air flames containing a little hydrocarbon.

10.5.2. Carbon Monoxide.

The effect of adding CO to a premixed ethylene/oxygen flame is shown in Fig.X(15), which shows n_e/n_c calculated from the total saturation current. These results, and those for the addition of CO_2 , H_2 , and N_2 shown in Figs.X(14), (16), and (17), are for a series of premixed ethylene/oxygen flames at a constant thermocouple reading corresponding to a final flame temperature of about 1550°K . The oxygen flow was constant at 5.50 l min^{-1} . When additives were present the thermocouple temperature was kept constant by reducing the ethylene flow rate.

10.5.3. Hydrogen.

The result of adding hydrogen to a premixed ethylene/oxygen flame (see section 10.5.2) is shown in Fig.X(17). Results for other oxygen flames containing hydrogen are given in Table X(2).

10.5.4. Nitrogen.

Fig.X(16) shows the effect of adding nitrogen to a premixed ethylene/oxygen flame (see section 10.5.2). Nitrogen added to premixed ethylene/air flames gave increases in the saturation currents which corresponded approximately to the increase in the final flame temperatures.

10.5.5. Bromine.

Results for premixed air flames are given below. The burning velocity was constant at 0.034 m s^{-1} . The third column gives the changes in the final flame temperature resulting from the addition of bromine and is probably accurate to about 20%. The fifth column shows the change in the saturation current due to the change in flame temperature, calculated assuming an activation energy of 210 kJ mol^{-1} . The sixth (last) column is the change in the saturation current which must be due to the bromine.

Flame	% Br ₂	T _f , °K	i _t , μA	Δi _t , %	Δi _t due to T _f , %	Δi _t , due to Br ₂ %
Near limit	0.38	+17	3.30	- 2	+24	-21
C ₃ H ₈ /air	0.61	+18	3.08	-16	+26	-33
CH ₄ /air	0.13	+ 4	2.10	+15	+ 5	+10
ϕ = c 0.55	0.16	+ 5	2.28	+10	+ 6	+ 3
	0.27	+11	2.38	+ 9	+15	- 5
	0.46	+26	2.32	+13	+40	-20

10.5.6. Metallic Salts.

To determine whether the rate of chemiionization in flames containing hydrocarbon is altered by the addition of metallic additives, and in particular whether chemiionization of the metal occurs, small amounts of sodium and lead salts were added to a premixed CO/C₂H₄/air flame as described in Ch. IX. The results obtained are shown in Fig. X(18). Doubling the height of the upper electrode from the flame approximately doubled the saturation current due to sodium addition, which confirms that most of the sodium added was not ionized.

10.6. Luminous Flames.

Two ethylene/air flames having the same

stoichiometric ratio (approximately 3.0) were investigated. The probe saturation currents, i_p , at height h above the flame are shown in Fig.X(13).

The brightness temperature, T_{br} , at 6550 \AA of the luminous region above the flame was measured by an optical pyrometer. The optical path length was approximately 40 mm. A_p was 1.1 cm^2 . The results obtained are given below:

S_u , m s^{-1}	T_f , $^{\circ}\text{K}$	T_{br} , $^{\circ}\text{K}$	di_p/dh mA m^{-1}	J , A m^{-3}
0.103	1784	1250	0.155	1.41
0.146	1880	1132	0.066	0.62

Samples of soot taken from the two flames were examined under an electron microscope. It was found that most of the particles had a diameter of about 300 \AA . The cooler flame yielded many more particles.

The yellow luminosity did not start for a distance of about 7 mm above the flame. The results show that little ionization occurred below this height.

It was found that the emissivity of the luminous region above the flame per unit path length was not altered by an applied field. The variation of i_p with voltage, V , was measured for the cooler flame with an electrode separation of approximately 13 mm. The results, given below, show that the saturation current had a well defined value (0.71 \mu A in

this case):

V, volt	104	190	385	590	830	978	
i_p , μA	0.016	0.026	0.053	0.089	0.143	0.179	
V, volt	1380	1670	1990	2900	4080	5910	7000
i_p , μA	0.27	0.37	0.54	0.65	0.70	0.74	1.0

10.7. Summary.

The variation of saturation current density with final flame temperature has been measured for lean premixed flames of methane, ethane, propane and ethylene with air and with oxygen at several different stoichiometric ratios in each case. Measurements were also taken for rich luminous and non-luminous ethylene/air and methane/oxygen flames. The saturation currents of flames of hydrogen and carbon monoxide were also measured, and found to be low.

The saturation current densities of the non-luminous flames increased with the final flame temperature and were greater for flames with air than with oxygen. The highest saturation currents were given by near stoichiometric flames.

Measurements were carried out to find the effect of the addition of small proportions of hydrogen, carbon monoxide, bromine, nitrogen, and carbon dioxide. The effects obtained were not large. Carbon dioxide reduced the saturation currents of certain flames. Measurements were

also made to determine the effect of the addition of sodium and lead salts to carbon monoxide flames with and without ethylene added. The saturation currents due to the metals and the hydrocarbon were found to be additive.

The significance of these results will be discussed further in Ch.XII.

Table X(1).

Saturation current densities of non-luminous premixed hydrocarbon/air flames.

Methane/air:

$$A_f = 13.2 \text{ cm}^2, \quad A_p = 1.3 \text{ cm}^2, \quad A_f/A_p = 10.2.$$

ϕ	$T_f,$ $^{\circ}\text{K}$	$i_t,$ μA	$j_s,$ mA m^{-2}	ϕ	$T_f,$ $^{\circ}\text{K}$	$i_p,$ μA	$j_s,$ mA m^{-2}
0.6	1574	1.23	0.93	1.04	1818	2.39	18.4
	1602	1.88	1.42		1896	4.78	36.8
	1638	3.05	2.31		1924	5.7	43.9
	1646	3.38	2.56		1980	8.2	63
	1671	4.05	3.07		2000	8.95	69
0.87	1550	1.96	1.49	2009	9.63	74	
	1575	2.61	1.98	2035	11.0	83	
	1628	5.40	4.09	2046	12.9	99	
	1667	7.87	5.96	2059	13.7	104	
	1713	12.0	9.1	2061	14.8	114	
	1767	17.1	13.0	2079	16.1	124	
	1818	25.9	19.6	2112	18.0	138	
	1833	28.8	21.8	1.25	1832	2.56	19.7
	1836	29.1	22.0		1871	3.98	30.6
	1861	30.3	23.0		1891	4.47	34.4
	1904	40.1	30.4		1926	7.05	54.1
	1939	50.0	32.8		1941	9.0	69
	1963	54.8	41.5		1960	10.3	79
	2004	71.5	54.1		1982	14.2	109
2020	81	61.3	2013	18.9	145		
2039	98	74					
0.87	1681	8.7	6.6				
check	1837	27.6	20.9				
run	1988	52.0	39.4				
	2028	91.9	69.5				

ϕ	$T_f,$ $^{\circ}\text{K}$	$i_p,$ μA	$j_s,$ mA m^{-2}	$i_t,$ μA	$\frac{i_t}{i_p}$
1.30	1792	1.06	8.2	15.8	14.9
	1859	2.02	15.6	26.3	13.0
	1909	3.35	25.8	41.9	12.5
	1931	4.77	36.7	57.1	12.0
	1957	6.15	47.3	73	11.8
	1980	8.9	66	92	10.7
	2017	11.8	91	121	10.3
1.39	1752	0.37	2.84		
	1866	1.74	13.4		
	1913	3.3	25.4		
	1942	4.8	37		
	1969	6.43	44.5		
1.64	1747	0.025	0.19		
	1812	0.35	2.7		

Ethane/air:

$$A_f = 13.2 \text{ cm}^2$$

$\phi = 0.70$			$\phi = 0.91$		
$T_f,$ $^{\circ}\text{K}$	$i_t,$ μA	$j_s,$ mA m^{-2}	$T_f,$ $^{\circ}\text{K}$	$i_t,$ μA	$j_s,$ mA m^{-2}
1451	1.45	1.10	1605	7.1	5.4
1512	2.6	1.97	1712	19.7	14.9
1603	6.6	5.0	1746	32	24.2
1632	10.0	7.6	1823	54.5	41.1
1689	18.0	13.6	1883	81	61
1735	24.1	18.3	1955	127	96
1741	27.0	20.5	1984	178	135
			2018	203	154

ϕ	$T_f,$ $^{\circ}\text{K}$	$i_t,$ μA	$j_s,$ mA m^{-2}	j_s at 1675°K mA m^{-2}	$f(\text{C}_2\text{H}_6)$ l min^{-1}	n_e/n_c $\times 10^{-7}$	n_e/n_c at 1675°K $\times 10^{-7}$
0.74	1661	15.7	11.9	13.4	0.829	1.34	1.42
0.80	1671	18.0	13.6	14.1	0.716	1.77	1.80
0.91	1681	18.8	14.3	13.5	0.653	2.03	1.97
0.97	1689	17.8	13.5	11.9	0.578	2.17	2.04

j_s and n_e/n_c at 1675°K were calculated taking j_s and the reaction rate to have effective activation energies of 210 kJ mole^{-1} .

Propane/air:

$$A_f = 13.2 \text{ cm}^2, \quad A_p = 1.3 \text{ cm}^2, \quad A_f/A_p = 10.2$$

ϕ	$T_f,$ $^{\circ}\text{K}$	$i_t,$ μA	$j_s,$ mA m^{-2}	ϕ	$T_f,$ $^{\circ}\text{K}$	$i_t,$ μA	$j_s,$ mA m^{-2}
0.69	1449	2.75	2.1	1.02	1837	56	42.5
	1515	4.5	3.4		1887	77	58.4
	1588	6.7	5.1		1949	103	78
	1638	9.8	7.4		2010	161	126
	1689	15.0	11.4		2038	192	145
	1736	22.7	17.2		2050	210	159
	1814	31.8	24.1		2071	259	196
	1839	36.0	27.3		2080	272	206
1.02	1584	8.9	6.7	2090	300	227	
	1680	21.0	15.9	2102	338	256	
	1757	34.9	26.4				

ϕ	$T_f,$ $^{\circ}\text{K}$	$i_p,$ μA	$j_s,$ mA m^{-2}	$i_t,$ μA	$\frac{i_t}{i_p}$
1.27	1630	0.4	3.1	8.7	21.8
	1687	1.0	7.7	16.9	16.9
	1754	2.52	19.4	33.7	13.4
	1807	5.0	38.4	61.5	12.3
	1857	7.7	59.4	90	11.6
	1909	12.0	92	132	11.0
	1947	17.0	131	188	11.1
	1972	22.7	175	241	10.6
	1990	26.9	207	283	10.5

Ethylene/air:

$A_F = 13.2 \text{ cm}^2$ for $\phi = 0.69, 0.85, 1.05$ to 1.83 ;

$A_F = 18.8 \text{ cm}^2$ for $\phi = 0.52, 2.0, 2.4$;

$A_p = 1.1 \text{ cm}^2$

ϕ	$T_f,$ $^{\circ}\text{K}$	$i_t,$ μA	j_s mA m^{-2}	ϕ	$T_f,$ $^{\circ}\text{K}$	$i_t,$ μA	$j_s,$ mA m^{-2}
0.52	1374	0.45	0.24	0.69	1708	33.7	25.5
	1408	0.88	0.47		1751	46.0	34.8
	1448	1.87	1.00		1800	63.8	48.4
	1479	3.06	1.63	0.85	1648	24.3	18.4
	1503	4.09	2.17		1727	38.6	29.2
	1532	4.35	2.31		1783	58	44.0
	1559	5.7	3.03		1801	66	50.0
					1828	78	59.1
0.69	1390	0.63	0.48	1859	100	76	
	1446	1.38	1.05	1894	125	94.5	
	1497	3.20	2.42	1920	139	105	
	1540	6.02	4.56				
	1599	12.1	9.2				
	1631	17.0	12.9				
	1677	25.8	19.5				

\emptyset	$T_f,$ $^{\circ}\text{K}$	$i_t,$ μA	$j_s,$ mA m^{-2}	\emptyset	$T_f,$ $^{\circ}\text{K}$	$i_p,$ μA	$j_s,$ mA m^{-2}				
1.05	1772	90	68	1.83	1739	0.029	0.26				
	1814	119	90		1800	0.15	1.36				
	1827	148	112		1856	0.52	4.7				
	1849	157	119		1929	1.35	12.4				
	1888	199	151		1964	2.38	21.8				
	1920	239	181		2001	4.03	36.8				
	1930	233	177		2042	6.7	61				
	1950	270	205		2.0	1750	0.010	0.09			
	1981	312	236	1776		0.013	0.12				
2037	352	266	1817	0.042		0.38					
\emptyset	$T_f,$ $^{\circ}\text{K}$	$i_p,$ μA	$j_s,$ mA m^{-2}	1851		0.10	0.92				
				1884	0.23	2.1					
				1904	0.40	3.6					
				1920	0.80	7.5					
				1.17	1753	5.32	48.4	2.4	1747	0.001	0.01
					1826	8.9	81		1792	0.003	0.03
					1874	11.9	108		1824	0.009	0.08
1910	15.7	143	1860		0.020	0.18					
1945	20.0	181	1869		0.030	0.27					
1981	25.1	228	1902		0.09	0.83					
2037	34.1	310	1918	0.12	1.10						
1.61	1838	3.7	33.6								
	1902	7.5	68								
	1908	7.5	68								
	1943	11.5	104								
	1992	18.1	165								

ϕ	$T_F,$ $^{\circ}K$	$i_t,$ μA	$j_s,$ $mA\ m^{-2}$	j_s at $1569^{\circ}K$ $mA\ m^{-2}$	$f(C_2H_4)$ $l\ min^{-1}$	n_e/n_c $\times 10^{-7}$	n_e/n_c at $1569^{\circ}K$ $\times 10^{-7}$
0.50	1546	6.0	3.2	3.8	0.54	0.78	0.93
0.56	1548	6.9	3.7	4.3	0.515	0.95	1.03
0.70	1554	9.6	5.1	5.8	0.48	1.41	1.51
0.80	1570	13.7	7.3	7.2	0.46	2.10	2.09
0.83	1563	12.0	6.4	7.0	0.42	2.02	2.12
0.94	1589	16.1	8.6	7.4	0.40	2.84	2.64
1.03	1611	19.1	10.2	7.8	0.395	3.41	3.00

j_s and n_e/n_c at $1569^{\circ}K$ were calculated taking j_s and the reaction rate to have effective activation energies of $210\ kJ\ mole^{-1}$. A_f was $18.8\ cm^2$.

Table X(2)

Saturation current densities of premixed hydrocarbon/hydrogen/oxygen flames.

Methane/hydrogen/oxygen:

For $\phi = 0.137$: $A_f = 18.3\ cm^2$, $j_s = i_t/A_f$.

$A_p = 1.3\ cm^2$

For $\phi = 0.30$: $i_p/i_t = 0.050$, $j_s = (i_p/i_t)i_t/A_p$.

For $\phi = c\ 1.0$, $i_p/i_t = 0.027$.

For higher values of ϕ , $j_s = i_p/i_t$ was taken.

ϕ	%H ₂	T _f , °K	i _t , μA	j _s , mA m ⁻²	
0.187	0	1547	0.032	0.02	
		1609	0.101	0.06	
		1656	0.21	0.12	
		1700	0.37	0.20	
		1722	0.50	0.27	
		1767	0.79	0.43	
		1797	1.15	0.63	
		3.4	1610	0.16	0.09
	1685		0.42	0.23	
	1739		1.04	0.57	
	0.30	0	1498	0.10	0.04
			1623	0.38	0.15
			1693	0.78	0.30
			1752	1.54	0.59
1795			2.40	0.93	
1845			4.10	1.58	
4.9			1739	1.92	0.74
		1804	3.70	1.42	

In the case of near stoichiometric and rich methane/oxygen flames, below, it was difficult to measure the temperature accurately. The final flame temperatures, T_f, were estimated from graphs of the measured temperature, T_{obs}, versus the burning velocity, S_u.

ϕ	$S_u,$ $m s^{-1}$	T_{obs} $^{\circ}K$	$T_f,$ $^{\circ}K$	$i_t,$ μA	i_p μA	$j_s,$ $mA m^{-2}$
0.99	0.062	1896	1885	26.7		5.5
0.99	0.079		1935	52.9		11.0
1.00	0.083	1928				.
0.95	0.103	1991	2005	77		16.0
1.00	0.122	2082	2065	148		30.7
1.05	0.124	2066	2070	168		35
1.00	0.147		2140	192+		40+
1.45	0.072	1918	1910		0.09	0.7
1.58	0.103	1941	1955		0.17	1.3
1.50	0.104	1944	1960		0.24	1.8
1.50	0.130	2010	2010		0.46	3.5
1.52	0.170	2076	2055		0.65	5.0
1.50	0.189	2086				
2.04	0.063*	1875	1870		0.33	2.5
2.05	0.109 ⁺		1900		0.072	0.55
2.05	0.116	1897			.	.
2.08	0.131		1920		0.052	0.40
2.05	0.168	1960	1955		0.067	0.52

*, yellow luminosity above centre of flame,

⁺, slight yellow luminosity above flame.

The mean values of ϕ for the above three sets of results are 1.00, 1.51, 2.05.

Ethane/hydrogen/oxygen:

For $\phi = 0.152$: $A_p = 13.2 \text{ cm}^2$, $j_s = i_t/A_p$.

For $\phi = 0.262, 0.272$: $A_p = 1.5 \text{ cm}^2$, $i_p/i_t = 0.071$,

$$j_s = (i_p/i_t)i_t/A_p.$$

ϕ	%H ₂	T _f °K	i _t μA	j _s mA m ⁻²
0.152	0	1462	0.011	0.01
		1521	0.068	0.05
		1559	0.114	0.09
		1605	0.32	0.24
		1637	0.51	0.39
		1677	0.80	0.61
		1701	1.03	0.79
		1724	1.33	1.01
0.262	0	1516	0.255	0.12
		1571	0.50	0.24
		1625	0.81	0.38
		1677	1.97	0.93
		1702	3.0	1.41
		1743	6.0	2.8
0.272	4.8	1478	0.45	0.21
		1535	0.92	0.44

Propane/hydrogen/oxygen:

for $\phi = 0.15$, $j_s = i_t/A_f$.

for $\phi = 0.275$: $A_p = 1.5 \text{ cm}^2$, $i_p/i_t = 0.074$, $j_s = (i_p/i_t)i_t/A_p$.

ϕ	% H ₂	T _f , °K	i _t , μA	A _f , cm ²	j _s , mA m ⁻²
0.15	0	1487	0.22	18.3	0.12
		1540	0.39	18.3	0.21
		1560	0.58	18.3	0.32
		1600	0.81	18.3	0.44
		1614	0.83	18.3	0.45
		1646	0.68	13.2	0.57
		1663	1.32	18.3	0.72
		1713	1.55	13.2	1.17
	2.9	1461	0.09	18.3	0.05
		1487	0.15	18.3	0.08
		1530	0.25	18.3	0.14
		1548	0.33	18.3	0.18
		1569	0.44	18.3	0.24
		1615	0.84	18.3	0.46
0.275	0	1453	1.53		0.76
		1541	1.70		0.84
		1598	1.88		0.93
		1686	3.65		1.8
		1729	6.4		3.2
		1746	7.5		3.7
		5.1	1444	0.22	
	1533		0.60		0.30
	1577		1.10		0.54
	1650		2.8		1.38
	1699		5.4		2.7
	1709		6.4		3.15

Ethylene/hydrogen/oxygen:

For $\phi = 0.155$: $A_f = 13.2 \text{ cm}^2$, $j_s = i_t/A_f$.For $\phi = 0.254$: $A_p = 1.5 \text{ cm}^2$, $i_p/i_t = 0.068$, $j_s = (i_p/i_t)i_t/A_p$.

ϕ	% H ₂	T _f , °K	i _t , μA	j _s mA m ⁻²		
0.155	0	1349	0.01	0.01		
		1438	0.03	0.02		
		1492	0.09	0.07		
		1560	0.26	0.20		
		1593	0.44	0.33		
		1628	0.72	0.55		
		1653	1.21	0.92		
	2.9	1543	0.21	0.16		
		1575	0.47	0.36		
		1620	0.64	0.49		
		1635	1.16	0.88		
		0.254	0	1397	0.08	0.04
				1488	0.17	0.08
				1559	0.50	0.23
1613	1.50			0.68		
1663	2.95			1.33		
1724	5.7			2.6		
1744	7.0			3.2		
4.6	0	1526	0.54	0.25		
		1585	1.51	0.68		
		1662	3.1	1.4		
		1725	6.0	2.7		

Table X(3).

Saturation current densities of hydrogen and carbon monoxide flames.

$$A_f = 13.2 \text{ cm}^2$$

j_s at 2000 °K is calculated assuming an activation energy of 239 kJ mol⁻¹ (see section 12.5.1).

Calculated j_s at 1667°K = 0.063 x j_s at 2000°K.

Flame	H ₂ /air					H ₂ /O ₂	CO/O ₂
$i_s, \mu\text{A}$	0.005	0.032	0.019	0.057	0.030	0.008	1.43
$T_f, \text{°K}$	1525	1732	1653	1811	1715	1649	2398
j_s at 2000°K mA m ⁻²	0.28	0.20	0.26	0.18	0.23	0.12	0.11

Flame	H ₂ /CO/air			CO/air			
$i_s, \mu\text{A}$	0.033	0.072	0.029	0.9	0.6	0.4	0.72
$T_f, \text{°K}$	1700	1796	1762	2208	2038	2112	2160
j_s at 2000°K mA m ⁻²	0.29	0.25	0.15	0.19	0.35	0.15	0.20

Small amounts of H₂ were added to some of the CO/air flames to stabilize them.

Table X(4).

Burning velocities of methane flames.

Values marked with an asterisk are estimated by interpolation.

Burning velocities for stoichiometric and rich CH_4/O_2 flames are from values given in Table X(2).

% CH_4		8.4	8.6	9.9	11.6	13.0
T_f , °K		1797	1797	1798	1796	1795
ϕ	CH_4/air	0.87		1.04	1.25	
	CH_4/O_2		0.19			0.30
S_u , m s ⁻¹	CH_4/air	0.132		0.092	0.109	
	CH_4/O_2	0.207*	0.205	0.190*	0.167*	0.154
ϕ		1.0	1.04	1.25	1.5	2.05
T_f , °K		1960	1959	1960	1958	1960
S_u , m s ⁻¹	CH_4/air		0.165	0.221		
	CH_4/O_2	0.084	0.084*	0.090*	0.104	0.168

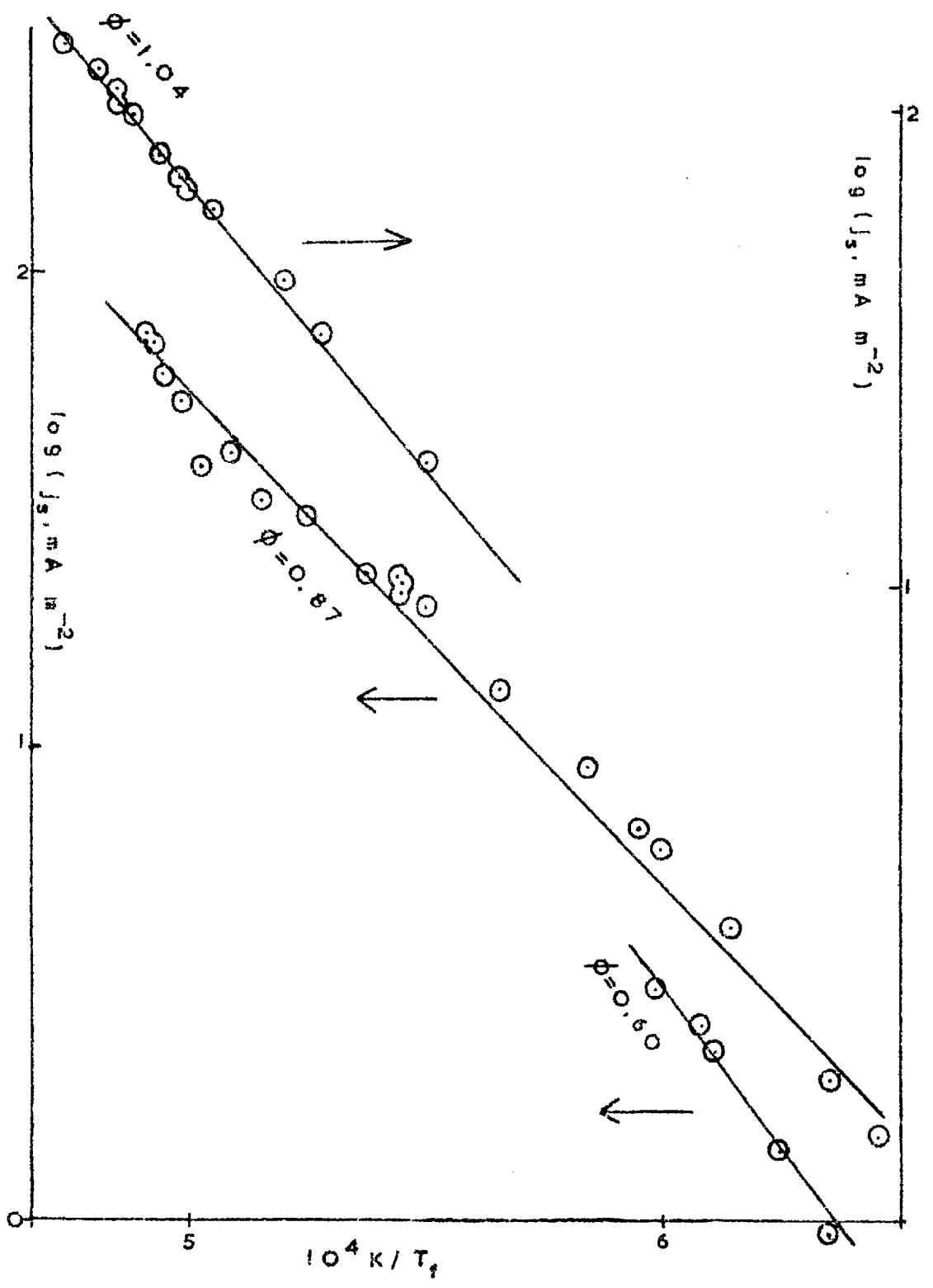
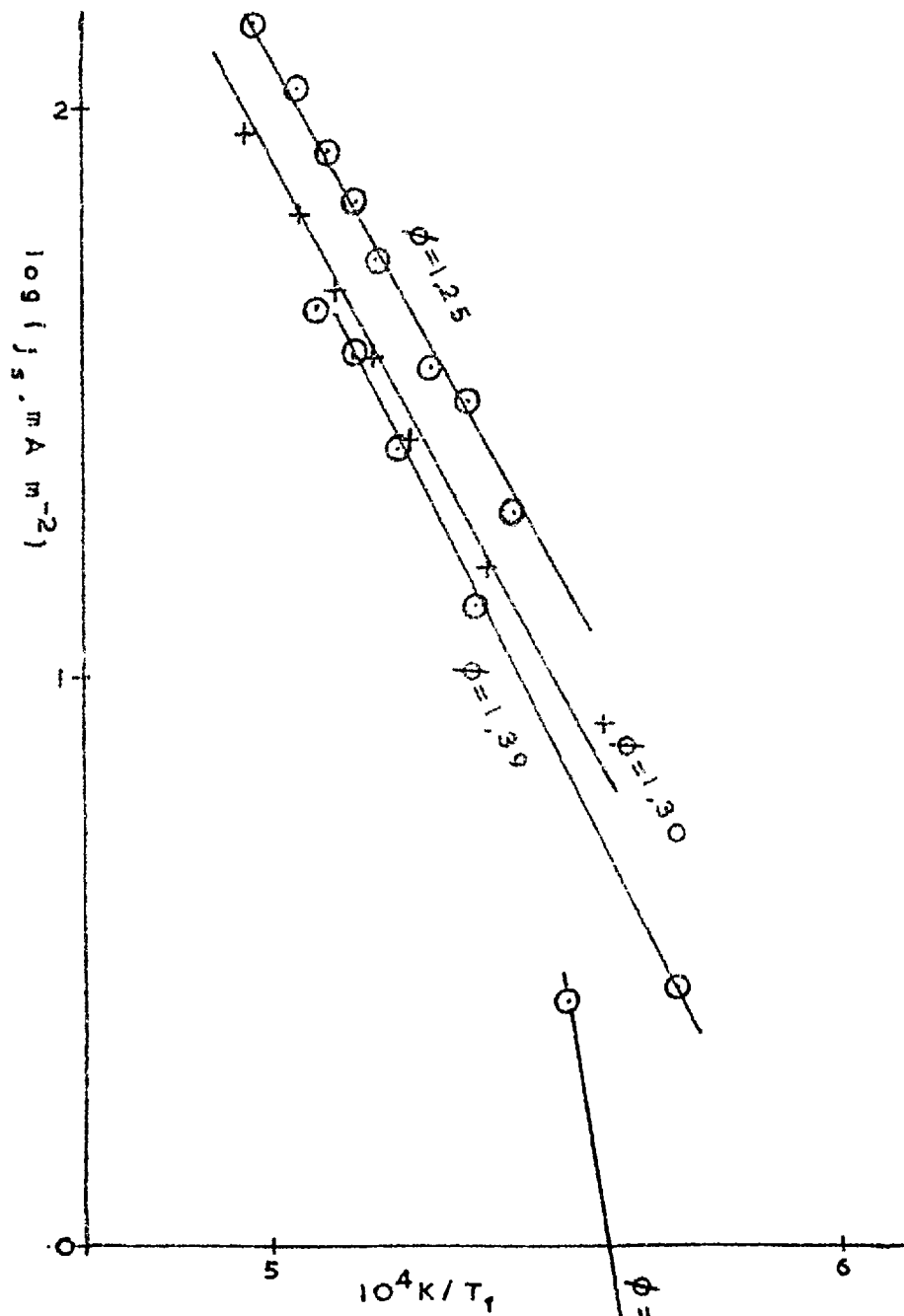
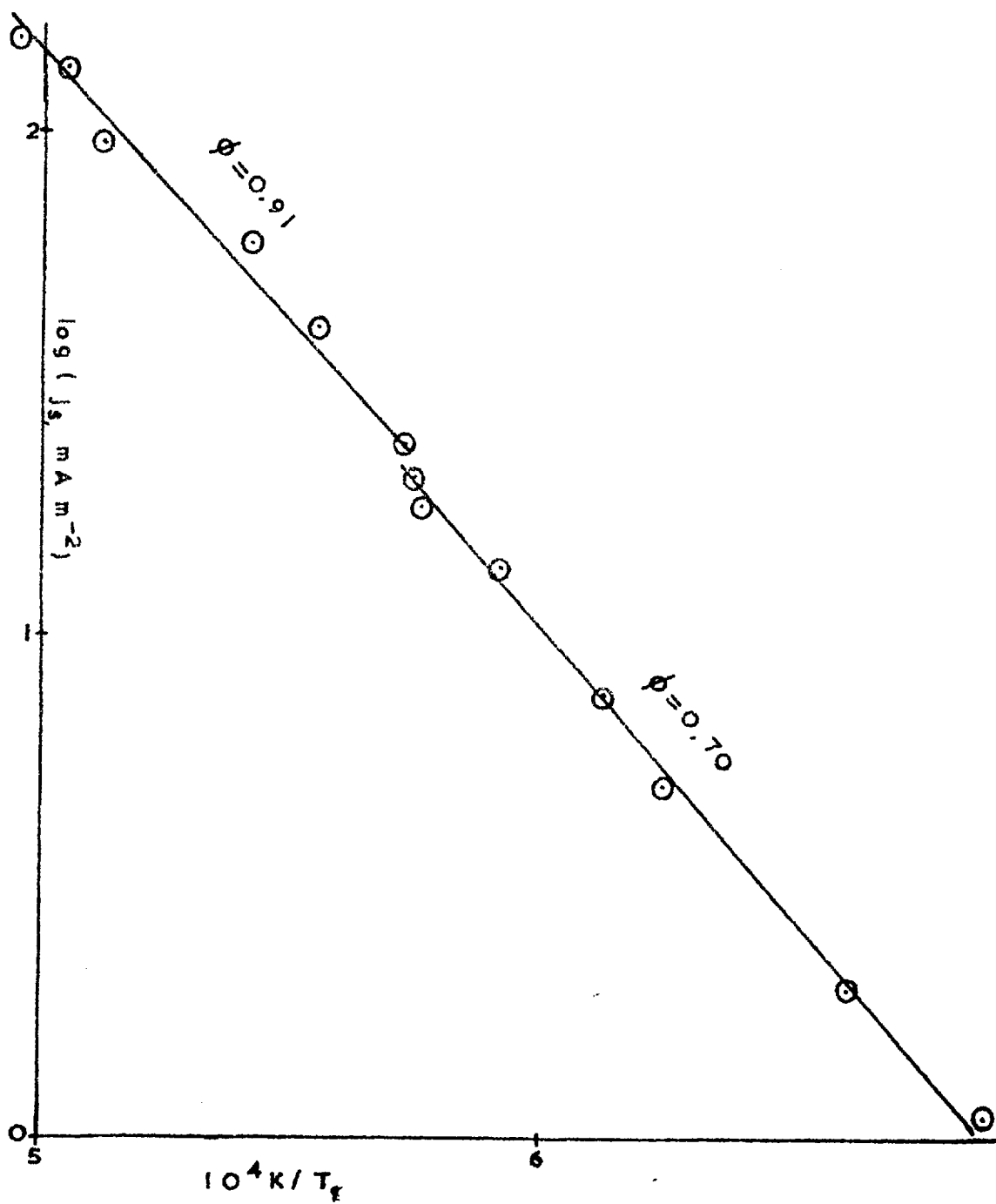
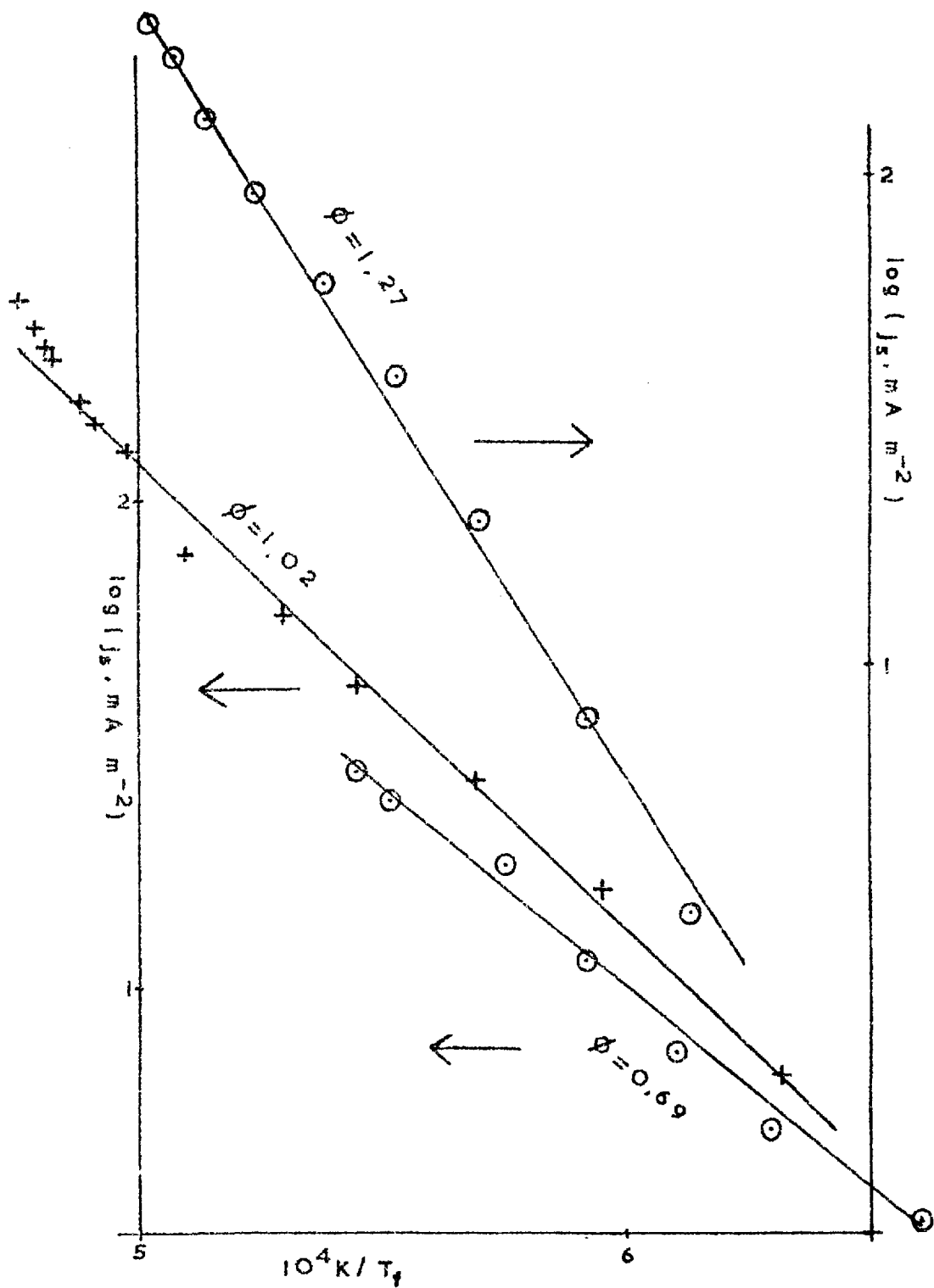
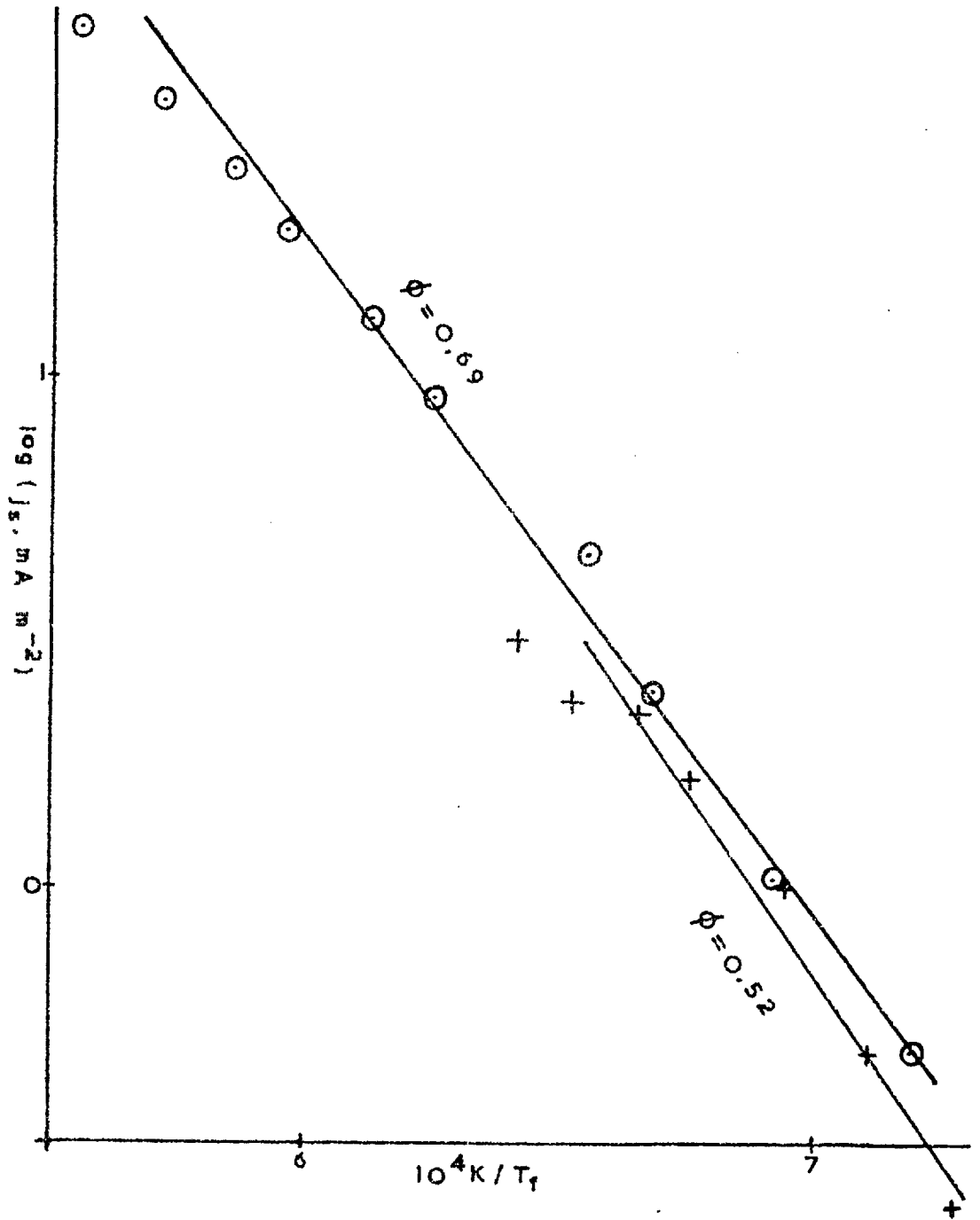


FIG. X (1). CH₄/air

FIG. X(2). CH₄/air

FIG. X(3), $\text{C}_2\text{H}_6/\text{air}$

FIG. X(4). $\text{C}_3\text{H}_8/\text{air}$

FIG. X (5). C_2H_4 /air

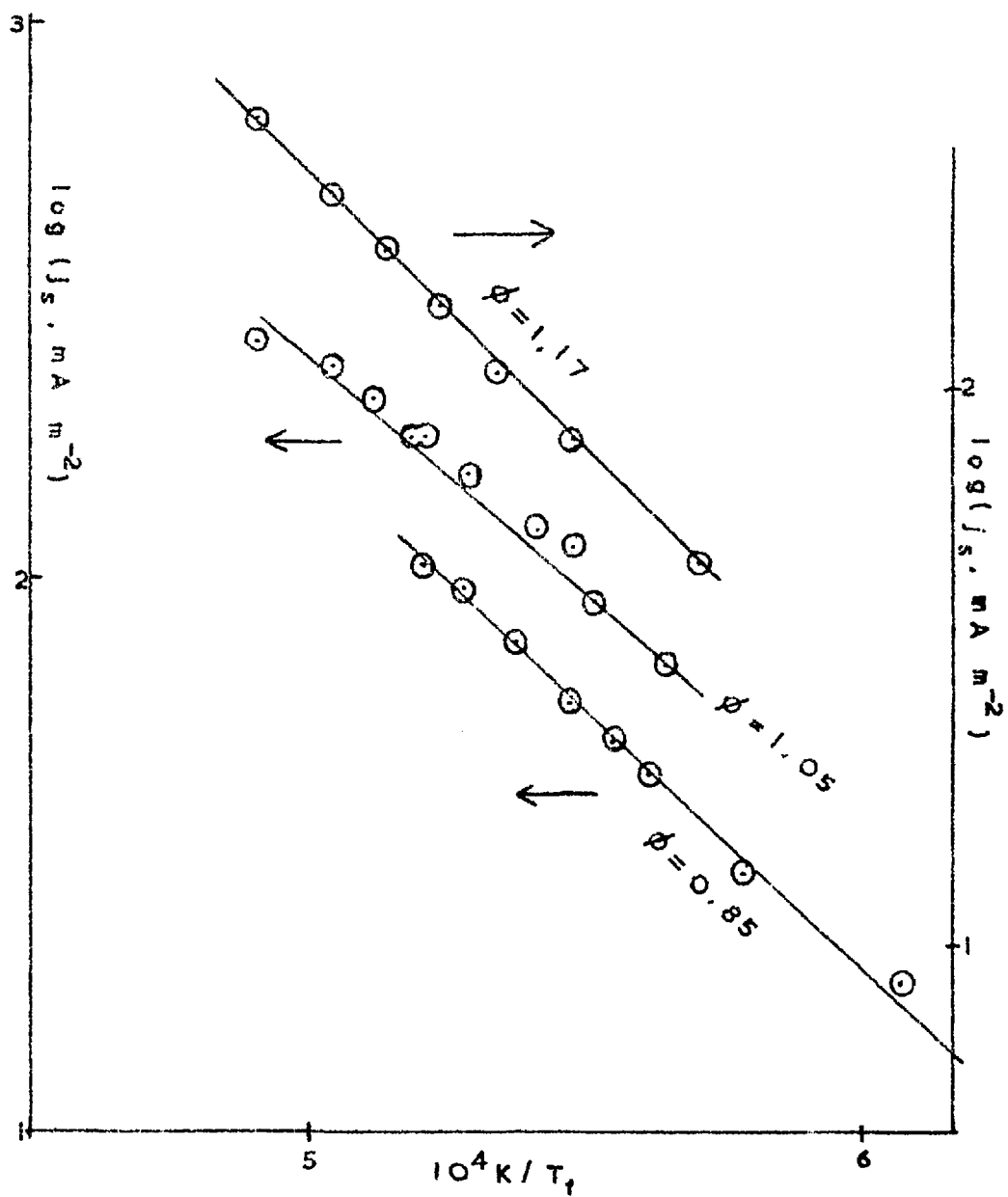
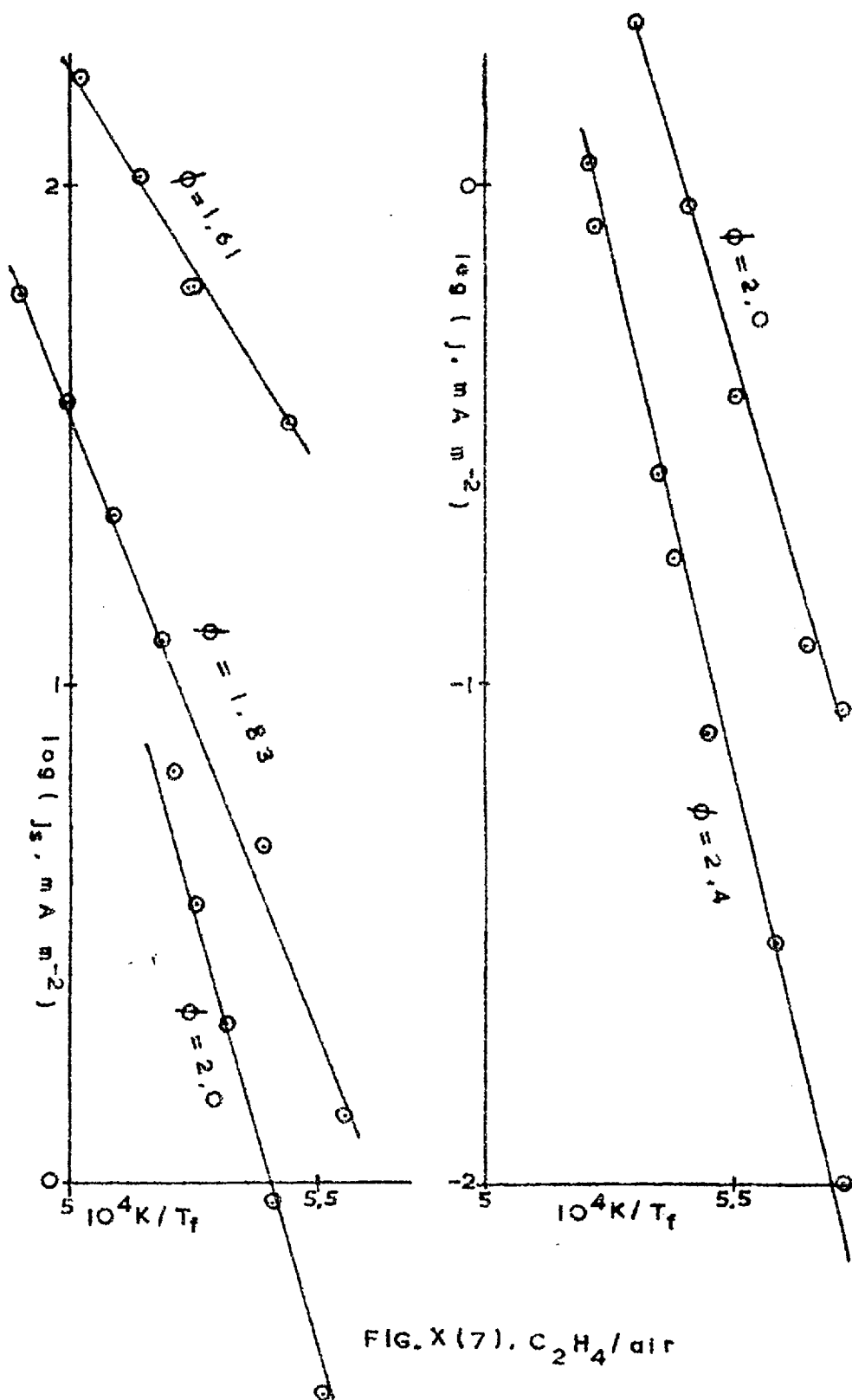
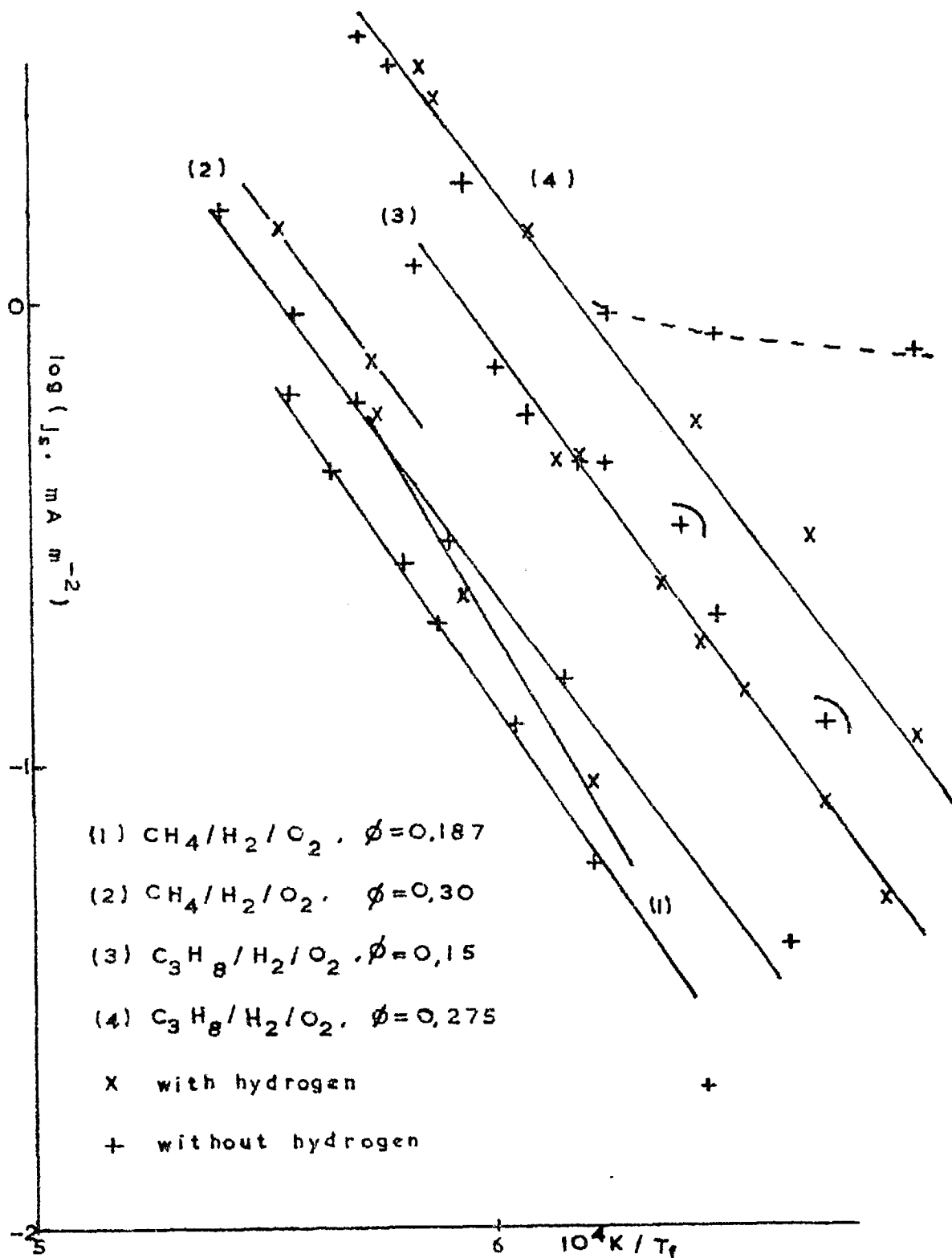


FIG. X(6). $\text{C}_2\text{H}_4/\text{air}$

FIG. X(7). C_2H_4/air


 FIG. X (8), $\text{CH}_4/\text{H}_2/\text{O}_2$ AND $\text{C}_3\text{H}_8/\text{H}_2/\text{O}_2$

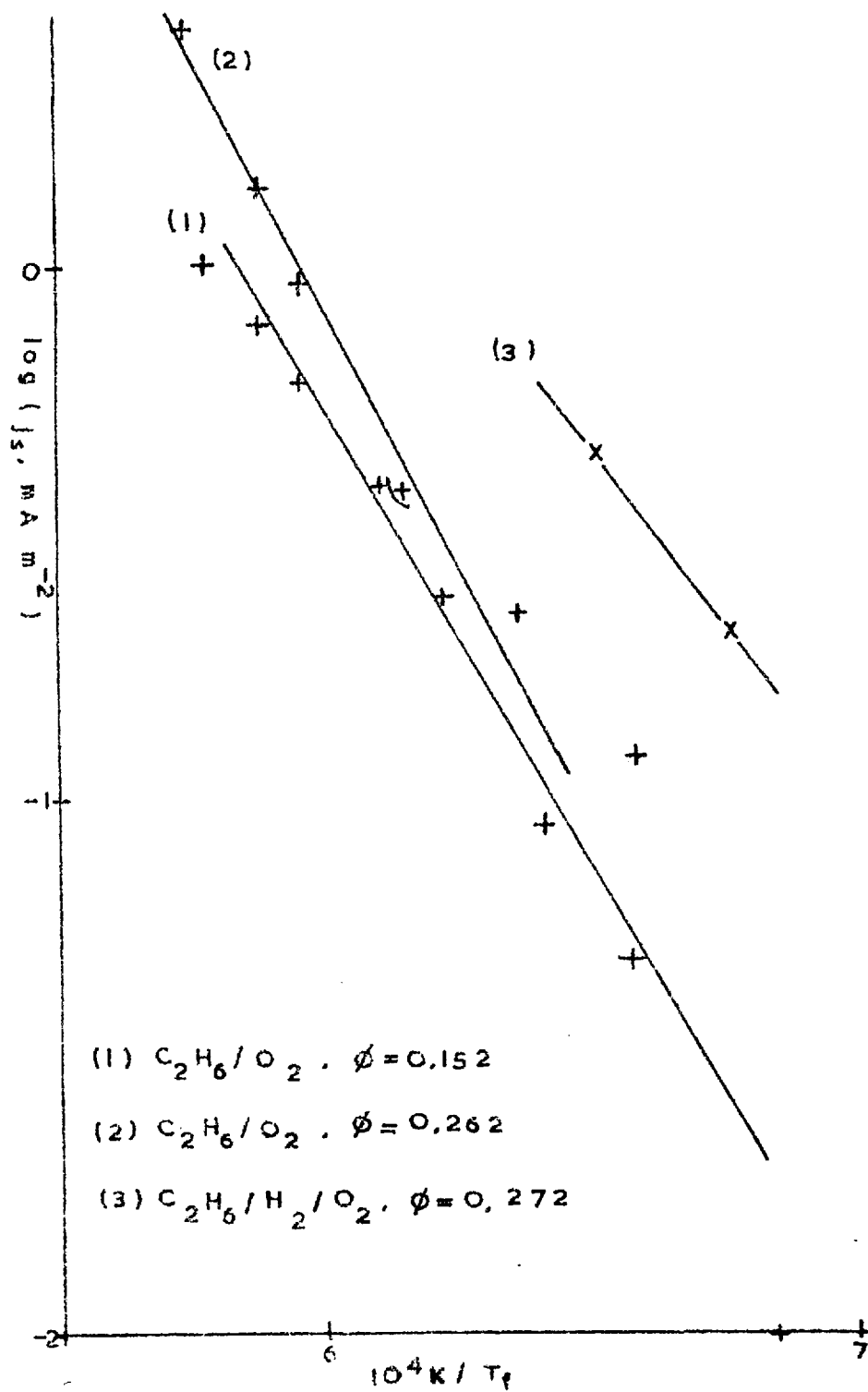


FIG. X (9). $C_2H_6/H_2/O_2$

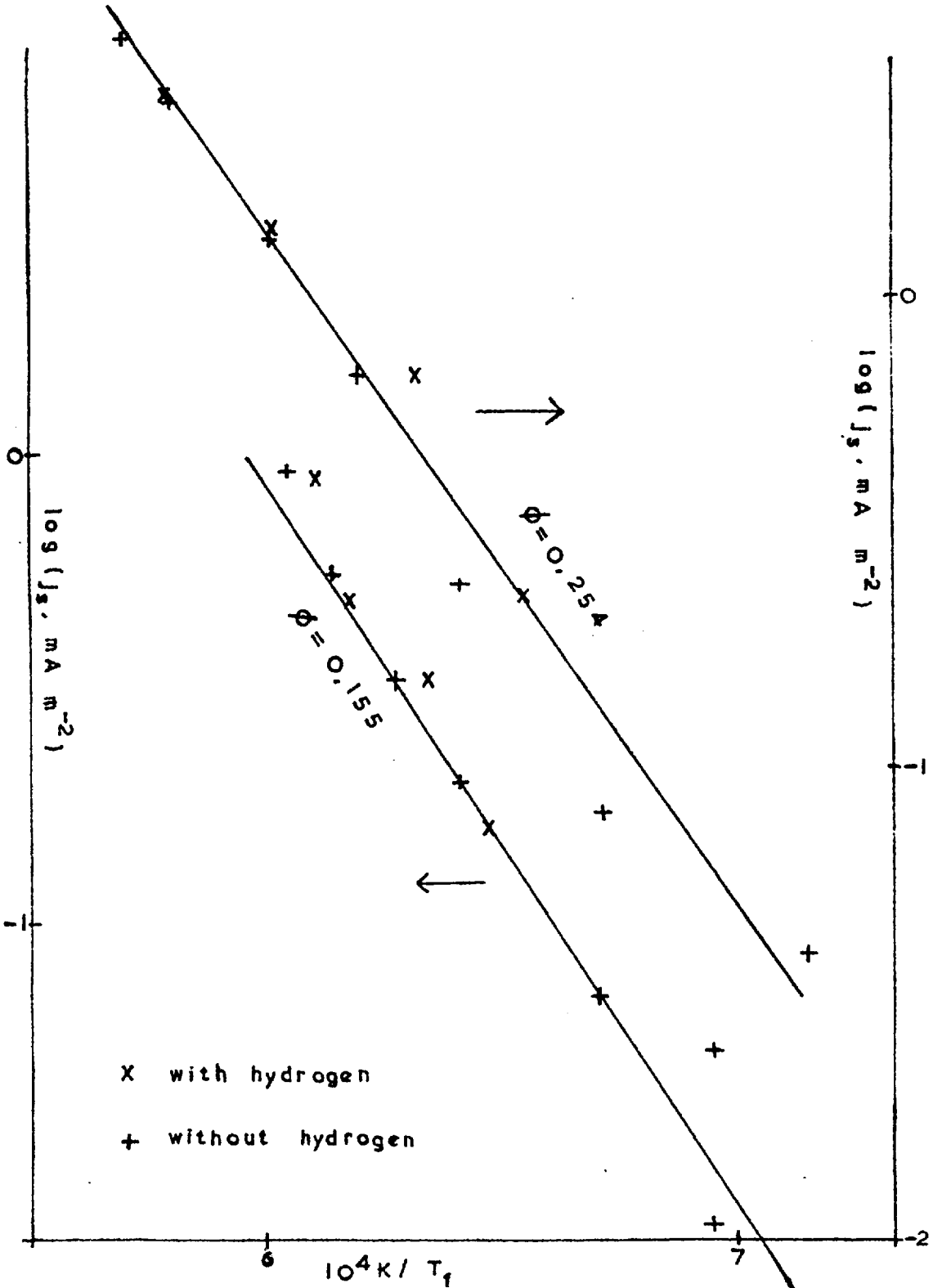
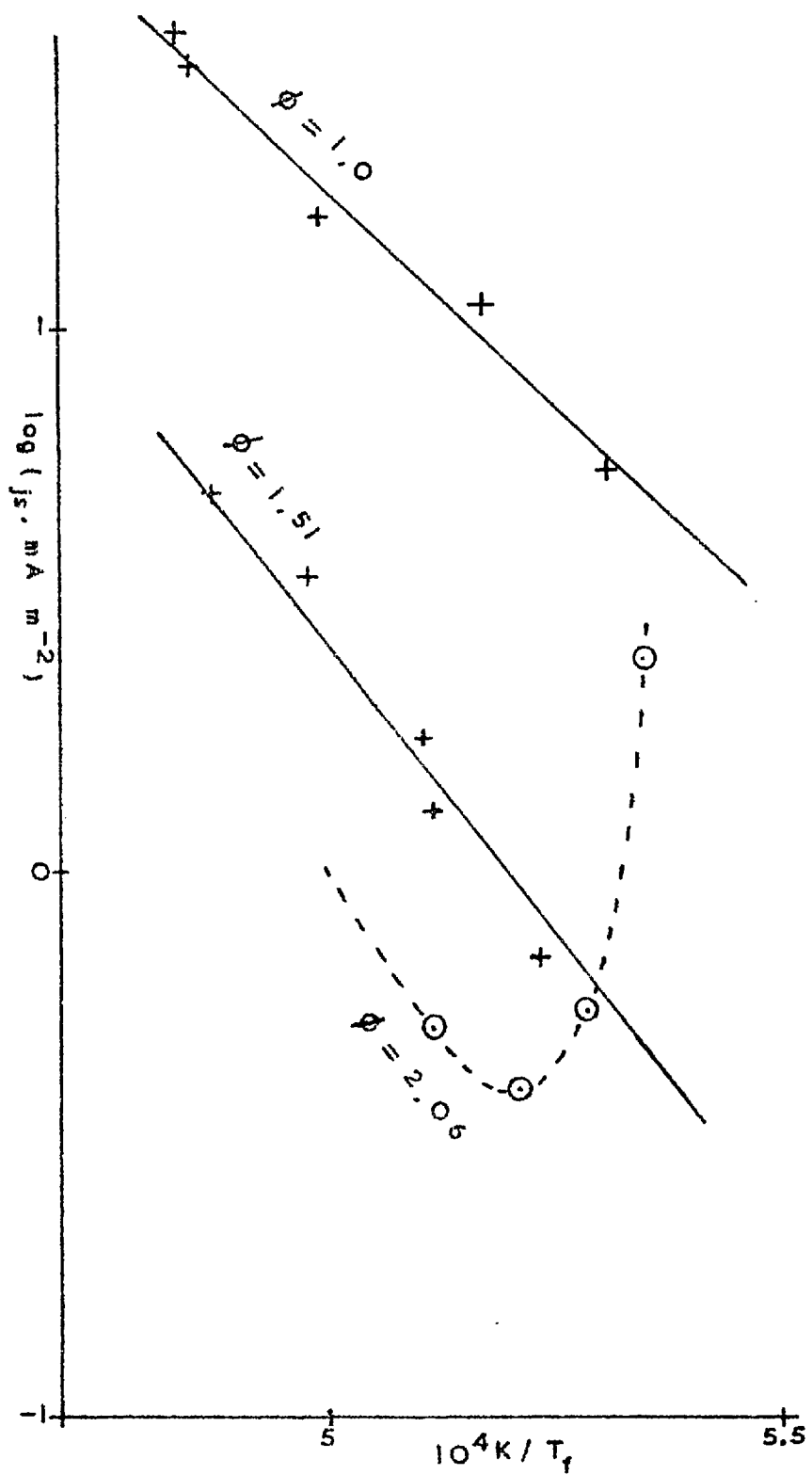


FIG. X (10). $C_2H_4/H_2/O_2$

FIG. X (II). CH_4 / O_2

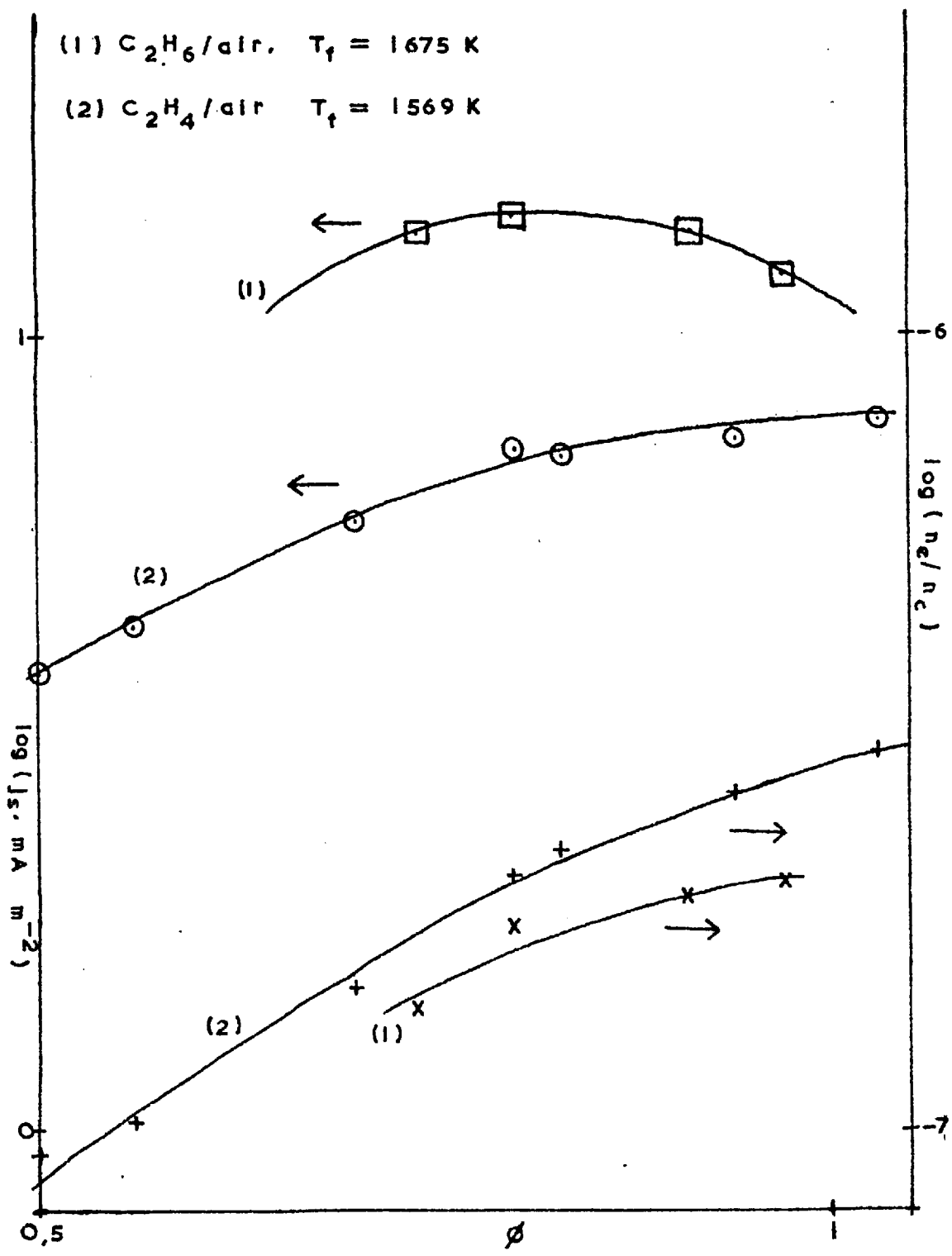
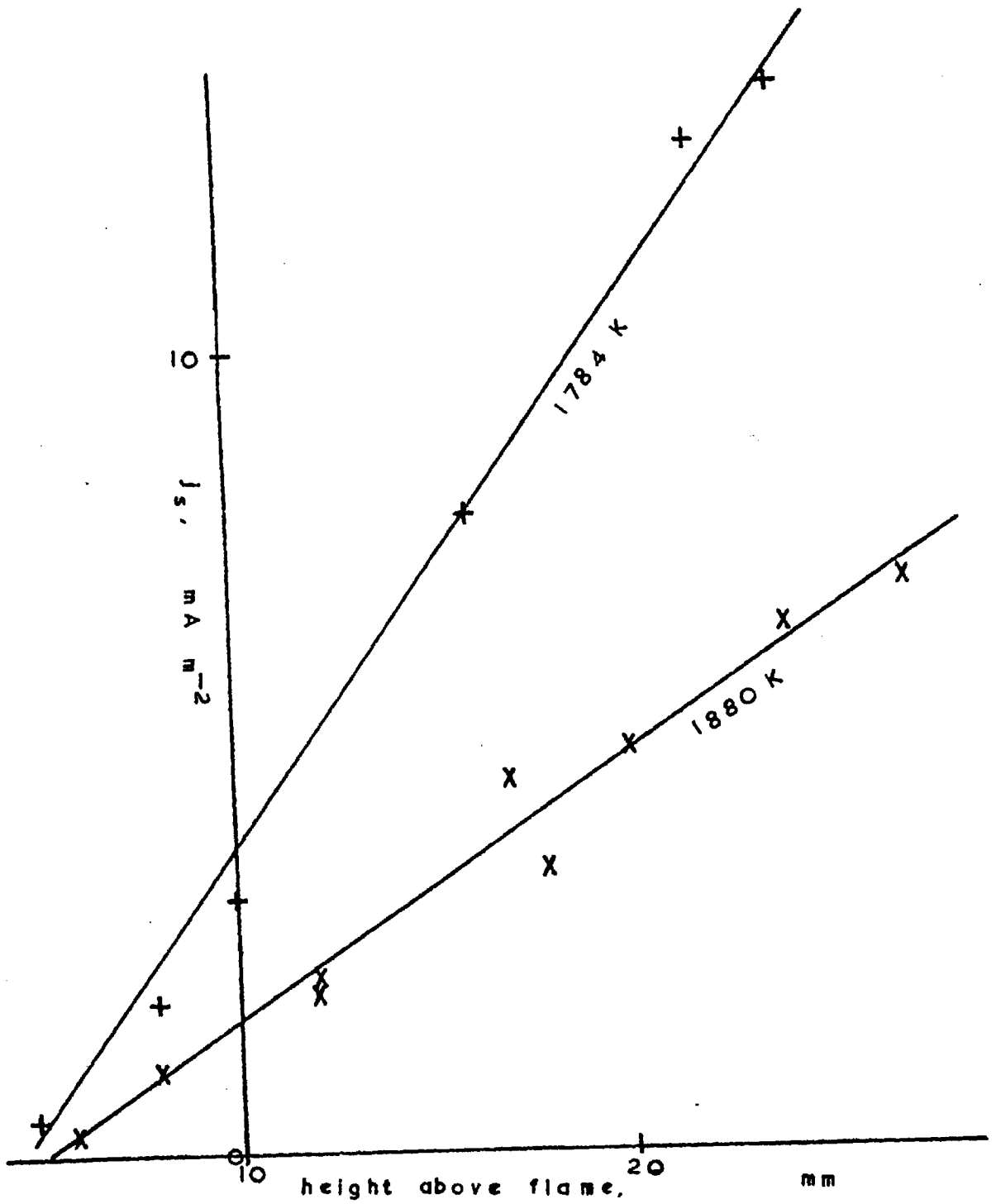


FIG. X(12). VARIATION OF J_s AND n_e/n_c WITH ϕ



Saturation current density of sooting flame

FIG. X (13)

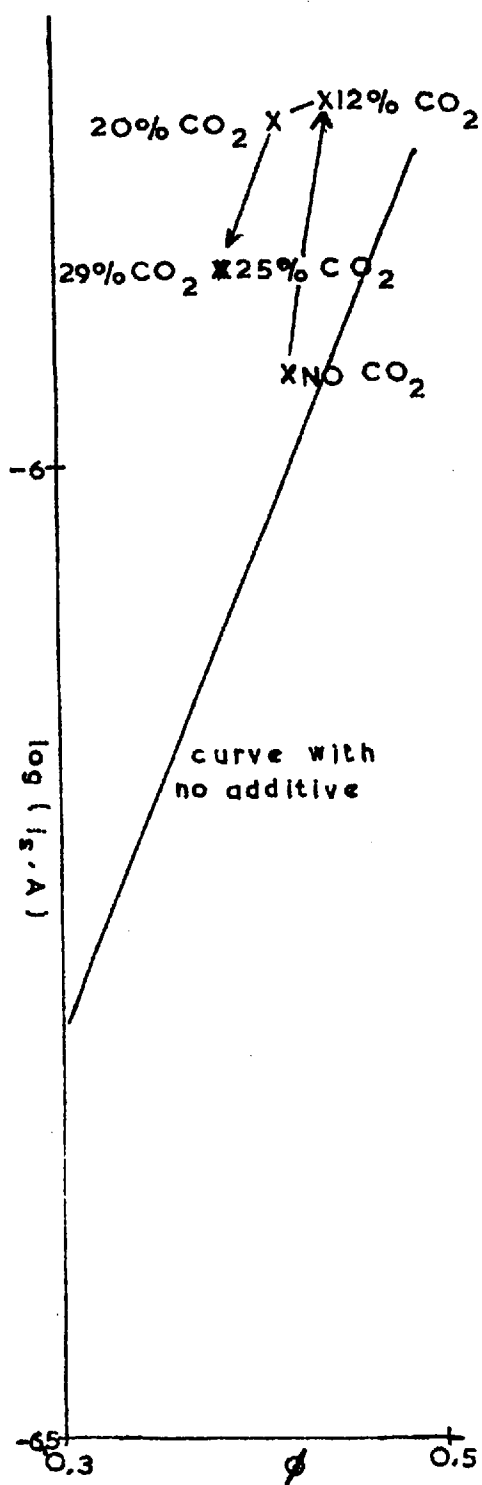


FIG. X (14), ADDITION
OF CO_2 TO $\text{C}_2\text{H}_4/\text{O}_2$

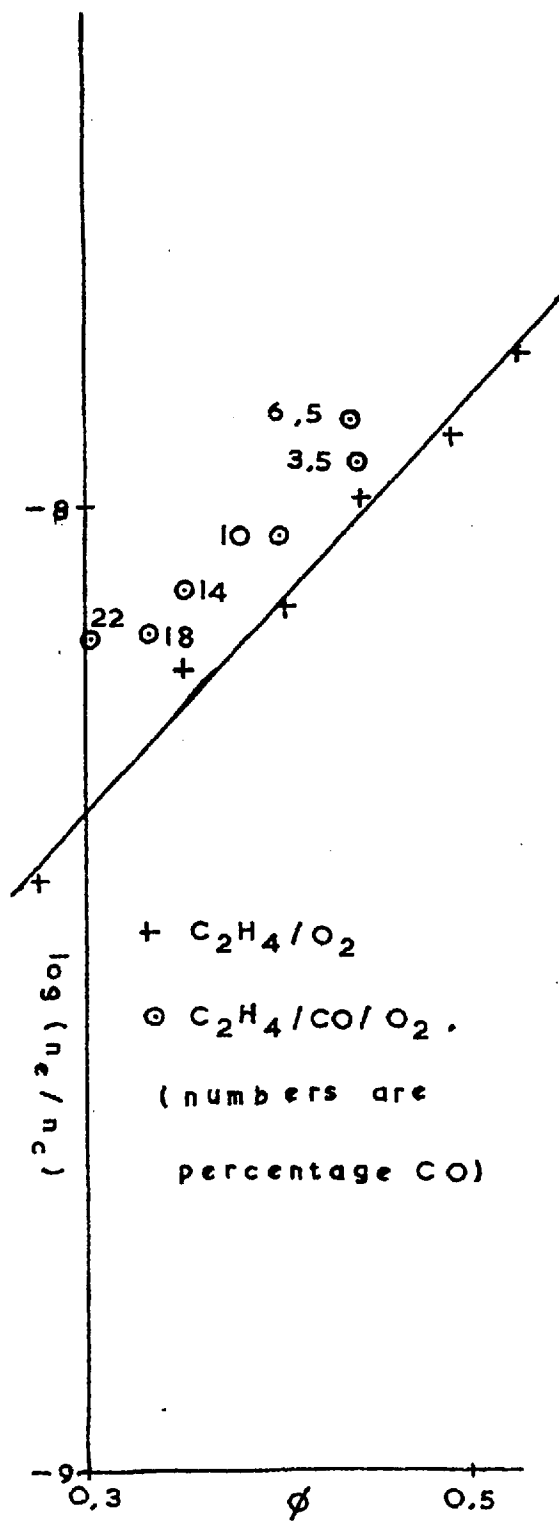


FIG. X (15), ADDITION
OF CO TO $\text{C}_2\text{H}_4/\text{O}_2$

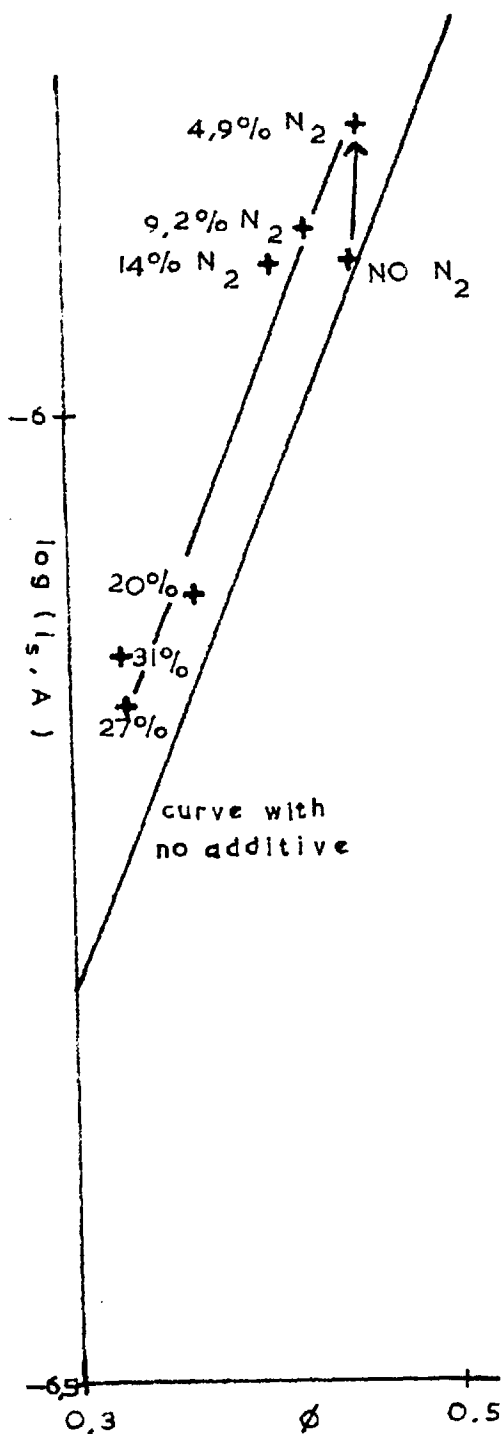


FIG. X (16). ADDITION OF N_2 TO C_2H_4/O_2

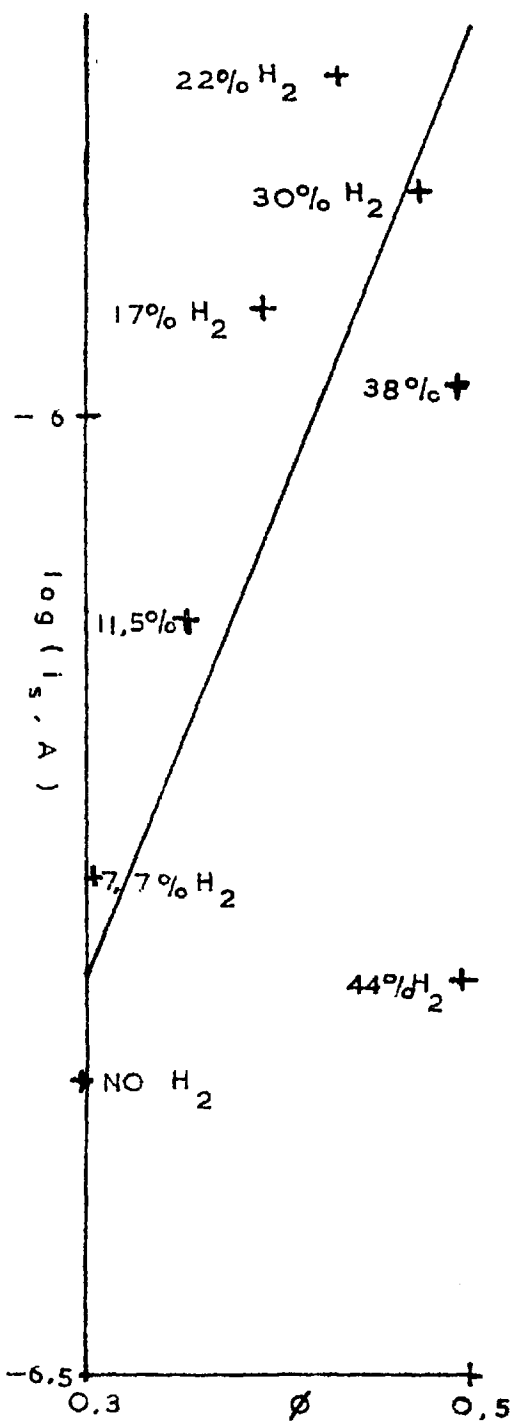


FIG. X (17). ADDITION OF H_2 TO C_2H_4/O_2

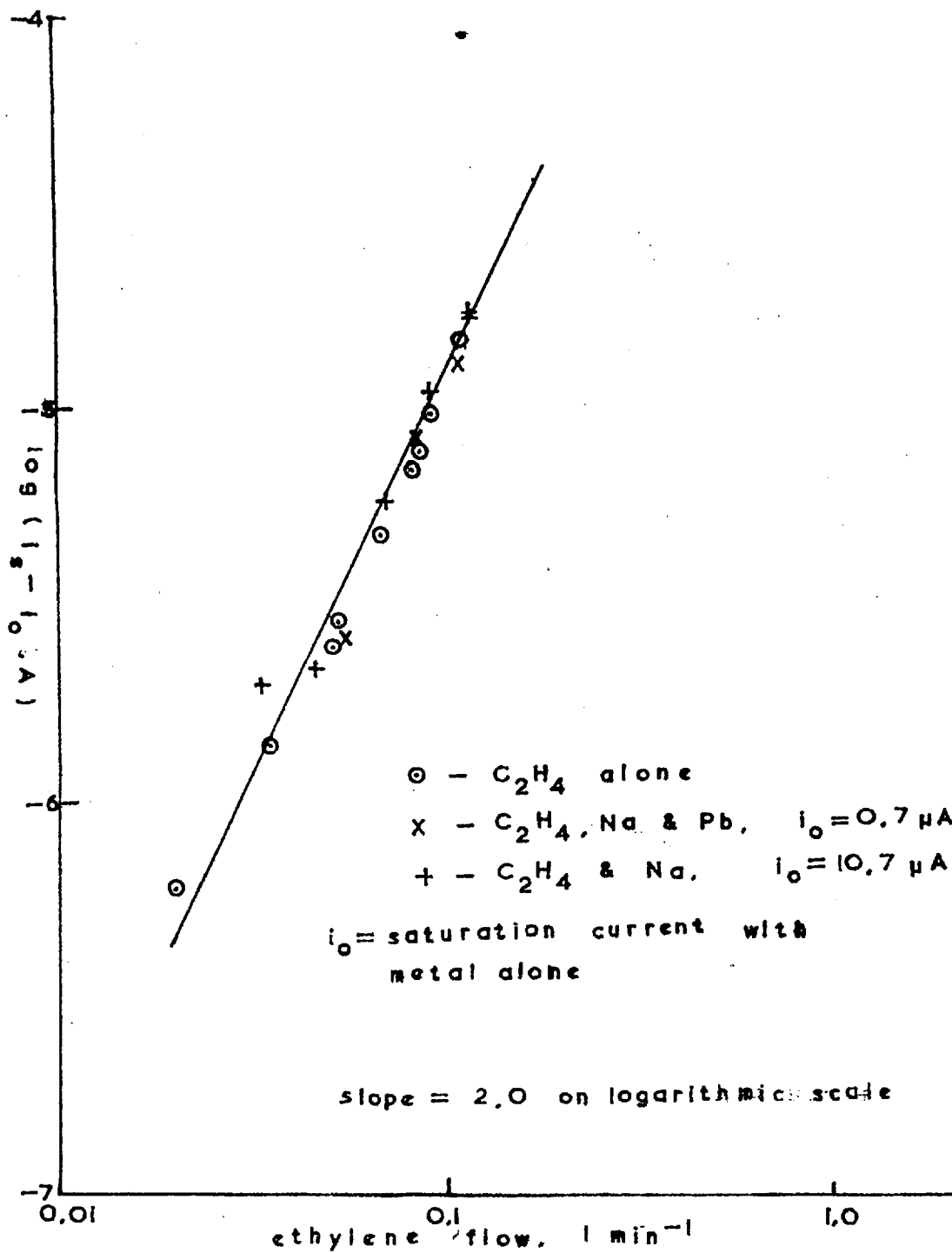


FIG. X (18). ADDITION OF Na AND Pb TO PREMIXED CO/ C_2H_4 /air FLAME

CHAPTER ELEVEN.DIFFUSION FLAMES.

All measurements are at atmospheric pressure unless otherwise stated.

Measurements were first made with flames on nozzles. It was found that the flames were deflected towards the cathode and touched it for all but the lowest fuel flow rates. When the cathode was a gauze the flame tended to burn on both sides of it so that some of the saturation current might not be collected. An aluminium sheet was used as the cathode and a gauze as the anode. The electrodes were made large enough to prevent the flame extending beyond the edges. It was found that the saturation current did not depend much on the electrode separation or the nozzle position. For too great electrode separations breakdown tended to occur before saturation.

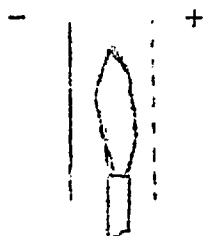


Fig.IX(1) - Experimental arrangement for the measurement of saturation currents of flames on nozzles.

Measurements were also made on circular flames produced by directing a jet of fuel vertically upwards

against a horizontal plate, as described in Ch. VII. The upper plate was made the cathode. In addition measurements were obtained on flames on a porous disc.

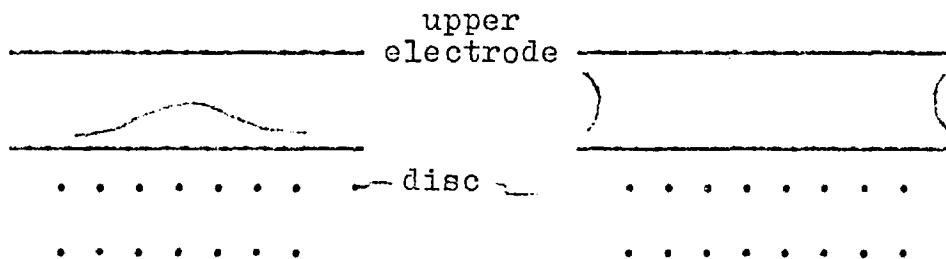


Fig.XI(2) - Experimental arrangement for the measurement of saturation currents of flames on porous discs.

11.1. Results for Methane.

Methane was found to be the easiest hydrocarbon on which to take measurements and was therefore studied most extensively. It sooted least and the volume flowing for any given flux of carbon atoms was greater and therefore easier to measure. Results for methane/air diffusion flames on different burners are given in Table XI(1). The average values over a wide range of fuel flow rates are given below:

The results show that for a variety of flames over a large range of fuel flow rates the saturation current is approximately proportional to the fuel flow rate. It was observed that the saturation current per unit area of flame is not constant, although the variation of fuel flow rate per unit area is small.

Burner	i_s/f $\mu\text{A per l min}^{-1}$	f/A $\text{l min}^{-1} \text{ m}^{-2}$
3 mm id jet	35	180
8 mm id jet	35	240
31 mm id jet	28	140
Batswing burner	27	220
Porous disc	22	-
Jet of fuel against plate	20	140

i_s is the saturation current, f the fuel flow rate, and A the flame area.

11.2. Results for Other Hydrocarbons.

Results for air diffusion flames of hydrocarbons other than methane on the batswing burner are given in Table XI(2). Approximate values of $i_s/(f n_c)$, where n_c is the number of carbon atoms per fuel molecule, are given below:

n_H = number of hydrogen atoms per fuel molecule.

Fuel	CH_4	C_2H_6	C_3H_8	C_2H_4	C_2H_2
n_H/n_c	4	3	2.7	2	1
$\frac{i_s}{f n_c} \frac{\mu\text{A}}{\text{l min}^{-1}}$	30	41	44	45	60+

These results show that the number of electrons produced per carbon atom, n_e/n_c , is approximately the same for these gases. The average value of n_e/n_c is about 5×10^{-7} .

A candle flame was also studied. When the candle lost 1.1 grams in five minutes, the current collected was $20 \mu\text{A}$. Assuming the composition of the candle was C_nH_{2n} , these results give $i_s/(f n_c)$ to be $55 \mu\text{A}$ per 1 min^{-1} , which is of the same order as the value obtained for hydrocarbon gases.

11.3. Counter-Flow Diffusion Flames.

Counter-flow diffusion flames seem the obvious flames on which to measure saturation current for diffusion flames since they are likely to be comparatively little affected by the field. However, it was found that i_s/f varied greatly with the incident flow velocities of the fuel and oxidant and it was not possible to obtain any constant value for i_s/f . The results did not fall into any obvious pattern. In most cases i_s/f increased when the flux of the reactants was increased, which indicates that the variation was not due to fuel escaping unburnt or burning beyond the flanges of the burners at higher fuel fluxes. The size of the flames obtained varied from 20 to 50 cm^2 in most cases. The increase of i_s/f may have resulted from greater disequilibrium (see section 13.7.3).

Results for counter-flow diffusion flames are shown in Figs. X(3-5), in which i_s/f versus f is plotted for methane flames with air and with oxygen at different electrode separations. The results are represented by vertical lines, which show the range of i_s/f obtained by varying the oxidant flow rate. The solid part of the lines represents oxidant flows in excess of stoichiometric, the dotted part lower flows. The horizontal line on each vertical line represents the point at which the flows are in approximately stoichiometric proportions.

11.4. Effect of Experimental Conditions.

The following results were obtained using the arrangement shown in Fig.XI(2):

CH₄/air: $f = 0.594 \text{ l min}^{-1}$, $i_s = 12 \text{ } \mu\text{A}$, $i_s/f = 20.2 \text{ } \mu\text{A l}^{-1}\text{min}$.

CH₄/O₂ : $f = 0.435 \text{ l min}^{-1}$, $i_s = 1.9 \mu\text{A}$, $i_s/f = 4.4 \text{ } \mu\text{A l}^{-1}\text{min}$.

$f = 0.337 \text{ l min}^{-1}$, $i_s = 1.5 \mu\text{A}$,

$i_s = 1.1 \mu\text{A}$ 'a' decreased

$i_s = 2.5 \mu\text{A}$ 'a' further decreased,

where a = electrode separation.

CH₄/O₂, $a = 17 \text{ mm}$, upper electrode positive:

$f, \text{ l min}^{-1}$	0.24	0.33	0.38	0.51
$i_s, \mu\text{A}$	0.50	1.31	1.49	2.29
$i_s/f, \mu\text{A l}^{-1} \text{ min}$	2.1	4.0	4.0	4.5

These results indicate that i_s/f is less constant for oxygen flames than air flames.

The current obtained from diffusion flames did not always increase to a steady value as the voltage was increased. In some cases it reached a maximum value and then decreased slightly. The saturation current was taken to be the value to which the current tended at high voltages. Although the flames were greatly affected by the field the current was not much affected by increases in voltage once the voltage was sufficient to draw the saturation current.

Measurements were made to find the effect of changes in polarity and electrode separation on the saturation current. A methane/air diffusion flame with a constant flow rate of methane (85 ml min^{-1}) was burnt on a jet between horizontal electrodes as shown below:

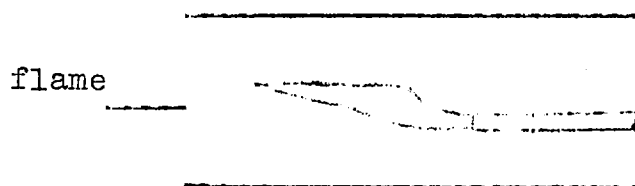


Fig XI(6)

The upper electrode was a metal plate, the lower one a porous disc with air passing through it. Thus when the upper electrode was positive, the wind effect due to positive ions was opposed by the air flow and buoyancy. The pressure was 614 mm Hg.

The saturation current was 4.5 μA with the upper electrode positive and 6 μA with it negative. At a smaller electrode separation saturation currents of 4.1 and 4.4 μA respectively were obtained. These results show that the variation of the saturation current with electrode separation was not great. It was least with the upper electrode positive. The variation with polarity was 33% at the larger electrode separation but only 7% at the smaller separation.

The effect of the air flow from the lower disc was investigated. The flame shape depended on the methane flow rate and whether there was a flow of air against the flame. However, the current was not greatly affected by such an air flow, as shown by the following results:

$f, \text{ml min}^{-1}$		53	83	117	160	189	254
$i_s/f,$	no air flow from disc	20.2	28.9	32.0	30.6	25.9	31.5
$\mu\text{A l}^{-1} \text{ min}$	air flow from disc	-	28.0	28.2	33.1	25.4	45.4

11.5 Effect of Pressure.

Measurements were made to find the variation with pressure, p , of the saturation current from diffusion flames. A methane/air diffusion flame was used. The experimental arrangement was that shown in Fig XI(6). The upper plate was made the anode, since it has been shown that the saturation current is then less dependent on the electrode separation. The following results were obtained:

p, mm Hg	136	216	231	264	270	324	387	388	399	422	434
f, ml min ⁻¹	135	132	133	65	60	130	58	59	67	140	61
i _s , μA	25	15	18	6.1	4.9	12	4.5	4.4	5.4	8.0	3.4
p.i _s /f x10 ⁻²	255	245	310	248	220	301	293	291	323	238	242

p, mm Hg	518	528	556	558	562	611	611	615	617	618
f, ml min ⁻¹	131	130	63	139	62	130	226	106	133	65
i _s , μA	7.2	5.6	3.8	5.9	3.1	6.0	10	6.3	6.1	3.2
p.i _s /f x10 ⁻²	285	227	336	234	281	282	273	366	283	300

It will be seen that $p.i_s/f$ is approximately constant from 140 to 620 mm Hg. Its value is $27770 \pm 12\%$ in mm Hg $\mu A l^{-1} min$. This result shows that the saturation current is inversely proportional to the pressure.

The following results were obtained with a methane/oxygen flame using the arrangement shown in Fig XI(2). The electrode separation was 17 mm and the upper electrode was positive.

p, mm Hg	108	161	186	236	315	404	547	614	770
f, ml min ⁻¹	350	350	350	350	350	340	320	310	330
i _s , μA	10.8	9.8	6.9	5.3	4.0	3.3	1.6	1.45	1.3
p.i _s /f	3320	4490	3660	3690	3650	3950	2740	2820	3030

11.6. Effect of Additives.

11.6.1. Nitrogen.

The effect of adding nitrogen to some diffusion flames with oxygen is shown below. The nitrogen was added to the fuel. The percentage of nitrogen in the fuel and that in the corresponding stoichiometric mixture are given.

i) Methane/oxygen flame on disc:

The methane flow rate, $f(\text{CH}_4)$, before addition of nitrogen was approximately 0.4 l min^{-1}

%N ₂ in CH ₄	0	14.7	32.8	45.0	55.2	63.2	62.4	74.4	78.1	81.6
%N ₂ in stoichiometric mixture	0	5.4	14.0	21.4	29.1	36.4	41.9	49.2	54.3	59.6
i_s , μA	1.3	1.55	1.8	2.3	2.8	3.5	4.4	6.1	7.5	9.1
$i_s/f(\text{CH}_4)$, $\frac{\mu\text{A}}{\text{l/min}}$	3.3	3.9	4.5	5.8	7.1	8.8	11.4	15.8	19.9	21.9

ii) Methane/oxygen flame on 3 mm id nozzle:

0.249 l min^{-1} of methane (before addition of nitrogen).

%N ₂ in methane	0	42.0	58.5	74.0	82.8	87.3
%N ₂ in stoichiometric mixture	0	19.4	31.9	48.7	61.6	69.6
i_s , μA	16.5	16.1	22	31.7	35	25.7
$i_s/f(\text{CH}_4)$, $\frac{\mu\text{A}}{\text{l/min}}$	66	65	88	127	140	103

iii) $(\text{H}_2 + \text{CH}_4)/\text{O}_2$ flame on porous disc.

Hydrogen flow 0.975 l min^{-1} , methane flow 57 ml min^{-1}

The background current with no methane was small (about $0.03 \mu\text{A}$) and has been allowed for.

%N ₂ in fuel	45.5	65.0	70.6	73.9	74.6	76	77
%N ₂ in stoichiometric mixture	36.2	52.3	59.0	62.9	63.9	65.5	66.5
$i_s, \mu\text{A}$	0.07	0.43	0.81	1.1	1.4	1.5	1.56
$i_s/f(\text{CH}_4), \frac{\mu\text{A}}{\text{l/min}}$	1.2	7.4	14.5	19.3	24.6	26.8	27.8

Note: stoichiometric methane/air contains 71.4% nitrogen; stoichiometric hydrogen/air contains 55.3% nitrogen. Some results for hydrocarbon/air flames with nitrogen added are given in section 11.6.4.

11.6.2. Hydrogen.

Hydrogen added to hydrocarbon diffusion flames was found to reduce i_s . Results for hydrogen addition to a methane/air diffusion flame on a 3 mm id nozzle are given below: The methane flow was constant and equal to 0.128 l min^{-1} .

flow of H ₂ , l min^{-1}	0	0.39	0.81	1.52
%H ₂	0	75.3	86.3	92.2
$i_s, \mu\text{A}$	7.0	2.0	1.2	0.8
$i_o = i_s$ without CH ₄ , μA	-	0.1	0.2	0.4
$i_s - i_o, \mu\text{A}$	7.0	1.9	1.0	0.4
$i_s/f(\text{CH}_4), \mu\text{A/l min}^{-1}$	55	15	7.8	3.1

11.6.3. Carbon Monoxide.

i) A flame of carbon monoxide plus methane in air was burnt on a batswing burner. The carbon monoxide flow was 3.38 l min^{-1} . With no methane a saturation current of $0.3 \text{ } \mu\text{A}$ was obtained, which was probably due to impurities from the air.

$f(\text{CH}_4)$, ml min^{-1}	40	78	130	250	450	840
$i_s' = i_s - 0.3 \text{ } \mu\text{A}$	2.3	4.2	7.4	12.7	19.7	29.7
$i_s' / f(\text{CH}_4)$, $\frac{\mu\text{A}}{\text{l/min}}$	57	54	58	51	44	36

ii) Addition of CO to methane/air diffusion flames on a batswing burner gave the following results:

Flow of CO, l min^{-1}	0	0.16	0.38	0.74	1.3	2.2	3.4
$i_o = i_s$ without CH_4 , μA	-	0.0	0.1	0.1	0.15	0.25	0.31
i_s (with 128 ml/min CH_4) $-i_o$, μA .	-	5.2	6.1	6.1	-	6.9	7.4
i_s (with 835 ml/min CH_4) $-i_o$, μA .	24.2	24.6	25.7	25.7	26.6	27.6	-

iii) Addition of CO to propane/air diffusion flames on a batswing burner gave:

Flow of CO, l min^{-1}	0	0.16	0.38	1.3	2.2	3.4
$i_o = i_s$ without C_3H_8 , μA	-	0.0	0.1	0.15	0.25	0.31
i_s (with $61 \text{ ml min}^{-1} \text{ C}_3\text{H}_8$) $-i_o$, μA	12.5	20.0	19.2	16.1	16.7	18.3

The currents given by diffusion flames of hydrogen and carbon monoxide with air are thought to be due to impurities, in particular sodium, from the laboratory air. The currents fluctuated and intermittent orange colouration of the flame was visible.

It was found that the addition of nitrogen, hydrogen, or carbon monoxide to hydrocarbon diffusion flames tended to reduce or eliminate sooting and yellow luminosity.

11.6.4. Carbon Dioxide.

The effect of the addition of carbon dioxide to diffusion flames was compared to that of nitrogen.

i) Methane/air diffusion flame on batswing burner:

Methane flow 0.446 l min^{-1}

Flow of N_2 , l min^{-1}	0	0.38	0.71
i_s , μA	14.7	13.3	12.0

i_s with 0.29 l min^{-1} of $\text{CO}_2 = 11.9 \mu\text{A}$.

Estimated value of i_s with 0.29 l min^{-1} of $\text{N}_2 = 13.7 \mu\text{A}$.

ii) Propane/air diffusion flame on batswing burner:

$i_s = 57 \mu\text{A}$ with 0.42 l min^{-1} of propane.

$i_s = 48 \mu\text{A}$ with 0.33 l min^{-1} of CO_2 or 0.65 l min^{-1} of N_2 added.

iii) Hydrogen plus propane/air diffusion flame on batswing burner:

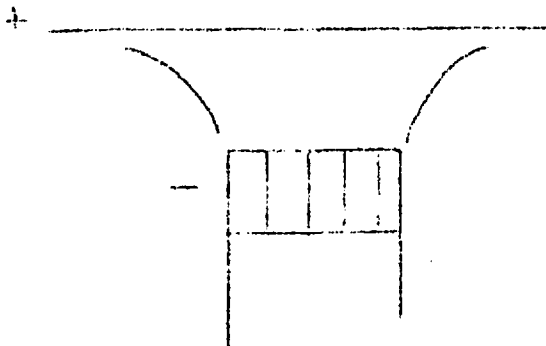
1.51 l min⁻¹ of hydrogen, 61 ml min⁻¹ of propane.

Flow of N ₂ , l min ⁻¹	0	0.7	1.2
i _s , μA	2.3	3.0	4.0

Flow of CO ₂ , l min ⁻¹	0.4	1.4	2.1
i _s , μA	2.7	4.0	4.6
Est. i _s at equal flow of N ₂	2.6	4.5	-

11.6.5. Bromine.

Flames were burnt on a circular matrix burner illustrated below:



It was found that the shape and appearance of the flames were little altered by the addition of bromine.

i) Methane/air flames:

no bromine added:

f, l min ⁻¹	0.25	0.37	0.47	0.64	0.69	0.84
i _s , μA	3.6	6.3	8.5	12.5	13.9	17.5
i _s /f, μA l min ⁻¹	14.2	17.3	18.1	19.7	20.2	20.8

Methane plus 21% bromine:

Flow of CH ₄ , f, l min ⁻¹	0.25	0.34	0.46	0.57	0.69	0.80	0.91
i _s , μA	3.5	4.9	7.5	9.8	12.9	14.0	18.5
i _s /f, μA l ⁻¹ min	14.2	14.3	16.4	17.4	18.8	17.6	20.4

0.70 l min⁻¹ of methane:

Flow of CH ₄ , f, l min ⁻¹	0.71	0.70	0.69	0.66	0.69
% Br ₂	0	2.1	3.7	11	21
i _s , μA	14.7	12.5	12.0	12.5	12.7
i _s /f, μA l ⁻¹ min	20.7	17.9	17.5	18.9	18.5

0.38 l min⁻¹ of methane:

% Br ₂	0	0.8	1.9	4.5	7.3	10	21
i _s , μA	6.3	6.2	6.0	5.9	5.5	5.3	5.3
i _s /f, μA l ⁻¹ min	17.3	16.3	15.8	15.6	15.0	14.3	14.0

ii) Propane/air flames:

Heavy sooting occurred.

No bromine added:

Flow of C ₃ H ₈ , f, l min ⁻¹	0.08	0.15	0.26
i _s , μA	3.6	11	22
i _s /(3f), μA, l ⁻¹ min	15.0	24.4	28.2

Propane plus 22% bromine:

Flow of C_3H_8 , f, $l\ min^{-1}$	0.08	0.15	0.26
i_s , μA	4.0	9.9	23
$i_s/(3f)$, $\mu A\ l^{-1}\ min$	16.5	22.0	29.4

Propane flow, f, $0.263\ l\ min^{-1}$:

% Br_2	0	3.0	8.2	22
i_s , μA	-	33	34	25
$i_s/(3f)$, $\mu A\ l^{-1}\ min$	28.3*	41.9	43.1	31.7

* extrapolated from results for propane/air.

The methane and propane flows above were measured before the addition of bromine.

11.6.6. Alkali Metals.

Alkali metals were added to counter-flow diffusion flames because the volume of gas at the final flame temperature which is contained between the electrodes is small in these flames, which reduces the amount of thermal ionization and makes it easier to measure the amount of chemiionization. Also it is easier to introduce alkali metals into these flames. The flames were burnt between two horizontal porous discs. A lean CO/air flame was burnt on the lower disc. The fuel was introduced through the upper disc and burnt in the products of the lean CO/air flame.

Alkali metals were introduced into the flame by placing a little of a salt of the metal on the lower disc. Some was volatilized by the premixed flame on the lower disc and carried into the diffusion flame, as shown by the colouration of the latter. The fuel emerging from the upper disc was hydrogen or carbon monoxide to which a small amount of hydrocarbon could be added. The following results were obtained for the saturation currents:

i) Hydrogen + hydrocarbon/carbon monoxide + air:

Hydrogen flow from upper disc c. 1.65 l min^{-1} .

Additive	i_s , microamps.					
propane	14.1	9.5	17.0	13.9	20.8	-
methane	-	-	-	-	-	5.7
borax	12.8	17.0	14.8	-	-	15.1
K_2CO_3	-	-	-	16	16	-
hydrocarbon plus alkali	30.7	27.0	32.2	32	34	23.9

ii). Carbon monoxide + hydrocarbon (or hydrogen)/carbon monoxide + air.

Additive	i_s , microamps.		Flow of CO from upper disc.
methane	5.8	21.1	1.51 l min^{-1}
borax	26	26	
both	26.5	37.3	

Additive	i_s , microamps	Flow of CO from upper disc.
borax	26	
borax + 30 ml min ⁻¹ CH ₄	23.2	1.51 l min ⁻¹
borax + 200 ml min ⁻¹ CH ₄	25.5	
200 ml min ⁻¹ CH ₄	6.6	
borax	11.1	0.84 l min ⁻¹
borax + 0.41 l min ⁻¹ H ₂	8.4	
Borax + 0.85 l min ⁻¹ H ₂	8.5	
borax	10.5	

11.7 Ionization Due to Pyrolysis.

Methane was passed into the hot products of a rich premixed hydrogen/air flame on a porous disc burner. In one case the methane was passed through the upper electrode into the flame products. In the other it was injected through a hypodermic needle.

i) Methane passed through upper electrode.

An earthed gauze with a hole of area 4 cm² was inserted between the burner and the upper electrode in order to exclude the current from the secondary flame in the surrounding air by measuring the current from the central portion only of the column of hot gases above the flame. The current obtained was very low (0.02 μ A). The current due to the methane burning in the surrounding air was 5.1 μ A.

ii) Methane injected through hypodermic needle.

The matrix upper electrode with an insulated probe at the centre was used. The end of the needle was placed under the probe and the current, i_p , to the probe measured. A current of 0.1 to 0.2 μA was obtained, depending on the height of the needle. The methane injected produced a faint blue colouration. The current given by combustion of the methane was 7 to 9 μA in air and 5 μA in oxygen.

The results show that the saturation current due to pyrolysis of methane was less than 3% of that given when the fuel burns in air.

11.8. Reversed Diffusion Flame.

The injection of 0.52 l min^{-1} of oxygen into excess methane gave a saturation current to a probe above of 11 μA . This oxygen flow is equivalent to the combustion of 0.26 l min^{-1} of methane, giving $i_s/f(\text{CH}_4) = 42.3$. The excess methane burnt in the surrounding air. The saturation current was 51 μA without and 45 μA with oxygen injection. For a higher methane flow rate the saturation current was 80 μA without and 70 μA with oxygen.

11.9. Summary.

The saturation currents of diffusion flames in air of several hydrocarbons have been measured over a range of

fuel flow rates, mostly using a batswing burner. Measurements were also taken with methane flames on a variety of different burners to investigate the effect of different flow patterns and flame shapes. The effect on flame saturation currents of changing the electrode separation and field polarity, and of forced convection were shown to be not very great except in the case of counter-flow diffusion flames. It was shown that most hydrocarbon/air diffusion flames give similar values of n_e/n_o although there is some small variation between different burners and different hydrocarbons.

Measurements were taken to find the effect of various additives: nitrogen, hydrogen, carbon monoxide, carbon dioxide, bromine, and alkali metals. The greatest effect was given by hydrogen, which reduced the saturation current by a factor of twenty. The ionization due to alkali metals and hydrocarbon in a hydrogen diffusion flame was shown to be additive. In carbon monoxide diffusion flames the ionization of alkali metals was reduced by the addition of hydrocarbons or hydrogen.

Some measurements were taken on diffusion flames in oxygen. The ionization efficiency for these flames was lower, in most cases, than for flames in air. However, it varied markedly with the flow conditions and type of burner.

The effect of injecting hydrocarbon into the hot products of a rich premixed flame was also investigated and found to be negligible.

The effect of pressure on the saturation currents of methane diffusion flames in air and in oxygen was investigated. It was found that the product of the pressure and the ratio of the saturation current to the fuel flow rate is constant, showing that the saturation current is inversely proportion to the pressure.

These conclusions will be discussed further in chapter XIII.

Table XI(1).

Saturation currents of methane/air diffusion flames.

Burner type	f , $l \text{ min}^{-1}$	i_s , μA	i_s/f , $\mu A \text{ l}^{-1} \text{ min}$	A , cm^2	f/A $l \text{ min}^{-1} m^{-2}$
Batswing	0.265	11	41.5	11	240
	0.51	20	39	24	210
	0.96	34.7	36	68	140
	1.72	51	29.5	81	210
	2.40	67	28	99	240
	3.14	81	26	119	260
	4.0	100	25	153	260

Burner type	f, l min ⁻¹	i _s , μA	i _s /f, μA l ⁻¹ min	A, cm ²	f/A l min ⁻¹ m ⁻²
3 mm id nozzle	0.058	3.1	53.5	2.5	230
	0.128	6.4	50	6.3	200
	0.25	12.3	49.5	12.5	200
	0.45	20	44	23.2	160
	0.65	26	40	41	160
	0.92	34	37	60	150
	0.96	33	34.5		
	1.37	45	33		
	1.72	56	32.5		
	3.0	(95)	32		
8 mm id nozzle	0.017	0.5	29.5		
	0.058	2.0	34.5	2.0	290
	0.128	4.3	33.5	4.8	270
	0.25	8.8	35.5	10.8	230
	0.45	16	35.5	20.3	220
	0.65	21	32	32.5	200
	0.92	29.3	32	41.5	220
	0.96	36	37.5		
	1.37	41	30	55	250
	1.43	54	38		
	1.72	62	36		
	2.20	91	44		
	2.92	100	34		
	3.3	130	39		
5.4	215	40			

Table XI(1) continued,

Burner type	$f,$ $l \text{ min}^{-1}$	$i_s,$ μA	$i_s/f,$ $\mu A \text{ l}^{-1} \text{ min}$	$A,$ cm^2	$f/A,$ $l \text{ min}^{-1} m^{-2}$
31 mm id nozzle	0.265	5.4	20.5		
	0.51	13.8	27	44	120
	0.96	28	29	107	90
	1.72	47	27.5	151	110
	2.40	66	27.5	170	140
	3.14	88	28	189	170
	4.0	118	29.5	214	190
Porous disc	0.202	4.7	23		
	0.272	5.4	20		
	0.355	7.2	20		
	0.425	9.5	22.5		
	0.52	11.6	22.5		
Jet of fuel against horizontal plate	0.050	2.9	50		
	0.128	4.2	33		
	0.25	5.3	21.5	12.3	200
	0.45	9.6	21	28	160
	0.65	12.2	18.5	49	130
	0.92	17.0	18.5	75	120
	1.37	24.8	18	138	100

Table XI(2)

Saturation currents of hydrocarbon diffusion flames in air on batswing burner.

Ethane

Flow, f , l min^{-1}	0.093	0.15	0.28	0.49	0.65	0.84
i_s , μA	8	15	24	34	50	67.5
$i_s/(2f)$, $\mu\text{A l}^{-1} \text{ min}$	43	50	43	35	38	40

Propane

Flow, f , l min^{-1}	0.061	0.14	0.26	0.42	0.55	0.69	0.92
i_s , μA	12.5	22	34	52.5	71.5	88.5	118
$i_s/(3f)$, $\mu\text{A l}^{-1} \text{ min}$	68	52	44	43	44	43	43

Ethylene

Flow, f , l min^{-1}	0.078	0.14	0.26	0.33	0.64	0.95
i_s , μA	6.0	12.5	25	27.5	50	111
$i_s/(2f)$, $\mu\text{A l}^{-1} \text{ min}$	38.5	45	48.5	41.5	39	58

Acetylene

Heavy sooting and the build-up of carbon tended to occur.

Flow, f , l min^{-1}	0.078	0.15	0.26	0.47
i_s , μA	10	19	42	72
$i_s/(2f)$, $\mu\text{A l}^{-1} \text{ min}$	64	63	81	77

Results for methane are given in Table XI(1).

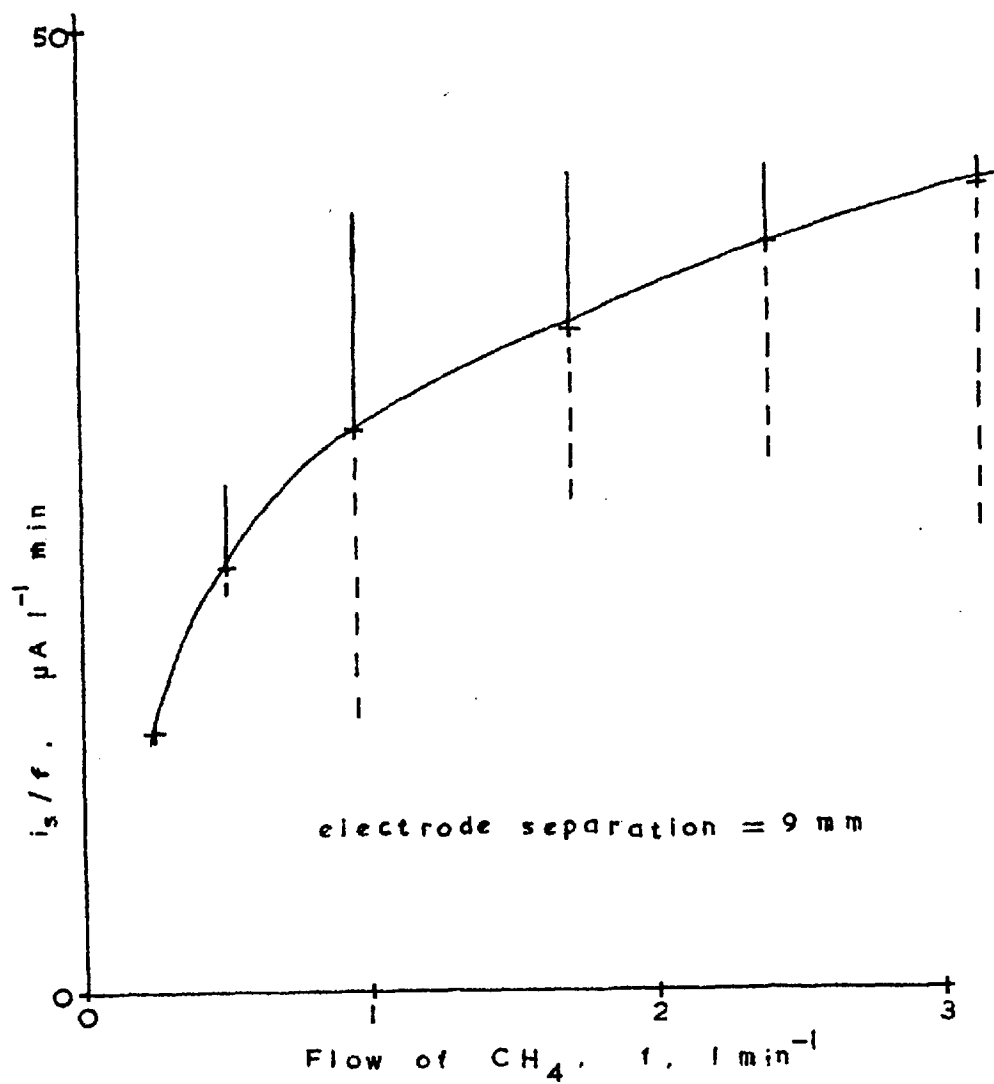


FIG. XI(3). CH₄/air COUNTER-FLOW
DIFFUSION FLAME

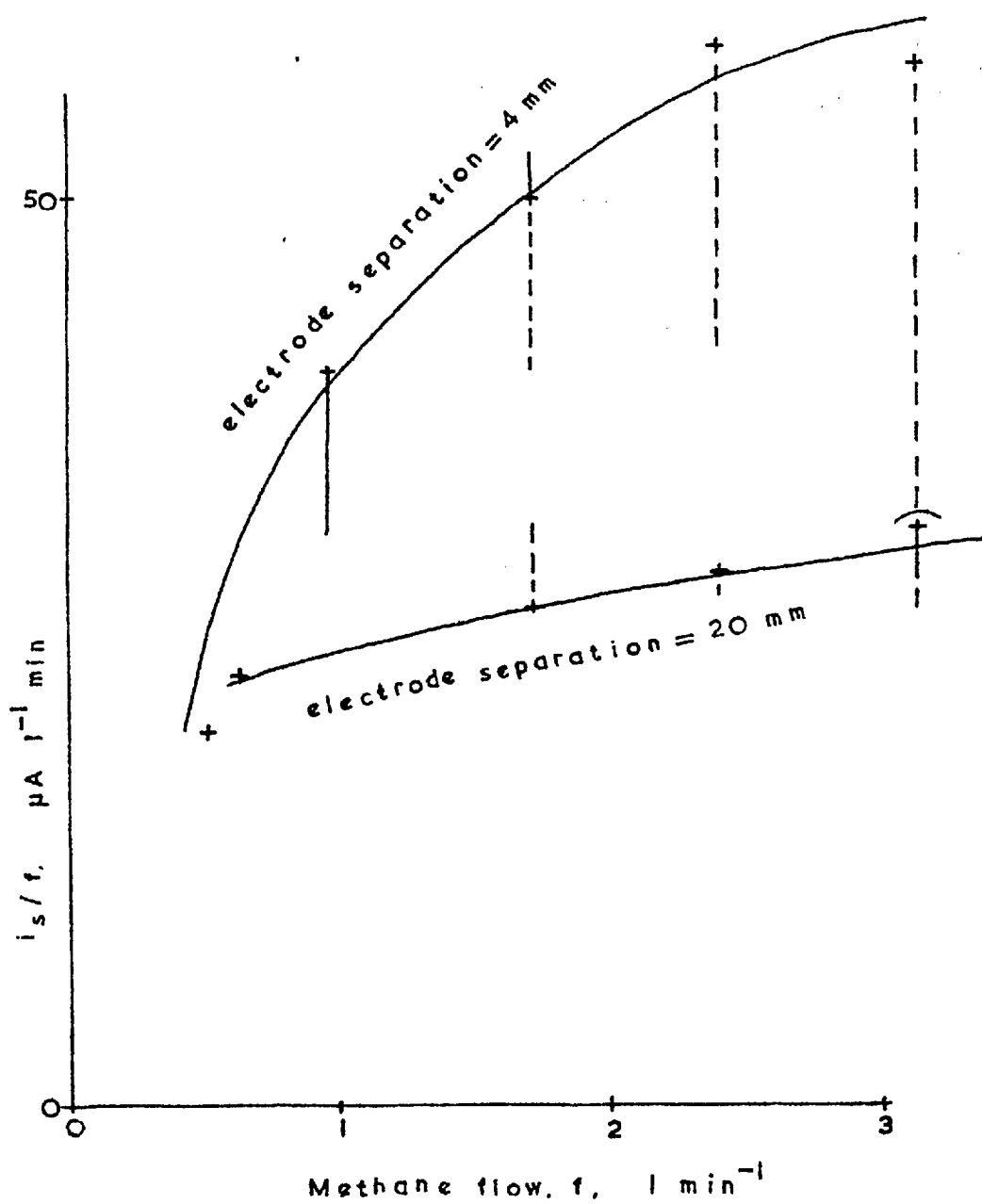


FIG. XI(4). CH_4/air COUNTER-FLOW
DIFFUSION FLAME

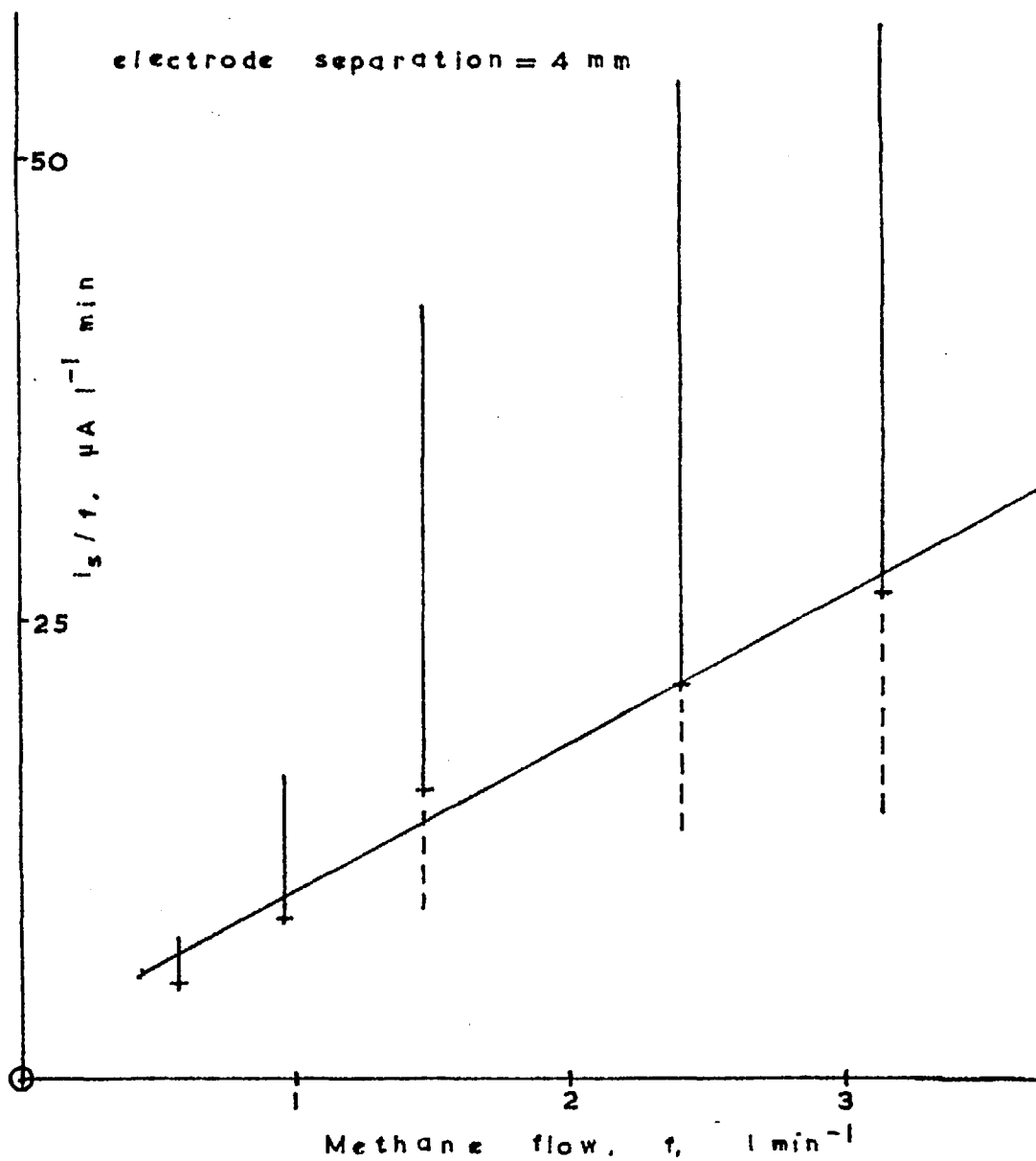


FIG. XI(5), CH_4/O_2 COUNTER-FLOW
DIFFUSION FLAME

PART IV. DISCUSSION.CHAPTER TWELVE.PREMIXED FLAMES.

Experimental results for the saturation current densities of premixed flames are given in Ch X. These results can be employed for practical purposes where it is necessary to know the maximum current which can be drawn per unit area of hydrocarbon flames. The results will now be considered and discussed from a number of points of view.

12.1 Comparison of Hydrocarbon Flames.

The results show that the saturation currents of hydrocarbon flames with air and with oxygen fall on a series of well defined curves. For a given composition, the saturation current density, j_s , is determined by the final flame temperature, T_f . The saturation current density increases rapidly as temperature increases, the rate of increase of j_s being of the order of 200% per 100 K. For a given value of T_f , the saturation current density varies comparatively little with stoichiometric ratio, ϕ , for lean flames; when ϕ is increased by increasing the initial fuel concentration, j_s reaches a maximum at about $\phi = 1$ and then decreases sharply for rich

mixtures. The number of ion pairs produced per carbon atom increases with ϕ for lean hydrocarbon/air flames by a larger factor than j_s does, as is shown by the results for ethane/air at 1675°K and ethylene/air at 1569°K. The increase of j_s with ϕ for lean air flames being comparatively small appears to be largely due to the fall in the fuel throughput required to keep the temperature constant as the mixture strength increases. The scatter of the results on the graphs indicates that the average random error of the results is about 10%. This corresponds to a temperature change of about 10 K. The results obtained for lean hydrocarbon/air flames are in reasonable agreement with those of Lawton (1963).

The results show that for flames with the same stoichiometric ratio and final flame temperature, propane and ethane/air gave similar saturation current densities. Ethylene/air gave values higher by a factor of the order of 1.5. Methane/air gave values lower by a factor of the order of three.

Propane/oxygen and ethylene/oxygen gave similar saturation current densities. Ethane/oxygen gave values about 40% lower. Methane/oxygen gave values lower by a factor of the order of five.

Lean methane, ethylene, and ethane/air flames gave

saturation current densities of the order of 20 to 25 times those given by flames with the same initial fuel concentration and final flame temperature but with oxygen instead of air. Lean propane/air gave values of the order of 15 times those for the corresponding propane/oxygen flames. These factors were a little lower at higher final flame temperatures.

The results for methane show that stoichiometric flames with air gave higher saturation current densities (by a factor of about four) than stoichiometric flames with oxygen with the same final flame temperatures.

The burning velocities of hydrocarbon/air flames are lower than those of oxygen flames with the same initial fuel concentration and final flame temperature. Table X(4) shows that for stoichiometric methane/air it is about half as great. The number of ion pairs produced per carbon atom in the fuel is therefore greater in air flames by a factor of the order of up to fifty.

12.2. Hydrogen and Carbon Monoxide Flames.

Saturation currents of flames of hydrogen and carbon monoxide with air and with oxygen are shown in Table X(3). The saturation current densities are equivalent to about 0.21 mA m^{-2} at 2000°K or 0.013 mA m^{-2} at 1667°K . The saturation current densities of hydrocarbon/air flames

at 2000°K are of the order of 150 mA m^{-2} . Those of the hydrocarbon/oxygen flames taken were from 0.2 mA m^{-2} at 1667°K. These results confirm that the saturation currents of flames of hydrogen and carbon monoxide are much lower than those of hydrocarbon flames. That flames containing hydrogen and carbon monoxide together give low ionization indicates that the ionization in hydrocarbon flames occurs during or as a result of the breakdown and oxidation of the hydrocarbon to CO. The low saturation currents obtained with hydrogen and carbon monoxide flames confirm that the ionization due to impurities is too small to affect the measurements on hydrocarbon flames. The saturation current given by hydrogen flames is equivalent to 7 ppm of propane, since $\frac{1}{2}\%$ of propane in hydrogen/air at 1667°K gives 9 mA m^{-2} (Lawton & Weinberg, 1964).

12.3 Effect of Additives.

12.3.1. Addition of Nitrogen, Carbon Dioxide, Carbon Monoxide.

The observation that saturation current densities of hydrocarbon/air flames are of the order of twenty times those of oxygen flames with the same initial fuel concentration and final flame temperatures indicates that excess oxygen can decrease rates of chemiionization. Dilution with large amounts of other inert additives would be expected to have an effect similar to that of nitrogen.

Figs. X(14) to (16) show the effect of small additions of nitrogen, carbon dioxide, and carbon monoxide to a premixed ethylene/oxygen flame. Small amounts of nitrogen and carbon dioxide (5 to 30%) gave a moderate increase (up to 50%) in j_s compared with the flame at the same stoichiometric ratio and final flame temperature without additive. The addition of 5 to 22% of carbon monoxide increased n_e/n_c by 20 to 40%.

The saturation current densities of ethylene/air flames diluted with nitrogen were approximately equal to those of the undiluted flames with the same final flame temperature and stoichiometric ratio. On the other hand, carbon dioxide added to hydrocarbon/air flames in concentrations of up to 15% decreased the saturation current density although it increased the final flame temperature. The saturation current densities with CO_2 added were about 40% less than for flames with the same final flame temperature and stoichiometric ratio and without CO_2 added. Carbon dioxide thus appears to have an appreciable chemical effect inhibiting ionization in hydrocarbon/air flames. The results for carbon dioxide added to carbon monoxide and hydrogen/air flames containing small amounts of methane indicate that carbon dioxide has an inhibiting effect on the ionization in the former but that it increases the amount of ionization in the latter. This effect may be due to

inhibition of the oxidation of hydrocarbons by CO_2 (see Rutherford & Fells, 1966), thereby giving more opportunity for ionization to occur.

Since the products of hydrogen flames do not contain CO_2 it is to be expected that any effect of carbon dioxide addition on these flames would be particularly marked.

12.3.2. Addition of Hydrogen.

The effect of hydrogen addition to hydrocarbon/oxygen flames is illustrated by the results given in Table X(2) and Fig X(17). Flames of $\text{C}_2\text{H}_4/\text{O}_2$ and $\text{C}_3\text{H}_8/\text{H}_2/\text{O}_2$ (which contained up to 30% of H_2) gave similar saturation current densities as flames without hydrogen but with the same stoichiometric ratio (including H_2 as fuel) and final flame temperature, provided the flames were quiet and stable. Hydrogen addition increased the saturation current density of CH_4/O_2 and, to a lesser extent, $\text{C}_2\text{H}_6/\text{O}_2$. This increase appears to be due to the fact that these flames are relatively poor ion sources, so that the addition of H_2 can give flames in which more of the hydrocarbon ionizes.

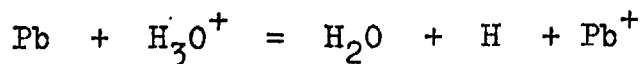
12.3.3. Addition of Bromine.

The results for the addition of bromine to premixed air flames show that the changes in the saturation current attributable to the addition of bromine were of the order of

20%. Thus the effect of bromine is small. Small additions of bromine gave a small increase in j_s and larger additions (up to about 1%) a net decrease. The effect of bromine is further discussed in section 12.8.

12.3.4. Addition of Metallic Salts.

The ionization of metallic additives downstream of flames is greater in the presence of hydrocarbons. The concentrations of the ions of many metals, including lead, have been found to reach several times the equilibrium value (Sugden & Knwestubb, 1956). Alkali metals have been found to ionize more rapidly in the presence of hydrocarbons (Hayhurst & Sugden, 1966). It has been suggested that these effects are due to charge transfer (Padley & Sugden, 1962). In the present investigation into the addition of sodium and lead salts to a carbon monoxide/air flame containing a small proportion of ethylene the results show that the saturation current is approximately equal to the sum of that due to the metal and that due to the hydrocarbon. This indicates that no appreciable chemi-ionization of these metals occurs as a result of the addition of hydrocarbon to premixed flames and that the high ion concentrations observed must be caused by changes in recombination rates due to charge transfer processes, such as



the atomic ion resulting in greatly reduced rates of recombination downstream of the reaction zone. The present results also show that the addition of sodium and lead do not affect the saturation current due to the hydrocarbon.

Lead was added in the presence of sodium so that the presence of the lead in the flame could be readily detected from the current given by the sodium. The saturation current due to the lead and sodium together was 0.7 μA , most of which must have been due to the sodium since sodium ionizes more readily (Sugden & Knewstubb, 1956). Less than half the sodium was ionized, so that the saturation current if all the sodium had been ionized would have been greater than 1.4 μA . The greatest saturation current obtained was 14 μA . The number of sodium atoms was therefore greater than one tenth of the number of ions. The molar concentration of the lead salt was ten times that of the sodium (see Ch IX). The number of lead atoms was therefore greater than the maximum number of ions. The saturation currents of seeded flames with hydrocarbon were 3 to 14 μA . Any additional current due to chemiionization of the lead must have been less than about 0.3 μA , which is 2% of the maximum current, and therefore less than 0.02 ion pairs per lead atom.

Petrol contains about 0.1% of lead of 7×10^{-5} lead atoms per carbon atom (Richardson et al, 1963). The production of 0.02 ion pairs per lead atom as a result of chemiionization would give 1.4×10^{-6} ion pairs per carbon atom. It is shown below that adiabatic stoichiometric hydrocarbon/air flames give about 7×10^{-6} ion pairs per carbon atom. The addition that can be given by chemiionization of the lead therefore appears to be small, which suggests that the action of lead as an antiknock does not result from its influence on the number of ions produced.

12.4. Noisy Flames.

Some hydrocarbon/oxygen flames were noisy. Propane gave this effect most easily. The phenomenon was observed also by Yunlu (1959) and is probably due to the flame vibrating. If the flame moves closer to the disc the heat loss increases, which reduces the flame temperature and the burning velocity, causing the flame to be carried downstream away from the disc. The flame temperature then begins to rise again and the burning velocity increases. It is thus possible for the flame to oscillate about its mean position.

The addition of hydrogen to noisy flames made them quiet, which was found to reduce the saturation current although the measured final flame temperatures were not

reduced. The higher saturation currents from noisy flames appears to be due to the periodic variation of the temperature, which makes the saturation current higher than that corresponding to the mean temperature because the saturation current does not vary linearly with T_f .

12.5. Effect of Final Flame Temperature.

Like most chemical reactions, ionization in flames has a global activation energy (Lawton & Weinberg, 1964). The saturation current density is given by an Arrhenius equation of the form $j_s = KT_f^n \exp(-E_a/RT_f)$ where K , n are constants. This equation gives $d(\ln j_s)/d(1/T) = -E_a/k - nT$, which is approximately equal to $-E_a/k$. Figs. X(1) to (12) show $\log j_s$ versus $10^4/T_f$ °K for hydrocarbon/air and hydrocarbon/oxygen flames. These graphs are mostly straight lines, which confirms the above relationship and that n is small. In the case of some oxygen flames it was necessary to take mixtures containing hydrogen in order to obtain straight lines. The fact that straight graphs were obtained over large ranges of T_f shows that the saturation current density was not much affected by quenching of active species on the porous disc.

12.5.1. Effective Activation Energies.

Values of $d(\log j_s)/d(10^4/T_f)$ are given in Ch X.

Activation energies calculated from these gradients, taking $n = 0$, are given below:

E_a is in kJ mol^{-1}
 ($1 \text{ kJ mol}^{-1} = 0.24 \text{ kcal mol}^{-1}$).

Methane/air

ϕ	0.6	0.87	1.04	1.25	1.30	1.39	1.64
E_a	247	187	243	331	348	381	1072

Ethane/air

ϕ	0.70	0.91
E_a	218	205

Propane/air

ϕ	0.69	1.02	1.27
E_a	159	176	306

Ethylene/air

ϕ	0.52	0.69	0.85	1.05	1.17	1.61	1.83	2.0	2.4
E_a	276	251	198	174	193	306	477	695	821

Methane/hydrogen/oxygen

ϕ	0.187	0.187	0.30	0.30	1.0	1.51
% H_2	0	3.38	0	4.85	0	0
E_a	293	322	272	264	310	461

Ethane/hydrogen/oxygen

ϕ	0.152	0.262	0.272
% H_2	0	0	4.76
E_a	322	360	252

Propane/hydrogen/oxygen

ϕ	0.150	0.275
% H_2	0/2.91	5.05
E_a	276	259

Ethylene/hydrogen/oxygen

ϕ	0.155	0.254
% H_2	0/2.86	0/4.58
E_a	297	276

The average values of the activation energy from the above results, excluding rich flames of stoichiometric ratio above 1.1, are:

$$E_a = 210 \text{ kJ mol}^{-1} \text{ (50 kcal mol}^{-1}\text{) for hydrocarbon/air,}$$

$$E_a = 294 \text{ kJ mol}^{-1} \text{ (70 kcal mol}^{-1}\text{) for hydrocarbon/hydrogen oxygen.}$$

Lawton & Weinberg (1964) obtained an average value for hydrocarbon/air of 205 kJ mol^{-1} . Thus the average value of E_a for hydrocarbon/air flames is in good agreement with that of Lawton & Weinberg and the values obtained by other workers (Van Tiggelen, 1963; Calcote, 1963a).

Rich flames gave higher values of E_a . It appears that the measured saturation current density varied more rapidly with final flame temperature for rich flames because at low temperatures some of the ionizable constituents (unburnt or partially burnt fuel) escaped whereas at higher temperatures they did not. The fact that ionizable constituents passed through the flame was shown by the occurrence of ionization in the secondary flame with the surrounding air. This ionization in the secondary flame increased the total current but not the probe current, so that the ratio of the total current to the probe current was greater at lower values of T_f than the ratio of the flame area to the effective probe area, as shown by the results for methane/air at $\phi = 1.30$ and propane/air at ϕ

= 1.27. The products of moderately rich hydrocarbon flames are usually CO_2 , CO , and H_2O , which should not give further ionization. The results show that, at low temperature, equilibrium is not attained in the primary flame.

12.5.2. Alternative Methods of Calculating the Activation Energy.

The activation energies given above are calculated from the saturation current density. An activation energy could be obtained for the variation of the ionization efficiency, n_e/n_c , with final flame temperature. The variation of the burning velocity, S_u , with the final flame temperature (Kaskan, 1957) is about half the variation of the saturation current density, j_s . At constant composition n_e/n_c is proportional to j_s/S_u . The variation of n_e/n_c with temperature is therefore about half that of j_s and the activation energy for n_e/n_c about half that calculated from j_s , giving a value in good agreement with those obtained by Hand & Kistiakowsky (1962) in shock tube studies and by Peters & Van Tiggelen (1968).

The rate of ionization per unit volume is equal to the saturation current density divided by the thickness of the ionization zone. Van Tiggelen (1963) has calculated activation energies for the ionization reaction taking into account changes in a "flame thickness" based on the theory

of flame propagation.

The variation of the reaction zone thickness can be estimated by assuming that the temperature gradient, dT/dx , is constant. The flame thickness is then proportional to $(dT/dx)^{-1}$. For lean flames, the rate of heat release in the reaction zone is Gc_fH per unit area where G is the mass flux density, c_f the initial fuel concentration, and H is the calorific value of the fuel. If all the reaction occurs near T_f then the temperature at the beginning of the reaction zone is approximately equal to T_f . Since gas then enters and leaves the reaction zone at approximately the same temperature there is little net heat loss from the reaction zone by convection and most of the heat loss must be by conduction. The heat flux density due to conduction is equal to $-k dT/dx$, giving

$$k dT/dx = Gc_fH.$$

$$\begin{aligned} \text{Therefore flame thickness} &\propto (dT/dx)^{-1} \\ &\propto (Gc_f)^{-1} \\ &= (\text{fuel flow rate per unit area})^{-1} \\ &\propto S_u^{-1} \text{ at constant composition.} \end{aligned}$$

Thus simple thermal flame theory gives the flame thickness to be inversely proportional to the fuel flow rate, and, at constant composition, to the burning velocity. Flame theory based on the diffusion of radicals (Gaydon & Wolfhard, 1949) also gives the reaction zone

thickness to be approximately inversely proportional to the burning velocity. If the burning velocity increases with temperature at half the rate the saturation current density does, then the effective activation energy of the rate of ionization per unit volume is 1.5 times that of the saturation current density.

The reaction zone thickness of flames is difficult to estimate and the distance over which ionization occurs is not necessarily equal to the reaction zone thickness (see Ch III). It is therefore easier and more reliable to take activation energies calculated from the saturation current density since the latter quantity can be measured directly.

The activation energy calculated from the saturation current density is not necessarily more fundamental than that calculated from the ionization efficiency or the ionization per unit volume. However, the saturation current density is the quantity required for many practical purposes and it can be measured directly and easily. For this reason activation energies calculated from j_s are given.

12.6. Maximum Saturation Current Densities and Ionization Efficiencies.

Saturation current densities and ionization

efficiencies increase with final flame temperature and are also a maximum for near stoichiometric flames. The maximum value of these quantities must therefore be given by near stoichiometric adiabatic flames. Estimated maximum values of the saturation current densities and ionization efficiencies, calculated from the data given, are presented in the following table. The values at a single temperature (2069°K) are also given for the purpose of comparison.

	Fuel in air				CH ₄	H ₂ /air +
	CH ₄	C ₂ H ₆	C ₃ H ₈	C ₂ H ₄	/O ₂	½% C ₃ H ₈
T _f , °K	2079	2018	2010	1950	2069	1667
φ	1.04	0.91	1.02	1.05	1.05	
j _s , A m ⁻²	0.124	0.154	0.126	0.205	0.035	0.009
E _a , kJ mol ⁻¹	243	297	176	172	310	239
j _s at 2069°K	0.117	0.208	0.181	0.430	0.035	0.250
% fuel	9.96	6.28	4.54	7.40	33.3	
φ	1.06	0.96	1.13	1.14	1.00	
T _{ad} , °K	2491	2500	2505	2630	3049	2373
S _u , m s ⁻¹	0.34	0.40	0.39	0.68	3.28	2.69
j _s , A m ⁻² *	0.913	1.68	1.50	5.71	8.34	
n _e /n _c x 10 ⁶ *	6.7	8.4	7.0	12.4	1.9	
j _s , A m ⁻² **	1.27	1.52	1.01	3.10	11.1	1.43
n _e /n _c x 10 ⁶ **	9.3	7.6	4.7	6.8	2.5	9.1

*, calculated taking the average values of E_a (210 kJ mol⁻¹ for air flames, 294 kJ mol⁻¹ for oxygen flames, 239 kJ mol⁻¹ for hydrogen/air flames containing hydrocarbon). **, calculated taking the observed values of E_a given in the first part of the table.

T_{ad} represents the final flame temperature and S_u the corresponding burning velocity. The saturation current density for the hydrogen/propane/air flame is taken from Lawton & Weinberg (1964). For methane/oxygen and hydrogen/air the calculated adiabatic final flame temperature for the stoichiometric mixtures have been taken from Gaydon & Wolfhard (1960) and the burning velocities from Lewis & von Elbe (1961). For hydrocarbon/air flames the values for the mixtures of maximum burning velocity are taken. The values of S_u and the initial fuel concentration are from Perry (1963) and those for T_{ad} from Gerstein et al (1951).

The estimates of j_s and n_e/n_c for adiabatic flames are approximate since a comparatively large error would result from a small error in the value of E_a taken. The estimates were obtained by taking average activation energies or those observed for each mixture. The variation of j_s with ϕ at constant T_f was ignored. The two sets of values obtained differ by factors between 1.3 and 1.8, the correct values probably lying between the two estimates.

As shown in Ch VIII, the saturation current densities required to obtain maximum practical effects are of the order of 0.25 to 2.5 A m⁻². The above estimates of the maximum saturation current densities of hydrocarbon flames show that it is possible to obtain saturation current densities of this magnitude. In most cases, however, the saturation current densities are much lower than 2.5 A m⁻², when the maximum current density which can be drawn, and the maximum practical effect obtainable where this depends on the current density, becomes limited by the flame saturation current.

In cases where the flame saturation current is too low, it can be increased by making the flame turbulent, which increases its surface area, or by seeding. Additional ionization can be produced also by ionizing radiation (Langevin, 1903), electrical discharges (Schuster, 1887), or by the use of lasers.

12.7. Temperature At Which Ionization Occurs.

The combustion of hydrocarbons appears to occur in two stages (see Ch VII): oxidation to CO and H₂O followed by the oxidation of the CO to CO₂. These two stages tend to occur successively (Westenberg & Fristron, 1961). It is of interest to know at which stage in the combustion reaction the ionization occurs.

It is not to be expected that the ionization occurs in the preheat zone since the rate of ionization is much lower at low temperatures. Hydrogen added to hydrocarbon/oxygen flames probably burns early in the flame, which would alter the temperature distribution in the preheat zone. The saturation current density was unaltered in most cases, which suggests that the ionization does not occur in the preheat zone. Shock tube studies (Gardiner, 1961) show that chemiluminescence, which appears to be associated with chemionization (see section 12.10.2), does not occur before ignition.

It is thought that ionization in flames results from reactions involving radicals. The maximum rate of radical production in flames occurs during the oxidation to CO and H₂O (Fristrom & Westenberg, 1965). Fewer radicals are produced during the oxidation of the CO. Moreover, the combustion of CO does not normally give ionization. Thus, it might be expected that the ionization would occur during the oxidation of the fuel to CO and H₂O.

The rate of any reaction occurring during the oxidation to CO and H₂O should be a function of the temperature at which that stage is completed, T_{CO} , and not of the final flame temperature (Chase & Weinberg, 1963). If the reaction occurs throughout the reaction zone a mean temperature should be taken (Van Tiggelen, 1963). However,

it appears that most of the ionization occurs near the final flame temperature. This hypothesis is supported by the following evidence.

12.7.1. Experimental Evidence.

i) Flame traverses.

Measurements of the variation of positive ion concentrations with position (Wortberg, 1965; Bradley & Matthews, 1967) show that the maximum concentration occurs near the final flame temperature.

ii) Variation of j_s with T_{CO} and T_f .

Whether the ionization occurs at T_{CO} or T_f can be investigated by varying these temperatures independently. T_{CO} and T_f can be varied independently by altering the composition of the reactants, in particular by adding and subtracting CO and H_2 . The addition of CO increases the heat release between T_{CO} and T_f but not that up to T_{CO} . Hydrogen increases the heat release up to T_{CO} but not that from T_{CO} to T_f . It is simpler and more reliable to vary T_{CO} while keeping T_f constant since the latter can be easily measured. Flames with equal values of T_f but different reactant compositions generally have different values of T_{CO} .

For a set of ethylene/oxygen flames containing up to 21.7% of CO the numbers of ion pairs produced per carbon

atom in the ethylene were 20 to 40% higher than those for flames of the same final temperature and stoichiometric ratio without CO. The change in T_{CO} resulting from the addition of CO can be estimated by calculating the change in the heat release during the CO to CO_2 stage and assuming that all the heat released by any mass of gas goes into raising the temperature of that mass of gas. The increase in the gas temperature from T_{CO} to T_f is then equal to the heat release divided by the thermal capacity. The heat release during the oxidation of flame gases is approximately 31 J mol^{-1} . These figures give the decrease in T_{CO} to have been up to 1300 K. Thus, although the addition of carbon monoxide increased n_e/n_c , the calculated value of T_{CO} was greatly decreased.

When hydrogen was added to hydrocarbon/oxygen flames the saturation current densities were similar to those of flames of the same temperature and stoichiometric ratio but without hydrogen. In a typical case 4.58% of hydrogen was added to ethylene/oxygen and the ethylene concentration reduced by 0.75%. The decrease in the proportion of CO produced was thus $2 \times 0.0075 = 0.015$, giving the increase in T_{CO} to be about 140 K. The activation energies, with respect to T_{CO} , of the saturation current densities of hydrocarbon/air flames are about 48 J mol^{-1} (Lawton & Weinberg, 1964). Taking T_{CO} to be

1000°K, an increase in T_{CO} of 140 K should increase the saturation current density by a factor of about two if j_s is a function of T_{CO} . The average change in j_s was much less than this.

The above results show that when hydrogen and carbon monoxide, particularly the latter, are added to hydrocarbon flames and T_f kept constant the change in the rate of ionization is small and does not correspond to the calculated change in T_{CO} , which suggests that the rate of ionization depends on T_f and not on T_{CO} , in which case the ionization must occur near T_f .

In hydrogen flames containing small concentrations of added hydrocarbon T_{CO} and T_f are nearly equal, so that the activation energies obtained taking T_f or T_{CO} are the same. This activation energy is nearly equal to that calculated for hydrocarbon flames taking T_f but much greater than that calculated taking T_{CO} (Lawton & Weinberg, 1964). It seems reasonable to assume that the activation energies in both types of flame have similar values, suggesting once more that those calculated taking T_f are correct and the ionization occurs near T_f .

The results show that, for flames with equal final flame temperatures, the saturation current densities and n_e/n_c increase with increasing stoichiometric ratio to a maximum near $\phi = 1$, and then decrease. The heat release

and therefore the temperature rise from T_{CO} to T_f is greatest for stoichiometric flames and T_{CO} therefore least. The fact that the rate of ionization is greatest for stoichiometric flames would indicate again that it does not depend on T_{CO} .

Until the combustion reaction nears completion there is excess oxygen available, even in rich flames. It is only near completion that rich and lean flames differ in nature. The fact that the rate of ionization is a maximum for near stoichiometric flames therefore suggests that the ionization occurs during the latter stages of the combustion.

12.7.2. Discussion.

It has been assumed that the temperature rise from T_{CO} to T_f is equal to the heat release divided by the thermal capacity of the gas. This is true only if the two stages of the combustion are completely separate and no heat produced in the second stage is conducted upstream to the first. Measurements show that the temperature gradient does not become zero after the first stage before the second (Fristrom et al, 1953) and that the oxidation to CO and H₂O and that to CO₂ overlap (Westenberg & Fristrom, 1961).

A typical hydrocarbon/oxygen flame contained 7.8% of ethylene, which gives 15.6% of CO. If the oxidation to H₂O and CO and that of the CO were separate, the difference

between T_{CO} and T_f would be 1400 K. It has been found (Westenberg & Fristron, 1961) that the average temperature at which the oxidation to CO and H₂O occur is not more than about 250 K below the final flame temperature. Thus it is clear that $(T_f - T_{CO})$ cannot be equal to the heat released by the oxidation of the CO divided by the thermal capacity of the gas. The regions in which the oxidation to CO and H₂O and that of CO to CO₂ occur overlap. For many purposes the reaction zones of flames can be considered as well mixed homogeneous reactors (Van Tiggelen & Feugier, 1965).

It has been shown that the ionization in flames occurs near the final flame temperature. It does not necessarily occur as a result of the last step, ie. the oxidation of CO, which does not normally give ionization. Since the rate of ionization would tend to occur near T_f even if the reactants producing ionization are species occurring in larger concentrations earlier in the flame. That ionizable components can survive into the burnt gases is shown by the fact that some ionization occurs downstream of flames, as described in Ch VIII, and that the combustion of the products of rich flames in the surrounding air can give further ionization, as discussed in Section 12.5.1. Since all the steps of the combustion occur throughout the reaction zone to some extent it is possible for the

ionization to be given by one of the initial oxidation reactions occurring towards the end of the reaction zone at a temperature near the final flame temperature.

To investigate the mechanism of ionization in flames it is necessary to establish at what temperature the ionization occurs. This is known to be near the final flame temperature. It is not, however, necessary to determine the precise position at which the ionization occurs and the saturation current density method of measurements can be used despite the fact that it does not give any spatial resolution.

12.8. Ionization and Flame Propagation.

Ionization appears to be a side reaction (Hend & Kistiakowsky, 1962) not closely connected with the main flame propagation reactions. Electric fields have not been found to have any chemical effect on the propagation on non-sooting flames (see Ch II). Other evidence that ionization is not closely connected with flame propagation includes:

1) Effect of Initial Oxygen Concentration

As shown by Table X(4), the burning velocities of premixed air flames are not very much lower than those of oxygen flames with the same initial fuel concentration and final flame temperature. Replacement of part of the oxygen

by nitrogen in an ethylene/oxygen mixture reduces the burning velocity comparatively little (Linnett & Hoare, 1949) provided excess oxygen is present. In the present study it was shown that the substitution of air for oxygen increases the saturation current density of premixed flames by a factor of the order of twenty. The substitution of air for oxygen reduces the burning velocity but markedly increases the saturation current density, which shows that the ionization process is not closely connected with the flame propagation.

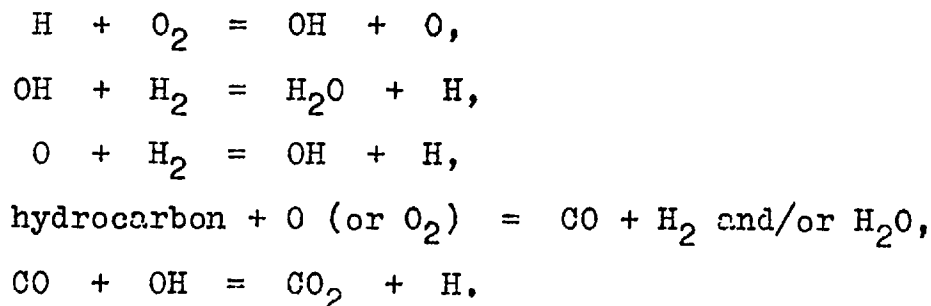
The replacement of oxygen by air in the case of diffusion flames increased the saturation currents in most cases, in spite of the much lower temperatures of the flames with air. Diffusion flames are discussed more fully in Ch XIII.

ii) Effect of Bromine.

Halogens have a marked inhibitory effect on combustion (Roser et al, 1959; Ibiricu & Gaydon, 1964). Bromine had no systematic effect on the saturation currents of diffusion flames (see Ch XI). The saturation current densities of premixed flames with bromine were between 10% and 33% more than those of flames without bromine with the same values of ϕ and T_f .

The fact that the ionization in flames does not appear to be closely connected with the propagation process

indicates that the species which control the rate of propagation do not control the rate of ionization. The main propagation reactions are thought to be



The H radical appears to be the most important in determining the reaction rate (Gaydon & Wolfhard, 1949; Tanford & Pease, 1947; Padley & Sugden, 1959). Bromine is believed to act as an inhibitor by combining with radicals, primarily H (Wise & Roser, 1963). Thus it appears that the H radical does not take part in the ionization process.

12.9. Mechanism of Ionization.

Possible mechanisms of ionization in flames are discussed by Calcote (1957). It has been suggested that thermal ionization is responsible. However, most species occurring in flames have very high ionization potentials and would not give detectable ionization. The only easily ionizable species likely to occur in flames in sufficient concentration to give appreciable ionization is solid carbon. The theory that ionization in flames is due to the thermal ionization of carbon is supported by Perkins et al (1962).

However, lean hydrogen flames containing small concentrations of hydrocarbon, which would not be expected to give solid carbon, give ionization. Rich flames, which should contain more solid carbon than stoichiometric ones, give less ionization. If ionization in flames is due to the thermal ionization of carbon, the activation energy should be equal to the work function of carbon, which is about 4.4 eV or 427 kJ mole⁻¹, which is much greater than the observed activation energy for lean and stoichiometric flames. Thus thermal ionization of solid carbon does not appear to be the mechanism of ionization in premixed flames, except perhaps in very rich ones, which have activation energies (see Section 12.5.1) up to and exceeding the work function of carbon.

Recently it has been suggested that ionization in flames might be due to secondary ionization by energetic electrons (Von Engel & Cozens, 1965), as occurs in the case of argon at high temperatures (Petschek & Byron, 1957). This mechanism would be feasible if the electron temperature were much higher than the gas temperature, which does not appear to be the case in all premixed flames (Trovers & Williams, 1965). In carbon monoxide flames, however, the electron temperature is considerably higher than the flame temperature (Bradley & Matthews, 1967). The fact that the current density reaches a steady value as the field is

increased is further evidence that it is unlikely that the ionization is caused by electrons. Otherwise it is probable that the current density would either decrease as a result of the removal of electrons or increase as a result of the field increasing the electron energies.

The addition of substances of high electron affinity to flames greatly reduces the electron concentration (King, 1962). Bromine has a high electron affinity (Creitz, 1961). The fact that the addition of bromine to premixed and diffusion flames did not markedly reduce the saturation current confirms that secondary ionization by electrons is not an important mechanism of flame ionization.

The results for premixed flames seeded with sodium show that the saturation currents due to the sodium and the hydrocarbon were additive. That due to the hydrocarbon was not increased by electrons drawn from the ionized sodium. That due to the sodium was not altered by positive ions from the reaction zone or by changes of the applied field.

The most probable mechanism of ionization in hydrocarbon flames is chemiionization, which is now discussed.

12.10. Chemiionization.

Various mechanisms have been proposed to account for ionization in flames containing hydrocarbons which fall

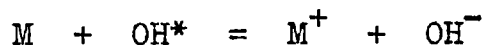
under the general heading of chemiionization. Chemiionization is non-equilibrium ionization resulting from the utilization of chemical energy before thermalization (Sternberg et al, 1962). Ions are produced in a narrow region in the flame reaction zone (Calcote, 1957) in concentrations usually far in excess of the equilibrium value, as is shown by the fact that the ion concentration decreases above the reaction zone.

Chemiionization in systems other than flames has been investigated by Fontijn et al (1965). Since such systems are less complex than the average flame there is more likelihood of the processes involved being elucidated.

It has been shown in the present work that the effective activation energy of the saturation current densities for lean hydrocarbon/air flames is 210 kJ mol^{-1} and for hydrocarbon/oxygen flames 294 kJ mol^{-1} . Hydrogen/air flames containing hydrocarbon give 239 kJ mol^{-1} (Lawton & Weinberg, 1964). These results could be interpreted as suggesting that there is more than one mechanism of ionization. The different activation energies obtained would then be explained by there being two or more ionization reactions of differing activation energies, which reaction predominates depending on the flame.

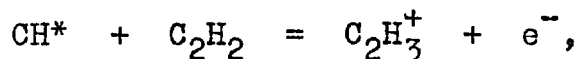
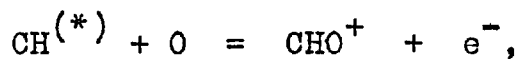
12.10.1. Possible Reaction Schemes.

It appears that most of the negative charge in flames is formed initially as electrons (see Ch VIII), in which case the ionization reaction cannot utilize the electron attachment energy by producing negative ions directly by reactions such as

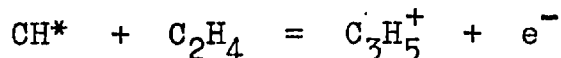


suggested by Tverdokhelbov (1956).

Fontijn et al (1965) give the most likely ionization reactions to be:



or, in ethylene flames,



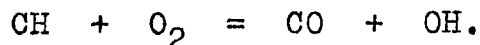
-suggesting that CHO^+ , $C_3H_3^+$, and $C_3H_5^+$ could all be primary ions.

Possible ionization reactions with $C_2^{(*)}$ are given by Calcote (1962).

The hypothesis that $CH^{(*)}$ is an ion precursor in premixed flames is probably correct. It exists in the excited state in concentrations much higher than the equilibrium value (Gaydon, 1957). The concentration of CH^* has been found in shock tube studies to increase with

the same time constant as the ion concentration (Glass et al, 1965). This radical, together with C_2^* , is not thought to be closely connected with the flame propagation process. Nor does ionization appear to be.

Replacing air by oxygen, increasing the oxygen concentration by a factor of 4.8, reduced the saturation current densities of premixed flames by a factor of the order of 20. This effect is so large that it appears that it must be due, partly at least, to competition by the oxygen for a species taking part in the reaction leading to ionization. This species may be CH, eg.



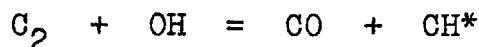
Oxygen is a well known free radical scavenger (Fontijn et al, 1965).

It has been shown in the present work that the saturation currents of hydrocarbon flames are a maximum for approximately stoichiometric flames (see Ch X) and that fuel injected into the hot products of a flame (see Ch XI) gives negligible ionization. These facts suggest that the reaction leading to ionization are between components from the fuel and from the oxidant. The saturation current is proportional to the concentration of hydrocarbon added for premixed (Lawton & Weinberg, 1964) and diffusion (Sternberg et al, 1962) hydrogen/air flames, showing that one

participant in the ionization reaction comes from the hydrocarbon.

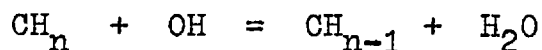
The present results for the addition of ethylene to a premixed CO/air flame (Fig X(15)) show that the saturation current is proportional to the square of the hydrocarbon concentration, which indicates that in this flame two reactants taking part in the reactions leading to ionization have to be supplied by the hydrocarbon, one of which is already present in hydrogen flames. This reactant, or reactants, must contain hydrogen. However, as shown above, the H radical does not appear to contribute to the ionization.

OH may contribute to ionization in flames by giving CH by the reaction



as suggested by Gaydon & Wolfhard (1960).

Another possible mechanism for the production of CH is dehydrogenation, such as by the reaction



There is a close parallelity between the rate of ionization in flames and the concentration of OH (Kinbara & Noda, 1969), which makes it likely that OH takes part in the reactions leading to ionization. CH produced by OH could give ionization by one of the reactions given above.

From the work of Ferguson (1957) it appears that

$C_2^{(*)}$ is produced by polymerization, as it must be in flames containing methane. Its concentration would therefore be expected to depend on a power of the fuel concentration higher than the first (Bulewicz, 1967). It is difficult to see how ionization in hydrogen flames, which is proportional to the hydrocarbon concentration, can be related to C_2 , although this mechanism might occur in other flames.

12.10.2. Role of Excited Species.

Chemionization and chemiluminescence have been shown to have the same time and temperature dependence (Hand & Kistiakowsky, 1962). It has been shown in the present study that the flames which give most chemionization are those which give most chemiluminescence: diffusion flames (see Ch XIII) give comparatively small saturation currents and give little chemiluminescence (Gaydon & Wolfhard, 1960); diffusion flames with air give higher saturation currents than those with oxygen and give more chemiluminescence. Thus flames which give chemionization give abnormal electronic excitation, whereas flames which do not give ionization, such as H_2 , CO , CS_2 , and $HCOH$, tend not to (Gaydon & Wolfhard, 1951). These results indicate that there is a connection between chemiluminescence and chemionization, as is to be expected since

both are forms of electronic excitation.

The question arises as to whether the ion precursors are excited. Miller (1967), Bulewicz (1967) and Arrington et al (1965) all question whether the excited radical CH^* can be responsible for ionization in flames. Unexcited CH has been detected in flames (Gaydon, Spokes & van Suchtelen, 1960). In the present study it was found that CO_2 reduces the saturation currents of premixed and diffusion flames of hydrocarbon/air and of premixed CO/air flames containing small amounts of hydrocarbon. The saturation currents of premixed and diffusion flames of hydrogen/air containing small amounts of hydrocarbon and of premixed hydrocarbon/oxygen flames were increased. CO_2 quenches excited species (Fontijn et al, 1965). Therefore it is likely that the ionization is produced by unexcited species in those flames the saturation currents of which are not reduced by CO_2 addition and by excited species in those flames where the saturation current is reduced. In particular, premixed CO flames containing hydrocarbon, the saturation currents of which are reduced by CO_2 addition, are known to give more disequilibrium than H_2 flames containing hydrocarbon (Bradley & Matthews, 1967), the saturation currents of which are not reduced by CO_2 addition.

It has been found that the concentration of C_3H_3^+

in flames is reduced by the addition of CO_2 (Calcote et al, 1965), which suggests that this ion may be produced by the excited radical CH^* . The proportion of the ionization due to C_3H_3^+ has been found to increase with hydrocarbon concentration (Green & Sugden, 1963). The present results are consistent with a high proportion of the primary ions formed in hydrocarbon/air flames being C_3H_3^+ and this ion being produced by CH^* , while most of those in the other flames are CHO^+ produced by unexcited CH . It is to be expected that C_3H_3^+ would constitute a higher proportion of the ions formed in air flames than in oxygen flames, in which species containing several carbon atoms would tend to be rapidly oxidized.

It has been suggested that the ionization produced during the oxidation of phosphorus results from ultra-violet chemiluminescence. This theory does not appear to be correct (Mayer & Muller, 1904). Similarly, the ionization in hydrocarbon flames is unlikely to be caused by radiation from the reaction zone since most of the ionization occurs over a narrow region.

12.11. Sooting Flames.

Very rich non-sooting flames gave very low saturation current densities. However, as shown by the results for methane/oxygen, sooting flames, that is flames

above which yellow luminosity occurred, gave higher saturation currents. Fig X(13) shows the variation of saturation current with height above two rich ethylene/air flames. Yellow luminosity commenced about 7 mm above the burner. The results show that the saturation current density was very small for electrode separations of less than about 5 mm and increased with electrode separation, showing that ionization occurred in the gas above the flame. It appears that this ionization is associated with the sooting and probably results from thermionic emission from the carbon particles.

The ethylene flames gave the following results:

Final flame temperature, T_f , °K	1784	1880
Brightness temperature at 6550 Å, T_{br} , °K	1250	1132
Ionization above flame, J , A m ⁻³	1.41	0.62

The optical path length through the flame, d , was approximately 40 mm.

The emissivity, e_λ , at wave length λ is given by

$$\begin{aligned}
 e_\lambda &= \frac{\exp(hc/(\lambda kT_f)-1)}{\exp(hc/(\lambda kT_{br})-1)} \\
 &= \exp(-(hc/(\lambda k))(T_{br}^{-1} - T_f^{-1})) \text{ approximately} \\
 &\hspace{15em} (1)
 \end{aligned}$$

since, because the soot particles are small, their temperature can be taken to be equal to the gas temperature.

Electron micrographs taken in the present work showed that the radius of the soot particles, r , was of the order of 150 \AA , which is much less than $\frac{1}{2} \lambda$. Therefore the formula given by Thring (1965), which is based on the Mie theory of scattering, can be used, giving

$$e_{\lambda} = \frac{33}{8} \frac{d}{\lambda} \times \text{volume of soot per unit volume} \quad (2)$$

$$= \frac{11}{8} \frac{rd}{\lambda} \times \text{surface area of soot per unit volume} \quad (3)$$

where the numerical constant is taken to be equal to that determined at a similar wave length of 5000 \AA .

Substituting for e_{λ} in (2) from (1) and taking the experimental values, gives the proportion of the carbon in the fuel converted into soot to be 0.4% and 0.03% in the cooler and hotter flames respectively. These flames sooted comparatively lightly. Since up to a few per cent of the carbon in the fuel can be released in premixed hydrocarbon flames (Thring, 1965) the values obtained are reasonable.

From the Dushman (1923) equation:

$$J = AT^2 \exp(-\psi/(kT)) \times \text{surface area of soot per unit volume} \quad (4)$$

where ψ is the work function for the emission of electrons from the soot.

Substituting for e in (3) from (1), dividing by (4), and substituting the experimental results gives two simultaneous equations, which give $\psi = 4.62 \text{ eV}$. This value

is close to that for graphite (4.4 eV).

If the random error in the measured temperatures (T_f and T_{br}) is 5 K, then the work function obtained is accurate to within about 10%.

It has been assumed that the surface of the carbon particles emits electrons in accordance with the same law as plane surfaces. The increase in the potential of a particle due to the emission of electrons is equal to $e/r\epsilon = 0.1$ volt per electron. This increase in potential has been ignored.

12.12. Catalytic Oxidation.

Ionization occurs during the catalytic oxidation of hydrocarbons at heated surfaces (Perkins et al, 1963). This ionization has been studied by passing air containing small concentrations of hydrocarbons over a filament. The ionization efficiency is near its maximum when the filament temperature is about 1043°K , when the number of ion pairs produced per carbon atom oxidized is about 7×10^{-8} to 3×10^{-6} , depending on the hydrocarbon used (Woods et al, 1965). Woods et al used filament temperatures up to 1293°K .

It is shown in Section 12.6 that the ionization efficiency for adiabatic paraffin/air flames at about 2500°K is of the order of 7×10^{-6} . The effective

activation energy for n_e/n_c is approximately 105 kJ mol^{-1} , allowing for the variation of the burning velocity with temperature. The ionization efficiency for combustion at 1043°K and 1293°K should therefore be of the order of 6×10^{-9} and 6×10^{-8} respectively. Thus catalytic oxidation in most cases gives greater ionization efficiencies than gas phase combustion would at the same temperatures. Catalytic oxidation also differs from combustion in other respects. The ionization efficiency is very dependent on the hydrocarbon structure. The ionization current depends on the field polarity, presumably as a result of the reaction being heterogeneous. As the temperature is increased the yield reaches a maximum value. This maximum may be due to a greater proportion of the oxidation occurring in the gas phase.

12.13. Analysis of Ion Concentration Measurements.

The rate of ion generation through a flame can be calculated from the ion concentration, n . The ion flux at any point is equal to $(nu - D \text{ dn}/\text{dx})$ where u is the flow velocity and D the diffusion coefficient. The rate of ion generation, J/e , is equal to the rate of recombination plus the rate of increase of the ion flux with distance, giving

$$\text{rate of ion generation} = \alpha n^2 + (d/\text{dx})(nu - D \text{ dn}/\text{dx})$$

$$= \alpha n^2 + u \frac{dn}{dx} - D \frac{d^2n}{dx^2} + n \frac{du}{dx} \quad \text{ion pairs per unit volume per unit time.}$$

Rates of ion generation were calculated from the results of Wortberg (1965). The following results (in ion pairs $\times 10^{18} \text{ m}^{-3} \text{ s}^{-1}$) were obtained at intervals of 0.37 mm.

αn^2	0.1	0.5	2.0	6.5	32.4	31.5	7.2	3.4	1.9
$u \frac{dn}{dx}$	0.6	1.1	2.1	4.4	1.7	1.5	-4.5	-1.9	-1.4
$-D \frac{d^2n}{dx^2}$	-0.4	-0.6	-1.7	-6.1	7.9	21.8	-5.3	-1.9	-0.5
$n \frac{du}{dx}$	0.1	0.1	0.2	0.4	0.9	0.8	0.1	0	0
J/e	0.4	1.1	2.5	5.2	42.9	52.5	-2.5	-0.4	0
αn^2	1.3	0.8							
$u \frac{dn}{dx}$	-	-0.6							
$-D \frac{d^2n}{dx^2}$	-	-0.2							
$n \frac{du}{dx}$	0	0							
J/e	-	0							

These results show that nearly all the ionization occurs in a region of width under 1 mm near the region of maximum ion concentration, which is also the region of maximum heat release rate and where the temperature reaches the final flame temperature. The presence of ions upstream of the region of maximum ion concentration is largely due to diffusion.

The saturation current is given by

$$j_s = e \int_{-\infty}^{\infty} \alpha n^2 dx.$$

The sum of the values of αn^2 is about $8.8 \times 10^{19} \text{ m}^{-3} \text{ s}^{-1}$, giving

$$\begin{aligned} j_s &= 1.6 \times 10^{-19} \times 8.8 \times 10^{19} \times 0.00037 \\ &= 5.2 \times 10^{-3} \text{ A m}^{-2}. \end{aligned}$$

The final flame temperature was 1500°K and the stoichiometric ratio 0.513. The measured saturation current density of a lean methane/air flame ($\phi = 0.6$) with a final temperature of 1574°K was 0.93 mA m^{-2} (Ch X). From this value, the saturation current density of Wortberg's flame could be estimated, when a value of 0.5 mA m^{-2} was obtained. Thus the saturation current density calculated from the measured ion concentrations is about ten times that obtained from direct measurements.

Calcote (1957) gives the maximum mole fraction of positive ions in a propane/air flame ($\phi = 0.84$, $T_f = 1535^\circ\text{K}$) to be 1.1×10^{-7} , which is equivalent to an ion concentration of about $6 \times 10^{17} \text{ m}^{-3}$. The ionization zone thickness was of the order of 0.1 mm, giving the saturation current density to be 600 mA m^{-2} , taking α to be $10^{-13} \text{ m}^3 \text{ s}^{-1}$. The measured value at $\phi = 0.69$, $T_f = 1535^\circ\text{K}$ was 4 mA m^{-2} (Ch X), which is less than the calculated value by a factor of 150.

The measurements of Wortberg give a saturation current density nearer to the measured value than the earlier measurements given by Calcote. The saturation current density calculated from the ion concentrations given by

Wortberg is nevertheless too high by a factor of ten. The most probable reason for the discrepancy is to be found in the uncertainty associated with the use of probes, especially at pressures of the order of atmospheric and above. Another reason may be that the recombination coefficient is less in the reaction zone than the value taken, which was obtained from measurements downstream of flames. In the reaction zone a higher proportion of the negative charge is in the form of electrons, which may have a lower recombination coefficient with positive ions than negative ions do (Gaydon & Wolfhard, 1960). These results show that the calculation of ion production rates from ion concentrations is unreliable.

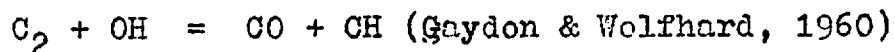
12.14. Summary.

Saturation current measurements have been made on a wide variety of flames. It was shown how the saturation current varies with temperature and stoichiometric ratio. Values of the saturation current densities given by different hydrocarbons and by flames with air and with oxygen were compared. Effects observed due to additives and the substitution of oxygen for air were discussed. Effective activation energies for the saturation current densities were obtained for different mixtures. Estimates were made of the maximum saturation current densities and ionization

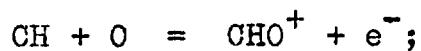
efficiencies obtainable. It was shown that the former are approximately 1 to 10 A m^{-2} and the latter of the order of 7×10^{-6} for stoichiometric flames of the gases taken.

From the results of the present work on premixed flames it appears that:

- a) the ionization occurs near the final flame temperature;
- b) the ionization is not directly connected with the flame propagation process;
- c) chemiionization of metallic additives does not occur in the flames;
- d) the ionization is unlikely to result from electron collision;
- e) the ionization is unlikely to result from the thermal ionization of flame carbon except in very rich luminous flames;
- f) in these the work function of flame carbon was deduced to be 4.6 eV, which is close to that of graphite;
- g) the ionization in non-luminous flames probably results from chemiionization;
- h) the H radical probably does not play an important part in the ionization reaction;
- i) the ionization is probably given by $\text{CH}^{(*)}$, which is possibly produced by OH. A likely reaction scheme is the production of CH by



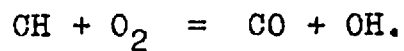
or by dehydrogenation, followed by



and possibly, in addition, in hydrocarbon/air flames and CO/air flames with hydrocarbon added,



j) oxygen inhibits the ionization reaction by competition for reactive species, e.g.



CHAPTER THIRTEEN.DIFFUSION FLAMES.

13.1. Variation with Fuel Flow Rate.

The results obtained for diffusion flames are given in Ch.XI. The values in Tables XI(1) and (2) show that the saturation currents obtained from hydrocarbon/air diffusion flames on a variety of burners were proportional to the hydrocarbon flow rate over large ranges of variation of the latter. The results for methane/air flames given in Table XI(1) show that the ratio of the saturation current to the fuel flow rate was similar for all the burners used although the fuel throughputs per unit area of flame differed, which shows that the saturation current is primarily a function of the fuel flow rate and not of the flame area. Data given in Table X(2) for flames of several hydrocarbons on a batswing burner are summarized in Table XIII(1) below.

Table XIII(1)

Saturation currents of diffusion flames in air on a batswing burner.

Fuel	Range of fuel flows(l/min)	Saturation current (μ A) Fuel flow (l/min)	Average n_e/n_c $\times 10^7$
CH ₄	1.7 - 4.1	27 \pm 2	3.8
C ₂ H ₆	0.1 - 0.84	78 \pm 8	5.5
C ₃ H ₈	0.26- 0.92	130 \pm 1	6.1
C ₂ H ₄	0.08-0.64	87 \pm 10	6.1
C ₂ H ₂	0.08- 0.47	140 \pm 12	9.9

For the candle flame $n_e/n_c = 7.7 \times 10^{-7}$.

The results confirm that the saturation currents of hydrocarbon diffusion flames are proportional to the fuel flow rate, giving an approximately constant value of the ionization efficiency, n_e/n_c , for each fuel. The value of n_e/n_c is similar for different hydrocarbons.

13.2. Counter-Flow Diffusion Flame.

The results for counter-flow methane diffusion flames show that although the ratio of the saturation current to the fuel flow rate is of the same order as for the other burners considered it varies very much with the fuel and oxidant flow rates, particularly in the case of flames with oxygen. Because of these variations, counter-flow diffusion flames do not appear suitable for saturation current measurements.

13.3. Effect of Additives.

13.3.1. Addition of Nitrogen.

Results given for the addition of nitrogen to two methane/oxygen flames show that the effect of the nitrogen is to increase the saturation current markedly. Methane/oxygen flames without nitrogen added gave lower ionization efficiencies in most cases than methane/air flames. Methane/oxygen flames at reduced pressure gave ionization efficiencies

lower than those for methane/air flames by a factor of about eight. These results show that whereas n_e/n_c for oxygen diffusion flames is less on average than for air it varies over a wide range with the burner and the flow conditions, as is confirmed by the results obtained using counter-flow diffusion flames.

The effect of the addition of nitrogen to a hydrogen/oxygen diffusion flame containing a little methane was particularly marked. The increase in the saturation current was of the order of twenty fold. An increase was obtained also in the case of a hydrogen/air flame containing a little propane (see section 11.6.4).

The addition of nitrogen to hydrocarbon/air flames tended to decrease the saturation current.

The result for propane plus nitrogen given in section 11.6.4 (61% nitrogen, $i_s = 48 \mu\text{A}$, propane flow, f , $= 0.42 \text{ l min}^{-1}$, $i_s/3f = 38.1 \mu\text{A min l}^{-1}$) is in satisfactory agreement with that of Pejack & Jones (1968). Their flame contained 81.5% nitrogen. The propane flow was 0.5 l min^{-1} and the saturation current about $35 \mu\text{A}$, both per 100 mm width of burner, giving $i_s/3f = 23.3 \mu\text{A min l}^{-1}$.

13.3.2. Addition of Hydrogen.

The addition of hydrogen to hydrocarbon/air flames reduced the saturation current. The results for the addition

of hydrogen to a methane flame on a 3 mm i.d. nozzle show that the ratio of the saturation current to the fuel flow was reduced from 55 to 3.1 μA per litre of methane per minute. Similarly, a hydrogen/propane/air flame (section 11.6.4) gave a lower saturation current per unit flow of propane than pure propane/air flames.

The results given in Table XIII(1) together with that for the candle flame are given below arranged in order of increasing $n_{\text{H}}/n_{\text{C}}$ where $n_{\text{H}}/n_{\text{C}}$ is the ratio of the number of hydrogen atoms to the number of carbon atoms in the fuel. $n_{\text{H}}/n_{\text{C}}$ for the candle would be 2 assuming the formula to be $(\text{CH}_2)_n$.

Fuel	C_2H_2	candle	C_2H_4	C_3H_8	C_2H_6	CH_4
$n_{\text{H}}/n_{\text{C}}$	1	2	2	2.7	3	4
$n_{\text{e}}/n_{\text{C}} \times 10^7$	9.9	7.7	6.1	6.1	5.5	3.8

These results show that burning a fuel containing more hydrogen reduces $n_{\text{e}}/n_{\text{C}}$. Thus burning a hydrocarbon containing more hydrogen appears to be equivalent to adding hydrogen to the fuel, as if the fuel decomposed before ionization.

The reduction of the saturation current of diffusion flames by the addition of hydrogen may be due to the hydrocarbon having less opportunity to mix with the oxygen. The hydrogen would tend to diffuse ahead of the

hydrocarbon and burn first. The initial oxidation of the hydrocarbon would be largely by OH. Oxidation by OH is not likely to give much ionization since the amount of ionization depends on the energy released by the oxidation process (Bulewicz, 1967).

13.3.3. Addition of Carbon Monoxide.

The effect on n_e/n_c of the addition of carbon monoxide in concentrations of up to 94% to hydrocarbon/air flames on a batswing burner was not large. For methane/air, n_e/n_c was increased by 14% at one methane flow rate and by 32% at a lower methane flow rate. For propane/air, n_e/n_c was increased by up to 46%. These increases are probably due to not all the fuel being burnt when no carbon monoxide was present, or to higher combustion efficiencies resulting from a reduction in the amount of soot produced. The results show that CO addition does not markedly affect the ionization of hydrocarbons in diffusion flames.

The results show that for the addition of methane to a carbon monoxide/air flame in concentrations of 1 to 7% the saturation current was proportional to the methane flow rate, which shows that the ionization of the methane was not affected by disequilibrium in the flame (see section 13.3.5) for methane concentrations of over 1%. That the saturation current is proportional to the methane concentration suggests

that it due to one component already present in the carbon monoxide flame and one component from the methane, probably $\text{CH}^{(*)}$ (see Ch XII). In the case of a premixed CO/air flame containing C_2H_4 it appears that both components must be supplied by the hydrocarbon (see Ch XII), which indicates that the reaction in premixed flames is faster.

13.3.4. Addition of Carbon Dioxide.

It was found that the addition of carbon dioxide to hydrocarbon/air diffusion flames decreased the saturation currents more than the addition of an equal flow of nitrogen. Flames with carbon dioxide added would have a lower temperature than those with nitrogen owing to the higher specific heat of the former. However, as shown below, the saturation currents of diffusion flames do not appear to depend markedly on the temperature. It thus seems that carbon dioxide has a chemical effect inhibiting ionization. This inhibition may be due to the quenching of an excited ion precursor (see Ch XII).

Carbon dioxide added to a hydrogen/air diffusion flame with small hydrocarbon addition had approximately the same effect as nitrogen, which indicates that both act as inert diluents and that the ionization in this flame is not due to excited species. This conclusion is supported by the fact that there is little connection between chemionization

and chemiluminescence in hydrogen flames containing hydrocarbons (Ackman, 1968).

13.3.5. Addition of Bromine.

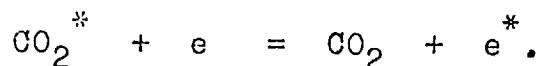
The results show that, as in the case of premixed flames, bromine does not have any marked effect on the saturation current of diffusion flames, the average change being about 10%. The effect of bromine is further discussed in Ch XII. In particular, the results indicate that the H radical, the concentration of which appears to be affected by bromine, is not important in the ionization process, and that secondary ionization by energetic electrons does not occur in hydrocarbon/air flames.

13.3.6. Addition of Alkali Metal Salts.

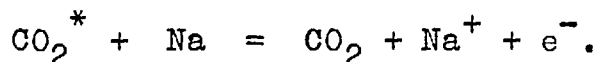
The results for the addition of alkali metal salts and/or hydrocarbon to a hydrogen/air diffusion flame show that the total current is approximately additive. The saturation current with hydrocarbon and alkali salt added was approximately the sum of that due to each by itself. Alkali metals have been found to ionize more rapidly in the presence of hydrocarbons (see Ch XII). The results show that no appreciable chemiionization of the alkali metals (sodium, potassium) occurred in the hydrogen/hydrocarbon/air diffusion flames.

The saturation currents of carbon monoxide/air diffusion flames seeded with sodium (borax) were reduced by the addition of small quantities of hydrogen or methane. The addition of larger quantities of methane gave saturation currents much smaller than the total of the current with methane but no borax and that with borax but no methane. These results show that the addition of hydrogen or hydrogen compounds reduces the ionization of sodium in carbon monoxide/air diffusion flames. Carbon monoxide flames are in marked disequilibrium. In particular the electron temperature in the reaction zone of carbon monoxide flames, but not in hydrogen flames, is much higher than the flame temperature (Bradley & Matthews, 1967). It thus appears that hydrogen, which catalyses the oxidation of carbon monoxide, reduces the disequilibrium in carbon monoxide flames. The reduction of the saturation currents of seeded carbon monoxide flames on the addition of hydrogen shows that in flames without hydrogen chemiionization of the sodium occurs.

The chemiionization of sodium in unseeded carbon monoxide/air diffusion flames may result from secondary ionization of the sodium by energetic electrons in accordance with the mechanism proposed by von Engel & Cozens (1965). Energetic electrons could be produced by inelastic collisions with excited species, such as by the reaction



Alternatively, excited species might cause ionization directly, e.g.



From the results it appears that hydrogen short circuits the production of the excited species. Thus it seems that von Engel & Cozens' mechanism may be important in seeded carbon monoxide/air diffusion flames but not in flames containing hydrogen or hydrocarbons.

13.4. Effect of Pressure.

The results for a series of methane/air diffusion flames on a nozzle and a series of methane/oxygen flames on a disc show that in each case the products of the pressure and the ratio of the saturation current to the fuel flow rate was approximately constant. This demonstrates that the saturation currents of diffusion flames are inversely proportional to pressure.

13.5. Effect of Temperature.

It has been shown that methane/oxygen diffusion flames give saturation currents lower, on average, than do methane/air flames. The addition of nitrogen to diffusion flames in oxygen of methane and of hydrogen containing a small proportion of methane initially gave a marked increase in the saturation current. The adiabatic flame temperature of methane/oxygen flames is about 500 K higher than that of methane/air flames. This temperature

difference would increase the saturation current of a premixed flame by a factor of the order of 60 at constant composition (see Ch XII). On the other hand, premixed adiabatic stoichiometric methane/air gives a somewhat higher value of n_e/n_c than a premixed adiabatic stoichiometric methane/oxygen flame, despite the higher temperature of the latter (see Ch XII).

Ibiricu & Gaydon (1964) using a counter-flow diffusion flame found that the temperature was reduced by the addition of inhibitors (including CH_3Br) and by higher incident oxidant flow rates. The results of the present study show that the addition of bromine to diffusion flames does not systematically affect the saturation currents, while increasing the oxidant flow rate to counter-flow diffusion flames increases the saturation current in most cases. Thus it appears that the saturation currents of diffusion flames do not depend on the flame temperature.

13.6. Accuracy of the Results.

The scatter of the results indicates that the random error was of the order of 10%, which is probably largely due to the effect of turbulence and distortion of the flames.

Diffusion flames were affected by the field and tended to be attracted to the cathode, particularly in the case of flames on nozzles. In addition, electric fields

affect the size and concentration of solid carbon in flames (Place & Weinberg, 1966), which would alter the amount of thermal ionization of the carbon and also the combustion efficiency. However, it was found that the current from flames increased to a steady value as the voltage was increased. This steady value was equal to or only slightly less than the maximum value and was not altered greatly by changes in the electrode separation or in the polarity. A wide range of burners gave similar results although the amount of quenching varied. It thus seems that quenching is unimportant and that diffusion flames have characteristic saturation currents.

Hydrogen and carbon monoxide diffusion flames without hydrocarbon added gave small saturation currents which are thought to be due to impurities from the air. This current, i_0 , was recorded when taking measurements on flames containing these gases. A hydrogen flame with oxygen from a cylinder gave a lower background current (section 11.6.1) than hydrogen and carbon monoxide flames burning in the open air (sections 11.6.2 and 3).

Values of i_0 for pure hydrogen and carbon monoxide flames burning in the open air are given below together with estimated saturation currents, i_s , of flames of methane with the same throughput.

$f(\text{H}_2)$, 1 min^{-1}	0.39	0.81	1.52
i_o , μA	0.1	0.2	0.4
i_s , for CH_4 , μA	18	31	50

$f(\text{CO})$, 1 min^{-1}	0.38	1.30	2.2	3.4
i_o , μA	0.1	0.15	0.25	0.31
i_s for CH_4 , μA	17	42	61	87

These magnitudes show that the currents due to impurities are much less than the saturation currents of a hydrocarbon/air flame with the same throughput. The effect of impurities from the air can therefore be ignored in the case of hydrocarbon flames.

The ionization efficiencies given by diffusion flames used in gas chromatography are of the same order as those obtained in the present study (Sternberg, 1963). The flames used in gas chromatography are diluted and small.

13.7. Discussion.

13.7.1. Mechanism of Ionization.

The addition of nitrogen and carbon monoxide to diffusion flames reduced or eliminated the sooting and yellow luminosity but gave higher saturation currents. The increase in the saturation current resulting from the addition of nitrogen was despite the reduction of the flame temperature resulting, which was of the order of up to 500 K. In addition, the saturation currents of unseeded diffusion flames do not appear to be greatly affected by polarity or

electric field strength (Place & Weinberg, 1966). Electric fields alter the size and concentration of carbon particles in flames. It is thus unlikely that the thermal ionization of carbon particles constitutes a large proportion of the saturation current in hydrocarbon diffusion flames, though it probably contributes to it.

Although it is probable that most of the ionization in flames is due to chemiionization (see Ch XII), the fact that the saturation current of diffusion flames does not increase with the flame temperature indicates that the rate of ionization, like the rate of combustion, is limited by the rate of diffusion and mixing of the reactants.

13.7.2. Comparison of Premixed and Diffusion Flames.

Ionization in diffusion flames differs in a number of respects from that in premixed flames. The most obvious is that the saturation currents of premixed flames increase steeply with temperature whereas those of diffusion flames appear to be independent of temperature. The second important difference is that premixed flames can give somewhat higher ionization efficiencies. n_e/n_c for stoichiometric adiabatic premixed hydrocarbon/air flames is of the order of 7×10^{-6} (see Ch XII). That for hydrocarbon/air diffusion flames is of the order of 5×10^{-7} .

Ionization in premixed flames is thought to be due to $\text{CH}^{(*)}$ and other radicals containing hydrogen (see Ch XII).

This does not appear to be the case for diffusion flames. Chemiionization can occur in diffusion flames containing no hydrogen (Galloway et al, 1964). Moreover, 2,2 dimethylbutane ($C(CH_3)_3C_2H_5$), in which one carbon atom is not initially joined to a hydrogen atom, gives a very similar ionization efficiency (n_e/n_c), when added to a suitable diffusion flame, as n-heptane and other hydrocarbons (Ackman, 1968). However, the main mechanism of ionization in most diffusion flames is probably similar to that in premixed flames.

13.7.3. Effect of Premixing and Disequilibrium.

In an ideal diffusion flame the reaction takes place in a thin zone in which there is chemical equilibrium, the reactant concentrations are zero and the temperature is equal to the stoichiometric adiabatic flame temperature. In practice the reaction rate is partially chemically limited and there is some premixing of the reactants. The temperatures of hydrocarbon/air diffusion flames are below the adiabatic flame temperature (Ibiricu & Gaydon, 1964; Pandya & Weinberg, 1964). On the other hand, the temperature of a hydrocarbon/oxygen diffusion flame has been found to be near the stoichiometric flame temperature (Wolfhard & Parker, 1949). The temperature of counter-flow diffusion flames is less at high incident oxidant flow rates (Ibiricu & Gaydon, 1964), which shows that the amount of

premixing is greater, presumably as a result of faster mixing due to the steeper concentration gradients, so that the rate of mixing tends to exceed the rate of reaction.

There is comparatively little chemical disequilibrium in diffusion flames since the reaction is diffusion limited and takes place gradually. There is more disequilibrium in flames with air than with oxygen because the dilution with nitrogen decreases the rate of chemical reaction. Spectroscopic studies confirm that there is more disequilibrium in premixed flames than in diffusion flames and that there is more disequilibrium in diffusion flames with air than with oxygen (Gaydon & Wolfhard, 1960). It appears also that there is more disequilibrium in hydrocarbon diffusion flames than in diffusion flames with hydrogen added (see section 13.3.4). Thus the flames having most disequilibrium are those giving most ionization, which is to be expected, since ionization is a disequilibrium phenomenon. In particular, it has been shown in the present investigation that diffusion flames tend to give lower values of n_e/n_c than premixed flames.

Reduction of pressure has been shown to increase the saturation currents of diffusion flames, and, as is well known, diffusion flames tend towards a premixed state

at low pressure (Gaydon & Wolfhard, 1960). Thus the higher saturation currents of diffusion flames at low pressures may be due to the increase in the mean free path giving greater mixing. Another possible explanation is that the rate of a competing reaction to the ionization reaction is reduced at low pressures. The amount of quenching of excited species would be reduced and it is possible that an excited species is an ion precursor (see Ch XII).

The saturation currents of counter-flow diffusion flames are greater at smaller electrode separations, when the concentration gradients are greater, increasing the rate of diffusion into the flame and giving a greater degree of premixing.

It has been shown that the amount of ionization in diffusion flames is greater in those flames with a greater degree of mixing, in particular flames at low pressure, diluted flames, and counter-flow diffusion flames with small electrode separations. More ionization occurs in the premixed region at the base of diffusion flames on nozzles than further up (Kinbara & Nakamura, 1955). It thus seems that the ionization in hydrocarbon diffusion flames occurs principally where the fuel and oxidant mix. The reactant concentration in this zone is greater in flames with a greater degree of premixing, giving higher

saturation currents. The results for premixed flames show that the maximum rate of ionization occurs when the fuel and oxidant are present in approximately stoichiometric proportions. It therefore seems unlikely that chemi-ionization occurs in the pyrolysis zone of diffusion flames.

13.7.4. Maximum Current Densities Obtainable.

The results obtained show that the saturation current densities given by diffusion flames are of the order of 3 to 20 mA m⁻². These values are less than the maximum space charge-limited saturation current density (see Ch VIII) so that the maximum current which can be drawn without secondary ionization is limited by the rate of ion generation.

Turbulent diffusion flames would enable larger flame areas, and hence larger saturation currents, to be obtained. They have the advantage for practical purposes that they can give combustion, and therefore ionization, throughout a large volume.

13.8. Summary.

The results obtained in the present study for diffusion flames have been analysed. Values of n_e/n_c have been obtained and shown to be of the same order (about 5×10^{-7} at atmospheric pressure) for all the hydrocarbon/air diffusion flames studied.

It was shown that the effect of temperature on the saturation currents of diffusion flames appears to be small. It was also found that the ionization efficiency, n_e/n_c , is inversely proportional to the pressure.

The effects of the addition of hydrogen, bromine, carbon dioxide, and carbon monoxide were considered. As in the case of premixed flames the addition of bromine and carbon dioxide appeared to have little chemical effect. The latter gave a small reduction in some cases. The effects of bromine and carbon dioxide are discussed in Ch XII. Carbon monoxide also had little effect. Hydrogen gave lower saturation currents, which is thought to be due to competition for the available oxygen.

The ionization of alkali metals in diffusion flames was considered. This ionization appears to be thermal except in the case of carbon monoxide flames, in which some chemiionization of the sodium was found to occur. It was concluded that secondary ionization by energetic electrons is probably unimportant in hydrocarbon flames.

It was shown that diffusion flames vary in the extent of mixing and that factors which increase the degree of mixing and disequilibrium, in particular dilution and reduced pressure, tend to increase n_e/n_c . Thermal ionization of flame carbon was shown to be unimportant. It is suggested that ionization in diffusion flames occurs

in the zone where the fuel and oxidant mix and that, as in premixed flames, it is primarily due to chemi-
ionization.

CHAPTER FOURTEEN.SUMMARY.

Total rates of ion generation in flames have been measured by the saturation current method. Hydrocarbon flames with air and with oxygen were studied. Factors affecting the saturation current, including temperature and the effect of additives and diluents, were investigated. In addition, the conduction of charge in the flame products has been studied.

Conduction to the electrodes was investigated in order to test the validity of the saturation current density method used. It was found that ion generation occurred above non-luminous premixed flames but that the amount was too small to affect the validity of the saturation current method, as applied to ionization in the reaction zone. A possible exception occurs in the case of oxygen flames which give very low saturation current densities. However, in such a case the variation of j_s with electrode separation provides a valuable means of determining the rate of ionization in the products.

It was shown that care had to be taken when using a probe/guard ring configuration in order to obtain the saturation current from part of a flame. The proportion of the current going to a probe was not always equal to the

ratio of the flame area - in particular the current could be influenced by impurities or foreign bodies in the flame gases. Field strengths and charge mobilities were measured. It was shown that the saturation current method, if used with care, is capable of giving valid results of absolute rates of ion generation.

The saturation currents of a large number of flames were measured. Premixed and diffusion flames of hydrocarbons with air and with oxygen were studied. The effects of various additives and diluents were determined. Additives investigated were nitrogen, hydrogen, carbon monoxide, carbon dioxide, bromine, and metallic salts. Some measurements were taken also on flames of hydrogen and carbon monoxide with and without hydrocarbon and other additives.

The variation of the saturation currents of premixed flames with final flame temperature and stoichiometric ratio was measured. Values of the effective activation energies were calculated. These were about 210 kJ mole^{-1} for lean hydrocarbon/air flames and 294 kJ mol^{-1} for lean hydrocarbon/oxygen flames. The rate of ionization and the soot particle size and concentration above two luminous flames were measured and a value of the work function of flame carbon of 4.6 eV was obtained.

It was found that diffusion flames of different hydrocarbons in air at ambient pressure on several burners gave similar ionization efficiencies, the value being about 5×10^{-7} . Some measurements were taken also at reduced pressures. The ionization efficiency was found to be inversely proportional to the pressure.

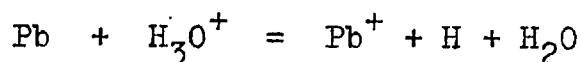
Premixed hydrocarbon flames with air gave higher saturation current densities (by a factor of the order of twenty) than flames with oxygen with the same initial hydrocarbon concentration and final flame temperature. Thus the effect of dilution with nitrogen is to increase the saturation current. This was accounted for in terms of competition by oxygen for precursors in the chemi-ionization process. The addition of nitrogen to diffusion flames in oxygen was also found to increase the saturation current. It was suggested that the increase in chemi-ionization due to dilution results from a greater degree of disequilibrium.

Carbon monoxide and bromine were found to have little systematic effect on n_e/n_c for premixed or diffusion flames. Hydrogen was found to have little effect on the saturation currents of premixed flames but decreased those of diffusion flames. Carbon dioxide reduced the saturation currents of some premixed and diffusion flames, which is

thought to be due to quenching of excitation. The effect of hydrogen and carbon monoxide in premixed flames indicates that the ionization occurs near the final flame temperature.

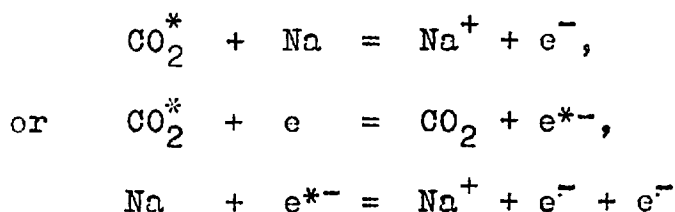
The results obtained indicate that H is not important in the ionization process but that OH and CH probably are.

The ionization due to metallic additives and small concentrations of hydrocarbon in a premixed carbon monoxide/air flame and a hydrogen/air diffusion flame were found to be additive, showing that no chemionization of the metals occurred due to reaction of the hydrocarbon. The additional ionization due to lead in a premixed carbon monoxide/air flame containing hydrocarbon was very small. This result suggests that the high ion concentration found downstream of flames containing hydrocarbon and seeded with metals such as lead is due to reduced recombination rates following charge transfer, e.g.



The saturation current of a carbon monoxide/air diffusion flame seeded with sodium was reduced by the addition of hydrogen or hydrocarbon, showing that enhanced ionization of the sodium did occur in this flame.

Probable reactions are



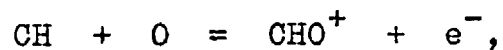
Secondary ionization by energetic electrons appears to be unimportant in hydrocarbon flames because of the existence of well defined saturation currents, the absence of chemiionization of or due to sodium in these flames, and the smallness of the effect of bromine.

Saturation currents of free burning flames were estimated. It was shown that the saturation current densities of diffusion flames and most premixed flames are lower than the maximum current densities which can be drawn without secondary ionization, so that the maximum current which can be drawn from flames for practical purposes is limited by the flame saturation current, though this limitation can be overcome by increasing the flame area per unit area of electrode (e.g. by the use of turbulent flames), or by seeding with easily ionizable materials. The results obtained give rates of ionization for a variety of different flames and enable a flame giving the required saturation current to be selected.

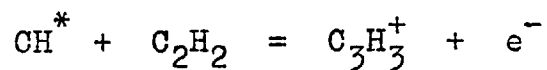
The mechanism of ionization has been considered and several conclusions reached. The main mechanism of ionization in diffusion flames and non-luminous premixed

flames is thought to be chemiionization. Results of the present study and those of other workers were compared.

The most likely ionization reaction appears to be



and possibly also,



in some flames.

REFERENCES.

The following special abbreviations have been used:

- Agard CP8 Fundamental Studies of Ions & Plasmas
(D.Wilsted, Ed.), Agard CP No 8, 1965.
- Prog.A.A.12 Progress in Astronautics & Aeronautics, Vol 12,
Ionization in High Temperature Gases
(K.E.Shuler, Ed.), Academic Press, 1963.
- 3rd Symp. Third Symposium (International) on Combustion,
Flames & Explosion Phenomena, Williams & Wilkins,
1949.
- 5th Symp. Fifth Symposium (International) on Combustion,
Reinhold, 1955.
- 6th Symp. Sixth Symposium (International) on Combustion,
Reinhold, 1957.
- 7th Symp. Seventh Symposium (International) on Combustion,
Butterworths, 1959.
- 8th Symp. Eighth Symposium (International) on Combustion,
Williams & Wilkins, 1962.
- 9th Symp. Ninth Symposium (International) on Combustion,
Academic Press, 1963.
- 10th Symp. Tenth Symposium (International) on Combustion,
The Combustion Institute, Pittsburgh, 1965.
- 11th Symp. Eleventh Symposium (International) on Combustion,
The Combustion Institute, Pittsburgh, 1967.
- 12th Symp. Twelfth Symposium (International) on Combustion,
The Combustion Institute, Pittsburgh, 1969.

- Ackman, R.G., 1968, *J. Gas Chromat.*, 6, 497.
- Arrhenius, S., 1891, *Annln. Phys.*, Series 3, 42, 18.
- Arrington, C.A., Brennen, W., Glass, G.P., Michael, J.V. & Niki, H., 1965, *J. chem. Phys.*, 43, 1489.
- Babcock, W.R., Baker, K.L. & Cattaneo, A.G., 1967, *Nature, Lond.*, 216, 676.
- Borgers, A.J., 1965, 10th Symp., 627.
- Botha, J.P. & Spalding, D.B., 1954, *Proc. R. Soc.*, A225, 71.
- Bradley, D. & Matthews, K.J., 1967, 11th Symp., 359.
- Brand, W.T., 1814, *Phil. Trans. R. Soc.*, 104, 51.
- Bulewicz, E.M., 1967, *Combustion & Flame*, 11, 297.
- Bulewicz, E.M. & Padley, P.J., 1963, 9th Symp., 638.
- Burgoyne, J.H. & Hirsch, H., 1954, *Proc. R. Soc.*, A227, 73.
- Calcote, H.F., 1949, 3rd Symp., 245.
- Calcote, H.F., 1957, *Combustion & Flame*, 1, 385.
- Calcote, H.F., 1962, 8th Symp., 184.
- Calcote, H.F., 1963a, *Prog. A.A.*, 12, 107.
- Calcote, H.F., 1963b, 9th Symp., 622.
- Calcote, H.F., 1965, *Agard CP 8*, 1.
- Calcote, H.F., Kurzius, S.C. & Miller, W.J., 1965, 10th Symp. 605.
- Calcote, H.F. & Pease, R.N., 1951, *Ind. Engng. Chem. Ind.*, 43, 2726.
- Chase, J.D. & Weinberg, F.J., 1964, *Proc. R. Soc.*, A275, 411.
- Chen, F.F., 1965, *Plasma Diagnostic Techniques* (R.H. Huddleston & S.L. Leonard, Ed.), Academic Press, Ch. IV.

- Chen, D.C.C., Lawton, J. & Weinberg, F.J., 1965,
10th Symp., 743.
- Cooper, J., 1966, Rep. Prog. Phys., 29(1), 35.
- Creitz, E.C., 1961, J. Res. ntn. Bur. Stand., 65A, 389.
- Cuthbertson, J., 1802, A Journal of Natural Philosophy,
Chemistry & the Arts (W.Nicholson, Ed.), 3, 188.
- Davies, A.J. & Evans, G.J., 1967, Proc. IEE, 114, 1547.
- Debiesse, J. & Klein, S., 1964, C. r. hebd. Seanc. Acad.
Sci., Paris, 259, 3470.
- Debiesse, J., Klein, S. & Kraus, P., 1965, C.r. hebd.
Seanc. Acad. Sci., Paris, 260, 465.
- de Gruchy, J., 1953, Wireless World, 59, 425.
- Dushman, S., 1923, Phys. Rev., Series 2, 21, 623.
- Egerton, Sir A. & Thabet, S.K., 1952, Proc. R. Soc.,
A211, 445.
- Erman, P., 1802, Annln. Phys., 11, 150.
- Fergusson, R.E., 1957, Combustion & Flame, 1, 431.
- Fontijn, A., Miller, W.J. & Hogan, J.M., 1965, 10 th Symp.,
545.
- Freck, V.D. & Wright, J.K., 1965, Nature, Lond., 205, 1192.
- Friedman, R. & Nugent, R.G., 1959, 7th Symp., 311.
- Fristrom, R.M., Prescott, R., Neuman, R.K. & Avery, W.H.,
1953, 4th Symp., 267.
- Fristrom, R.M. & Westenberg, A.A., 1965, Flame Structure,
McGraw Hill.
- Gallaway, W.S., Foster, R.A., Sternberg, J.C. & Dora, R.A.,
1964, U.S. Patent 3,140,919.

- Gardiner, W.C.J., 1961, J. chem. Phys., 35, 2252.
- Gaydon, A.G., 1957, The Spectroscopy of Flames, Chapman & Hall, London.
- Gaydon, A.G., Spokes, G.N. & van Suchtelen, J., 1960, Proc. R. Soc., A256, 323.
- Gaydon, A.G. & Wolfhard, H.G., 1949, Proc. R. Soc., A196, 105.
- Gaydon, A.G. & Wolfhard, H.G., 1951, Proc. R. Soc., A205, 118.
- Gaydon, A.G. & Wolfhard, H.G., 1960, Flames, their structure radiation & temperature, 2nd edn., Chapman & Hall.
- Gerstein, M., Levine, O. & Wong, E.L., 1951, J. Am. Chem. Soc., 73, 418.
- Giese, W., 1882, Annln. Phys., 17, 537.
- Gilbert, W., 1600, De Magnete, Lond.; translation: Fleury Mottelay, P., N.Y., 1893.
- Glass, G.P., Kistiakowsky, G.B., Michael, J.V. & Niki, H., 1965, 10 th Symp., 513.
- Green, J.A., 1965, Agard CP8, 191.
- Green, J.A. & Sugden, T.M., 1963, 9th Symp., 607.
- Grieg, J.R., 1965, Br. J. appl. Phys., 16, 957.
- Guénault, E.M. & Wheeler, R.V., 1932, J.Chem. Soc., 2, 2788.
- Hand, C.W. & Kistiakowsky, G.B., 1962, J.Chem.Phys., 37, 1239.
- Henley, W., 1774, Phil. Trans. R. Soc., 64, 389.
- Hertzberg, G., 1944, Atomic Spectra & Atomic Structure, 2nd edn., Dover, N.Y.

- Higashino, I., 1961, Bull. J.S.M.E., 4, 583.
- Hankel, W., 1851, Phil. Mag., 4th series, 2, 542.
- Hayhurst, A.N. & Sugden, T.M., 1966, Proc. R. Soc., A293, 36.
- Heaps, C.W., 1920, Phys. Rev., Series 2, 16, 238.
- Huddleston, R.H. & Leonard, S.L. (Ed.), 1965, Plasma Diagnostic Techniques, Academic Press.
- Ibiricu, M.M. & Gaydon, A.G., 1964, Combustion & Flame, 8, 51.
- Karlovitz, B., 1965, Chem. Engng. Prog., 61(8), 56.
- Kaskan, W.E., 1957, 6th Symp., 134.
- Kinbara, T. & Nakamura, J., 1955, 5th Symp., 285.
- Kinbara, T. & Noda, K., 1969, 12th Symp.
- King, I.R., 1958, J.chem. Phys., 29, 681.
- King, I.R., 1963, Prog. A.A., 12, 197.
- King, I.R. & Calcote, H.F., 1955, J. chem. Phys., 23, 2203.
- Klein, S., 1960, C. r. hebd. Seanc. Acad. Sci., Paris, 251, 657.
- Knapp, V.H., 1964, Elektrotech. Zeit., B16, 733.
- Langevin, P., 1903, Annls. Chim. Phys., 7th series, 28, 289.
- Langevin, P., 1905, Annls. Chim. Phys., 8th series, 5, 245.
- Lawton, J., 1963, Ph.D. Thesis, Lond.
- Lawton, J., 1965, Agard CP8, 135.
- Lawton, J., Mayo, P.J. & Weinberg, F.J., 1968, Proc. R. Soc., A303, 275.
- Lawton, J. & Weinberg, F.J., 1964, Proc. R. Soc., A277, 468.

- Lewis, B. & von Elbe, G., 1961, Combustion, Flames & Explosions of Gases, Academic Press, N.Y., 2nd Edn.
- Linnett, J.W. & Hoare, M.F., 1949, 3rd Symp., 195.
- Loeb, L.B., 1955, Basic Processes of Gaseous Electronics, University of California Press.
- Lovelock, J.E., 1961, Analyt. Chem., 33, 162.
- McClelland, J.A., 1898, Phil. Mag., 5th series, 46, 29.
- McWilliam, I.G., 1961, J.Chromat., 6, 110.
- Makios, W., Agard CP8, 419.
- Malinowsky, A.E. & Malyar, D.V., 1935, Zh. tech. Fiz., 5, 1260.
- Massey, H.S.W. & Burhop, E.H.S., 1952, Electronic & Ionic Impact Phenomena, Clarendon Press, Oxford.
- Mayo, P.J., Watermeier, L.A. & Weinberg, F.J., 1965, Proc. R. Soc., A284, 488.
- Meek, J.M. & Craggs, J.D., 1953, Electrical Breakdown of Gases, Clarendon Press, Oxford.
- Meyer, E. & Muller, E., 1904, Verh. Deut. Phys. Ges., 2, 332.
- Miller, W.J., 1967, 11th Symp., 311.
- Mitchell, J.H. & Ridler, K.E.W., 1934, Proc. R. Soc., A146, 911.
- Nakamura, J., 1959, Combustion & Flame, 3, 277.
- Padley, P.J., Page, F.M. & Sugden, T.M., 1961, Trans. Faraday Soc., 57, 1552.
- Padley, P.J. & Sugden, T.M., 1959, 7th Symp., 235.
- Padley, P.J. & Sugden, T.M., 1962, 8th Symp., 164.

- Pandya, T.P. & Weinberg, F.J., 1963, 9th Symp., 587.
- Pandya, T.P. & Weinberg, F.J., 1964, Proc. R. Soc.,
A279, 544.
- Payne, K.G. & Weinberg, F.J., 1959, Proc. R. Soc., A250, 316.
- Peeters, J. & Van Tiggelen, A., 1968, Combustion & Flame,
12, 394.
- Pejack, E.R. & Jones, C.D., 1968, Combustion & Flame,
12, 509.
- Perkins, jun., G., Rouayheb, G.M., Lively, L.D. &
Hamilton, W.C., 1962, Gas Chromatography, 3rd Symp.,
Academic Press, 269.
- Perkins, jun., G., Yang, K. & Folmer, jun., O.F., 1963,
Nature, Lond., 198, 780.
- Perry, J.H. (Ed.), 1963, Chemical Engineers' Handbook,
4th Edn., McGraw Hill.
- Petschek, H. & Byron, S., 1957, Ann. Phys., 1, 270.
- Place, E.R. & Weinberg, F.J., 1966, Proc. R. Soc., A289, 192.
- Richardson, W.L., Ryason, P.R., Kautsky, G.J. & Berusch, M.R.
1963, 9th Symp., 1023.
- Roser, W.A., Wise, H. & Miller, J., 1959, 7th Symp., 175.
- Rotherham, L., Nature, Lond., 216, 1071.
- Rutherford, A.G. & Fells, I., 1966, J.Inst. Fuel, 39, 307.
- Salter, I.W. & Travers, B.E.L., 1965, Agard CP8, 65.
- Scheller, K. & McKnight, W.E., 1959, 7th Symp., 369.
- Schnauffer, K., 1934, SAE J., 34, 17.
- Schofield, K. & Sugden, T.M., 1965, 10th Symp., 589.

- Schuster, A., 1887, Proc. R. Soc., 42, 371.
- Schuster, A., 1890, Proc. R. Soc., 47, 526.
- Snellerman, W., 1967, Combustion & Flame, 11, 453.
- Soundy, R.G. & Williams, H., 1965, Agard CP8, 161.
- Sternberg, J.C., Gallaway, W.S. & Jones, D.T.L., 1962,
Gas Chromatography, 3rd Int. Symp., Academic Press
231.
- Sternberg, J.C., 1963, Gas Chromatography, 4th Symp., 161.
- Sugden, T.M., 1963, Prog. A.A., 12, 145.
- Sugden, T.M., 1965, 10th Symp., 539.
- Sugden, T.M. & Knewstubb, P.F., 1956, Res., Res. Corr. 9, S32.
- Tanford, C. & Pease, R.N., 1947, J. chem. Phys., 15, 431.
- Taylor, G.N., 1964, Proc. R. Soc., A279, 497.
- Thieme, B., 1912, Z. phys. Chem., 89, 693.
- Thieme, B., 1915, Z. phys. Chem., 78, 490.
- Thomson, Sir J.J. & Thomson, G.P., 1928, Conduction of
Electricity Through Gases, 3rd edn., Vol.1, C.U.P.
- Thring, M.W., 1965, Chem. & Process Engng., 46, 544.
- Travers, B.E.L. & Williams, H., 1965, 10th Symp., 657.
- Turcotte, D.L. & Friedman, W., 1965, 10th Symp., 673.
- Tverdokhelbov, V.N., 1956, Zh. eksp. teor. Fiz., 30, 252.
- Van Tiggelen, A., 1963, Prog. A.A., 12, 165.
- Van Tiggelen, A. & Feugier, A., 1965, Rev. de l'Inst. Franc.
du petrol., 20, 1135.
- Von Wouterghem, J. & Van Tiggelen, A., 1954, Bull.Soc. Chim.
Belg., 63, 235.

- Von Engel, A. & Cozens, J.R., 1963, Proc. Phys. Soc., 82, 85.
- Von Engel & Cozens, J.R., 1965, Agard CP8, 123.
- Waroux, M., 1964, private communication.
- Watson, W., 1747, Phil. Trans. R. Soc., 44, 704.
- Weinberg, F.J., 1963, Optics of Flames, Butterworths, London.
- Weinberg, F.J., 1966a, Combustion & Flame, 10, 267.
- Weinberg, F.J., 1966b, IPPS Bulletin, 17, 116.
- Westenberg, A.A. and Fristrom, R.M., 1961, J. phys. Chem.,
65, 591.
- Williams, H., 1962, 8th Symp., 179.
- Wilson, H.A., 1931, Rev. mod. Phys., 3, 156.
- Wise, H. & Roser, W.A., 1963, 9th Symp., 733.
- Wolfhard, H.G. & Parker, W.G., 1949, Proc. Phys. Soc.,
A62, 722.
- Woods, F.J., Umstead, M.E. & Johnson, J.E., 1965, Naval Res.
Lab., Washington, D.C., report No. NRL-6316.
- Wortberg, G., 1965, 10 th Symp., 651.
- Yumlu, V.S., 1959, Ph.D. Thesis, London.

APPENDIX.

Consider the electric field downstream of a flame in the presence of negative ions and electrons, allowing for electron attachment and detachment.

Gauss's Law gives

$$\epsilon \frac{dE}{dx} = e (n_i + n_e) \quad (1).$$

$$j = eE (k_i n_i + k_e n_e) \quad (2).$$

Therefore
$$n_e = \frac{j}{e k_e E} - \frac{k_i}{k_e} n_i \quad (3),$$

and
$$\epsilon \frac{dE}{dx} = n_i e (1 - k_i/k_e) + \frac{j}{e k_e E} E \quad (4).$$

$$\begin{aligned} (d/dx)(k_i n_i E) &= \text{rate of increase of ion flux density} \\ &= v_a n_e - v_d n_i. \end{aligned}$$

Substituting for n_e from equation (3),

$$\frac{d}{dx} (k_i n_i E) = \frac{j v_a}{e k_i E} - n_i \left(v_d + \frac{v_a k_i}{k_e} \right).$$

Therefore
$$n_i \frac{dE}{dx} = \frac{j v_a}{e k_i k_e E} - n_i \left(v_d/k_i + v_a/k_e \right) - E \frac{dn_i}{dx}.$$

Multiplying by $(1 - k_i/k_e)e$,

$$\begin{aligned} n_i e (1 - k_i/k_e) (dE/dx + v_d/k_i + v_a/k_e) + E (d/dx)(n_i e (1 - k_i/k_e)) \\ = \frac{j v_a}{k_i k_e E} (1 - k_i/k_e). \end{aligned}$$

From equations (1) and (2),

$$n_i e (1 - k_i/k_e) = \epsilon \frac{dE}{dx} - j (k_e E)^{-1}$$

Therefore

$$\begin{aligned} \left(\epsilon \frac{dE}{dx} - \frac{j}{k_e E} \right) \left(\frac{dE}{dx} + \frac{v_d}{k_i} + \frac{v_a}{k_e} \right) + E \frac{d}{dx} \left(\epsilon \frac{dE}{dx} - \frac{j}{k_e E} \right) \\ = \frac{j}{k_e E} \frac{v_a}{k_i} (1 - k_i/k_e). \end{aligned}$$

Therefore

$$\begin{aligned} \left(\epsilon \frac{dE}{dx} - \frac{j}{k_e E} \right) \left(\frac{dE}{dx} + \frac{v_d}{k_i} + \frac{v_a}{k_e} \right) + \epsilon E \frac{d^2 E}{dx^2} + \frac{j}{k_e E} \frac{dE}{dx} \\ = \frac{j}{k_e E} \frac{v_a}{k_i} (1 - k_i/k_e). \end{aligned}$$

Expanding and rearranging:

$$\left(\frac{dE}{dx} \right)^2 + E \frac{d^2 E}{dx^2} + \left(\frac{v_d}{k_i} + \frac{v_a}{k_e} \right) \frac{dE}{dx} = \frac{j}{\epsilon k_i k_e E} (v_a + v_d),$$

Therefore

$$E \frac{d^2 j(E^2)}{dx^2} = \frac{2j}{\epsilon k_i k_e} (v_a + v_d) - \left(\frac{v_a}{k_e} + \frac{v_d}{k_i} \right) \frac{d(E^2)}{dx}.$$